A NON-PERMSELECTIVE MEMBRANE REACTOR FOR CATALYTIC GAS PHASE REACTIONS

H.J. SLOOT

DEVELOPMENT OF A NON-PERMSELECTIVE MEMBRANE REACTOR FOR CATALYTIC GAS PHASE REACTIONS

PROEFSCHRIFT

ter verkrijging van
de graad van doctor aan de Universiteit Twente,
op gezag van de rector magnificus,
prof. dr. ir. J.H.A. de Smit,
volgens besluit van het College van Dekanen
in het openbaar te verdedigen
op vrijdag 17 mei 1991 te 16.00 uur.

door

Henk Johan Sloot
geboren op 17 april 1964
te Hengelo.

Dit proefschrift is goedgekeurd door de promotoren

Prof. dr. ir. W.P.M. van Swaaij
Prof. dr. C.A. Smolders

en de assistent promotor

Dr. ir. G.F. Versteeg

ISBN 90-9004092-7
Druk: Febodruk, Enschede

Aan mijn ouders

SUMMARY

In this thesis a novel kind of membrane reactor is studied. In this reactor a porous membrane is used to keep the bulk of reactants separated from each other and to allow the reactants to come together and react in a controlled way inside the membrane. Permselectivity of the membrane is not used in this system, this in contrast to the usual application of membranes. The reactants A and B are fed to the opposite sides of a porous membrane and diffuse into the membrane from either side. The reactants come together inside the membrane, where a catalyst has been impregnated, and react. Provided the rate of the reaction is fast compared to the diffusion rate of the reactants a small reaction zone will exist inside the membrane. In the steady state the location of this reaction zone is such that the molar fluxes of both reactants are in stoichiometric ratio. If the concentration of one of the reactants, for instance A, increases this will result in an increase of the molar flux of A into the membrane. Therefore an excess of A will be present at the reaction zone diffusing further into the membrane until reaction can occur. This automatically results in a shift of the location of the reaction zone towards the side of the membrane where reactant B is present. Because of this change of the location of the reaction zone the distance from the membrane interface to the reaction zone increases for reactant A thereby decreasing the molar flux of A and vice versa for reactant B. The new location of the reaction zone will be such that the molar fluxes of both reactants are in stoichiometric ratio again. Finally the products of the reaction diffuse out of the membrane.

As the reactants must diffuse from opposite sides into the membrane no pressure difference over the membrane is required, contrary to the common applications of membranes. Another difference is that as permselectivity does not play a role in this system the pore diameter of the membrane can be relatively large in order to operate in the continuüm regime resulting in high molar fluxes and therefore relatively small required membrane areas.

Owing to the fast chemical reaction inside the membrane slip of reactants to the opposite side of the membrane is prevented. As this reactor controls the stoichiometric addition of both reactants automatically, this offers opportunities for processes where strict stoichiometric addition of reactants is important and troublesome, for instance because of fluctuation of the concentration of one of the reactants.

In this thesis first a literature survey of the main topics in membrane reactors, especially those using ceramic or metallic membranes, is given. All these systems have in common that the membrane is used because of its separation properties. Next the membrane reactor which is investigated in this thesis is presented and the structure of the present thesis is described.

The features of this membrane reactor are shown by means of mathematical modelling of molecular diffusion and viscous flow combined with an instantaneous, reversible reaction inside the membrane. This model uses Fick's law to describe diffusion and is therefore called the simplified model. As a model reaction the Claus reaction (Mark et. al., 1983) was selected and by conversion measurements the principle of a shifting reaction plane inside a porous membrane is demonstrated. Application of a moderate overall pressure difference over the membrane still permits the reactor to operate while products of the reaction can be forced to one side of the membrane only.

Surface diffusion of H_2S and SO_2 in alumina membranes with an average pore diameter of about 350 nm, impregnated with γ-Al_2O_3, is studied as a function of pressure at temperatures between 446 and 557 K. Diffusion through the gas phase in the pores of the membrane almost entirely takes place in the continuum regime. The pressure dependence of transport by diffusion through the gas phase and by surface diffusion is different, a fact which is used for the interpretation of the steady state diffusion measurements. It is observed that the contribution of surface diffusion to the total diffusion through the membrane can be up to about 40%. The surface diffusion data obtained are interpreted by a theoretical surface diffusion model using two parameters to be fitted, the product of the effective surface diffusion coefficient, the concentration of the adsorption sites and the adsorption parameter as well as the adsorption parameter itself. The parameters fitted for SO_2 show a remarkable change between 498 and 525 K which probably may be attributed to a change in the adsorbed species also reported in literature. The parameters fitted for H_2S show a maximum as a function of temperature, however, the product of the effective surface diffusion coefficient and the concentration of the adsorption sites still increases with temperature.

Then, a more complete mathematical model, based on the so-called 'Dusty-Gas Model' (Mason and Malinauskas, 1983) extended with surface diffusion, is presented. This model describes mass transport owing to molecular diffusion and viscous flow combined with an instantaneous reversible reaction inside a membrane with reactants fed to different sides of the membrane. Mass transfer resistances in the gas phase outside the membrane are taken into account. The extended model is used to determine the validity of the presented simplified model. From the comparison of both models it is concluded that the simplified model predicts the correct molar fluxes provided the system is very diluted and can therefore be considered a pseudo-binary system. From the present model it is concluded that in absence of an overall pressure difference over the membrane, a maximum or a minimum in the pressure profile inside the membrane is to be expected. This effect not only depends on the stoichiometry of the reaction but also on the mobilities of the different species.

The Claus reaction, mentioned before, has been used to verify experimentally the previously presented transport model in a non-permselective membrane reactor with a mean pore diameter of 350 nm. Both at a temperature of 493 K and at 542 K the experimentally determined molar fluxes are 10 to 20% lower compared to the molar fluxes predicted by the transport model. Conversion measurements performed at pressures of 220 kPa and 500 kPa demonstrate the importance of surface diffusion as a transport mechanism despite the large pore diameter of the membrane. In the presence of an overall pressure difference over the membrane still the agreement of the experimentally determined molar fluxes and those calculated by the transport model is reasonable.

Finally, this membrane reactor has been tested experimentally for the catalytic reduction of nitric oxide with ammonia. It is demonstrated that the reactor can cope with varying ratios of concentrations of nitric oxide and ammonia without detectable slip of reactants at a temperature of 569 K.

References

Mark H.F., D.F. Othmer, C.G. Overberger and G.T. Seaborg, 1983, Kirk-Othmer, Encyclopedia of chemical technology, vol. 22, 276 - 282, John Wiley & Son, New York

Mason E.A. and A.P. Malinauskas, 1983, Gas transport in porous media: The Dusty-Gas Model, Chemical Engineering Monographs 17, Elsevier, Amsterdam

SAMENVATTING

In dit proefschrift wordt een nieuw type membraan reactor bestudeerd. In deze reactor wordt een poreus membraan gebruikt om de bulk van de reactanten van elkaar gescheiden te houden en om de reactanten in het membraan bij elkaar te laten komen en te laten reageren op een gecontroleerde wijze. Van permselectiviteit van het membraan wordt geen gebruik gemaakt in dit systeem, dit in tegenstelling tot de gebruikelijke toepassing van membranen. De reactanten A en B worden aan verschillende zijden van het membraan toegevoerd en diffunderen van verschillende zijden het membraan in. De reactanten komen samen in het membraan, waarin een katalysator is geïmpregneerd, en reageren. Mits de reactiesnelheid hoog is in vergelijking tot de diffusie snelheid van de reactanten zal er een kleine reactiezone in het membraan ontstaan. In de stationaire toestand zal de plaats van deze reactiezone zodanig zijn dat de molfluxen van beide reactanten in stoechiometrische verhouding zijn. Indien de concentratie van een der reactanten, bijvoorbeeld A, toeneemt zal dit resulteren in een toename van de molflux van A het membraan in. Daardoor zal er een overmaat van A aan de reactiezone aanwezig zijn die verder het membraan in diffundeert totdat reactie plaats kan vinden. Dit leidt automatisch tot een verschuiving van de plaats van de reactiezone naar de zijde van het membraan waar reactant B aanwezig is. Vanwege deze verandering van de plaats van de reactiezone neemt de afstand van het membraan tot de reactiezone toe voor reactant A resulterend in aan afname van de molflux van A en vice versa voor reactant B. De nieuwe plaats van de reactiezone zal zodanig zijn dat de molfluxen van beide reactanten weer in stoechiometrische verhouding zijn. Tenslotte diffunderen de produkten van de reactie het membraan uit.

Aangezien de reactanten van verschillende zijden het membraan in moeten diffunderen is er geen drukverschil over het membraan vereist, dit in tegenstelling tot de gebruikelijke toepassing van membranen. Een ander verschil is dat aangezien permselectiviteit geen rol speelt in dit systeem de poriediameter van het membraan relatief groot kan zijn teneinde in het continuum regime te werken hetgeen de hoogste molfluxen geeft en daardoor in relatief kleine membraan oppervlakken resulteert.

Als gevolg van de snelle reactie in het membraan wordt doorbraak van reactanten naar de andere zijde van het membraan voorkomen. Aangezien deze reactor de stoechiometrische toevoer van reactanten automatisch regelt geeft dit mogelijkheden voor processen waarin een strikt stoechiometrische toevoer van reactanten vereist en moeilijk is, als gevolg van bijvoorbeeld een fluktuerende concentratie van een der reactanten.

In dit proefschrift wordt eerst een literatuur overzicht gegeven van de belangrijkste onderwerpen op het gebied van membraan reactoren, met name van de systemen die gebruik maken van keramische of metallische membranen. Al deze systemen hebben als gemeenschappelijk kenmerk dat het membraan gebruikt wordt voor zijn scheidende eigenschappen. Vervolgens wordt de membraan reactor die in dit proefschrift onderzocht is gepresenteerd en wordt de opbouw van dit proefschrift beschreven.

De mogelijkheden van deze membraan reactor worden aangetoond middels wiskundige modellering van moleculaire diffusie en visceuze stroming in combinatie met een instantane, reversibele reactie in het membraan. Dit model gebruikt Ficks diffusie wet en wordt daarom het

vereenvoudigde model genoemd. Als model reactie is de Claus reactie (Mark et.al., 1983) gekozen en door middel van conversie metingen wordt het principe van een verschuivende reactiezone in het membraan aangetoond. Opleggen van een bescheiden drukverschil over het membraan tast de werking van de reactor niet aan terwijl de reactieprodukten naar een zijde van het membraan kunnen worden geforceerd.

Oppervlakte diffusie van H_2S en SO_2 in alumina membranen met een gemiddelde poriediameter van circa 350 nm, geïmpregneerd met γ-Al_2O_3, is bestudeerd als functie van de druk bij een temperatuur van 446 tot 557 K. Diffusie door de gasfase in de poriën van het membraan geschiedt vrijwel geheel in het continuum regime. De drukafhankelijkheid van het transport ten gevolge van diffusie door de gasfase en oppervlakte diffusie is verschillend hetgeen gebruikt is voor de interpretatie van de steady state diffusie metingen. Het is waargenomen dat de bijdrage van oppervlaktediffusie ten opzichte van het totale diffusie transport door het membraan tot circa 40% bedraagt. De verkregen oppervlaktediffusie data zijn geïnterpreteerd met een theoretisch oppervlaktediffusie model met twee te fitten parameters, het produkt van de effectieve oppervlakte diffusie coëfficiënt, de concentratie aan adsorptie plaatsen en de adsorptie parameter alsmede de adsorptie parameter zelf. De voor SO_2 gefitte parameters geven een opmerkelijke verandering te zien tussen 498 en 525 K hetgeen waarschijnlijk verbonden is aan de verandering van de aard van de geadsorbeerde deeltjes die in de literatuur gevonden is. De voor H_2S gefitte parameters geven als functie van de temperatuur een maximum te zien, echter het produkt van de effectieve oppervlakte diffusie coëfficiënt en de concentratie aan adsorptie plaatsen neemt toe met de temperatuur.

Vervolgens wordt een uitgebreider wiskundig model gepresenteerd dat gebaseerd is op het zogeheten 'Dusty-Gas Model' (Mason and Malinauskas, 1983), uitgebreid met oppervlakte diffusie. Dit model beschrijft transport tengevolge van moleculaire diffusie en visceuze stroming gecombineerd met een instantane, reversibele reactie in een membraan waarbij de reactanten aan verschillende zijden van het membraan worden toegevoerd. Met stofoverdrachtsweerstanden in de gasfase buiten het membraan wordt rekening gehouden. Het uitgebreide model is gebruikt om de geldigheid van het vereenvoudigde model te bepalen. Uit de vergelijking van beide modellen kan geconcludeerd worden dat het vereenvoudigde model de correcte molfluxen voorspelt mits het systeem sterk verdund is en daarom als pseudo binair mag worden opgevat. Uit het huidige model volgt dat, in afwezigheid van een drukverschil over het membraan, een maximum of een minimum in het drukprofiel in het membraan kan worden verwacht. Dit effect hangt niet alleen af van de stoechiometrie van de reactie maar ook van de beweeglijkheid van de diverse deeltjes.

De reeds eerder genoemde Claus reactie is gebruikt om experimenteel het hiervoor beschreven transport model te verifiëren in een niet-permselectieve membraan reactor met een gemiddelde poriediameter van 350 nm. Zowel bij een temperatuur van 493 K als bij 542 K zijn de experimenteel bepaalde molfluxen 10 tot 20 % lager dan de molfluxen voorspelt met het transport model. Conversie metingen verricht bij drukken van 220 kPa en 500 kPa tonen het belang aan van oppervlakte diffusie als transport mechanisme ondanks de grote poriediameter van het membraan. Ook in aanwezigheid van een drukverschil over het membraan is de overeenkomst van de experimenteel bepaalde molfluxen en de berekende molfluxen redelijk.

Tenslotte is deze membraan reactor experimenteel getest voor de katalytische reduktie van stikstofoxiden met ammoniak. Aangetoond wordt dat deze reactor verschillende verhoudingen van concentraties aan stikstofoxiden en ammoniak aankan zonder meetbare doorbraak van reactanten bij een temperatuur van 569 K.

Referenties

Mark H.F., D.F. Othmer, C.G. Overberger and G.T. Seaborg, 1983, Kirk-Othmer, Encyclopedia of chemical technology, vol. 22, 276 - 282, John Wiley & Son, New York

Mason E.A. and A.P. Malinauskas, 1983, Gas transport in porous media: The Dusty-Gas Model, Chemical Engineering Monographs 17, Elsevier, Amsterdam

VOORWOORD

Aan het werk beschreven in dit proefschrift hebben velen een bijdrage geleverd. Om te beginnen wil ik mijn promotoren Prof. dr. ir. W.P.M. van Swaaij en Prof. dr. C.A. Smolders en mijn assistent promotor Dr. ir. G.F. Versteeg bedanken voor hun begeleiding. Hun kennis en ervaring zijn van grote waarde geweest bij het richting bepalen en op wetenschappelijke wijze verrichten van het onderzoek.

Gedurende het onderzoek is Paul Weersink bij het experimentele werk van zeer grote waarde geweest, waarvoor ik hem bij deze wil bedanken. Dankzij zijn kritische en zelfstandige werkwijze liepen het draaiend krijgen van de opstellingen en de metingen hiermee op voortreffelijke wijze. Zijn manier van werken en zijn nieuwsgierige instelling naar het hoe en waarom van interpretaties van metingen heb ik in hoge mate gewaardeerd.

Bedanken wil ik ook de technici van het HDL en de CTD. Met name wil ik daarbij Karst van Bree, Wim Leppink en Arie Pleiter noemen voor hun bijdrage in het ontwikkelen van de opstellingen, de bouw en het technisch onderhoud hiervan. Ben Haafkes, Wim Platvoet en Jan Jagt zorgden voor de bestellingen en aflevering van bestelde apparatuur. Rik Akse, Ferdinand Damhuis en Andries Groenink zorgden voor de financiële administratie van het project.

Afstudeeropdrachten werden verricht door Koert Ackerman en Norbert Kuipers, een keuzepracticum Proceskunde werd verricht door Arnoud Kamperman. In het kader van hun HTS afstudeeropdracht hebben Magriet de Jonge en Eugenie Nijmeijer hun opdracht in dit project verricht. Hen allen wil ik bij deze bedanken voor hun bijdrage.

Ook de leden van de gebruikerscommissie van mijn project, Drs. N.H.C.M. Boots (STW), Ir. A.E. Cornelisse (Shell), Dr. G. Desgrandchamps (Elf-Aquitaine), Ir. J.J. Gorissen (Akzo), Dr. G.W. Meindersma (DSM) en Prof. dr. ir. K. van der Wiele (Akzo) wil ik bedanken voor hun tijd en inbreng in de halfjaarlijkse vergaderingen over dit project.

De leden van de vakgroep wil ik bedanken voor de stimulerende omgeving waarin ik tijdens het project heb mogen werken. De goede sfeer en vele discussies hebben zeker een positieve bijdrage geleverd bij de totstandkoming van dit proefschrift.

Aangezien bovenstaande opsomming zeker niet volledig is wil ik tenslotte een ieder bedanken voor de bijdrage die hij of zij geleverd heeft voor het tot stand komen van dit proefschrift.

ACKNOWLEDGMENT

The National Dutch Program Committee on Membranes is gratefully acknowledged for its financial support of this work.

CONTENTS

Summary 5

Samenvatting 8

Voorwoord 11

Chapter 1: An introduction to membrane reactors 15
Abstract 15
1. Literature survey 16
2. A non-permselective membrane reactor 18
References 20

Chapter 2: A non-permselective membrane reactor for chemical processes normally requiring strict stoichiometric feed rates of reactants 23
Abstract 23
1. Introduction 24
2. Model description 25
3. Numerical results 30
4. Experimental verification 35
5. Conclusions 37
Notation 38
References 39

Chapter 3: Surface diffusion of hydrogen sulfide and sulfur dioxide in alumina membranes in the continuum regime 41
Abstract 41
1. Introduction 42
2. Theory 43
3. Experimental setup 47
4. Determination of the porosity-tortuosity factor, ε/τ, of the membrane 49
5. Determination of the mass transfer parameter in the gas phase k_g 51
6. Results from diffusion measurements 53
7. Conclusions 57
Notation 58
References 59
Appendix: Experimental and theoretically calculated surface diffusion data 60

Chapter 4: Mathematical modelling of mass transport combined with an instantaneous, reversible reaction inside a membrane 63
Abstract 63
1. Introduction 64
2. Model description 65
3. Solution method 70
4. Numerical verification 74
5. Numerical evaluation of the transport model 78
6. Comparison of the results of the numerical model with those of the previous model 84
7. Conclusions 89
Notation 89
References 91
Appendix: Approximate analytically molar fluxes in limiting situations 92

Chapter 5: A high temperature membrane reactor part 2: An experimental study 101
Abstract 101
1. Introduction 102
2. Theory 102
3. Experimental setup 104
4. Experimental results 105
5. Conclusions 110
Notation 111
References 111

Chapter 6: A non-permselective membrane reactor for the selective catalytic reduction of NO_x with ammonia 113
Abstract 113
1. Introduction 114
2. Theory 116
3. Experimental setup 118
4. Analysis system 120
5. Conversions of NO_x and NH_3 in the reactor 122
6. Conclusions 130
Notation 130
References 131

Levensloop 135

Chapter 1

AN INTRODUCTION TO MEMBRANE REACTORS

Abstract

A literature survey of the main topics in membrane reactors, especially those using ceramic or metallic membranes, is given. All these systems have in common that the membrane is used for its separation properties. Next the membrane reactor which is investigated in this thesis is presented. In this reactor permselectivity is not important as the membrane is used to keep reactants separated from eachother and to allow them to come together in a controlled way. Finally, the structure of this thesis is described.

1. Literature survey

A lot of research effort is invested in membrane reactors nowadays because the combination of separation and reaction in one apparatus offers very interesting opportunities to improve the efficiency of a large number of chemical and biochemical processes. In these reactors membranes of all kind of materials, polymers, ceramics or metals, can be used and each of these materials has its own specific advantages.

Polymeric membranes are mainly used in bioreactors as their use is limited to relatively low temperatures, 550 K at maximum. A survey of the use of these polymeric membranes in bioreactors is given by Matson and Quinn (1986). A number of reasons can be distinguished to integrate the bioconversion and the separation process e.g., the opportunity of obtaining relatively pure product streams, the increase of the product yield in case of bioreactions that suffer from product inhibition and the possibility of enzyme-catalyzed conversion of reactants that are not soluble in water.

The use of ceramic or metallic membranes offers the possibility of operation at high temperatures. Dense, non-porous, metallic membranes, made of palladium or palladium alloys, offer complete permselectivity as they are only permeable to hydrogen. A large disadvantage of dense metallic membranes however is the low molar flux that can be obtained compared to those obtained using porous ceramic membranes. For porous ceramic membranes permselectivity is often limited to the Knudsen selectivity which is equal to the square root of the ratio of the molar masses of the components to be separated. An excellent survey of the use of metallic and ceramic membranes in membrane reactors is given by Armor (1989). A survey of commercially available inorganic membranes is given by Hsieh (1988).

There are two main reasons for the combination of reaction and separation by membranes i.e.

i) selectivity improvement and

ii) increase of the conversion of reactions where conversion is limited by thermodynamics, by selective removal of one of the products of the reaction, mostly hydrogen.

Dense foils of palladium or palladium alloys were used as membrane material by Nagamoto and Inoue (1985), Gryaznov (1986) and Gur'yanova et. al. (1988) to study hydrogenation reactions. In these systems hydrogen diffuses through the membrane before the reaction takes place. Nagamoto and Inoue (1985) studied the hydrogenation of 1,3-butadiene and observed higher reaction rates using the hydrogen permeable membrane compared to the reaction rate with premixed reactants. They attributed this to strong adsorption of 1,3-butadiene on the catalyst surface. Gur'yanova et. al. (1988) studied the hydrogenation of CO and observed an influence of the introduction of hydrogen on the activity and the selectivity. Using dense Bi_2O_3-La_2O_3 oxygen permeable membranes Di Cosimo et. al. (1986) studied the oxidative dehydrodimerization of propylene and obtained selectivities higher compared to those obtained with oxygen supplied to the propylene feed. Gryaznov et. al. (1986) studied the oxidation of hydrocarbons, alcohols and ammonia using oxygen permeable silver membranes and also obtained improved selectivities.

Studies concerning the improvement of the conversion of dehydrogenation reactions where conversion is limited by thermodynamics by selective removal of hydrogen through a dense

metallic or porous ceramic membrane in literature are numerous. Wood (1968) studied the dehydrogenation of cyclohexane to cyclohexene using a palladium-silver alloy membrane. The dehydrogenation of cyclohexane to benzene was studied by Ito et. al. (1985) and by Sun and Khang (1988) both using porous Vycor-glass as a membrane material. Ito et. al. (1985) used the membrane as a permselective wall of a packed bed of Pd-Al_2O_3 or Pt-Al_2O_3 catalytically active particles and observed conversions higher compared to those obtained without permselective wall. They reported the existence of an optimal thickness of the membrane for maximal conversion which depends on the relative rates of permeation and reaction. A permeation rate high compared to the reaction rate results in excessive loss of reactant by permeation of cyclohexane whereas a permeation rate low compared to the reaction rate results in substantial hydrogen concentrations at the feed side limiting conversion. Sun and Khang impregnated the Vycor-glass membrane with the platinum catalyst and compared the conversions obtained with the situation of packed catalyst particles in the Vycor-glass tube. For high residence times the conversion in the reactor with the membrane impregnated with the catalyst was superior compared to the reactor using a packed bed of catalyst particles whereas at low residence times the latter configuration was superior.

Mikhalenko et. al. (1986) studied the dehydrogenation of isopropyl alcohol using a palladium foil as a catalytic membrane material. They showed that the conversion depends highly on the hydrogen concentration at the surface of the membrane and that a certain amount of adsorbed hydrogen is necessary for the dehydrogenation reaction to occur.

Ito et. al. (1984) studied the dehydrogenation of HI at 700 K in a membrane reactor with a wall of microporous Vycor-glass. The optimal membrane thickness was shown to be about 1 μm. Conversions of HI of about twice the conversion obtained without selectively removing hydrogen were reported.

Economically very interesting is the dehydrogenation of hydrogen sulfide which can be an alternative for the complicated Claus process as pointed out by Raymont (1975). Kameyama et. al. (1983) studied this reaction at 1100 K using a microporous Vycor-glass and a microporous alumina membrane for comparison. The hydrogen production in this case was about twice the amount of hydrogen produced without using a permselective membrane. A problem however was the relative low separation factor owing to the large pore diameters of about 100 nm resulting in excessive permeation of hydrogen sulfide through the membrane.

Recently, Champagnie et. al. (1990) used Pt-impregnated alumina membranes to increase the conversion of ethane to ethylene at 700 to 900 K. Reactor conversions were up to a factor 6 higher compared to those obtained without selective hydrogen removal.

Very interesting work concerning the operation of membrane reactors, co- or countercurrently, with or without recycle, has been published by Mohan and Govind (1988a, 1988b). To improve the performance of membrane reactors using membranes operating at Knudsen selectivity, they concluded that:

- permeated reactant should be recycled or allowed to permeate back
- the separation can be increased by shifting the feed location
- the permeation rates of the products should be high to reduce the reverse reaction.

The choice of a co- or countercurrently operated membrane reactor depends on system parameters

e.g., differences in permeability. An interesting proposal is the membrane reactor with recycle and intermediate feed location resulting in an enricher and a stripper section (Mohan and Govind, 1988b).

Porous ceramic membranes offer high molar fluxes compared to those obtained with dense metallic membranes but the permselectivities are often limited to the Knudsen selectivity. The occurrence of surface diffusion as a transport mechanism can improve the selectivity of the membrane (Asaeda and Du, 1986, Uhlhorn et. al., 1989) while maintaining the high molar fluxes. On the other hand the complete selectivity of dense metallic foils is attractive for hydrogen or oxygen permeation provided that their molar fluxes can be improved. To increase the molar fluxes of hydrogen or oxygen through these dense metallic membranes the membrane thickness should be reduced. This however results in membranes vulnerable for damage, which can be avoided if it is possible to locate the separating metallic layer somewhere inside a porous support, realized e.g. by a special vapour deposition technique (Gavalas et. al., 1989).

2. A non-permselective membrane reactor

A completely new application of membrane reactors is studied in this thesis. In the present study the membrane is not used to separate components from eachother but to keep reactants separated and to proceed the reaction in a controlled way. Reactants are fed to different sides of a porous, ceramic membrane and diffuse from either side into the membrane. Therefore no pressure difference over the membrane is used. Inside the membrane a catalyst has been impregnated resulting in a reaction between the reactants inside the membrane. Provided the rate of the reaction is fast compared to the diffusion rates of the reactants, the diffusion is rate limiting resulting in a small reaction zone inside the membrane, for instantaneous, irreversible reactions leading to a reaction plane. Finally the products diffuse out of the membrane. In Figure 1 concentration profiles in the membrane are presented schematically.

Figure 1: Concentration profiles inside the membrane

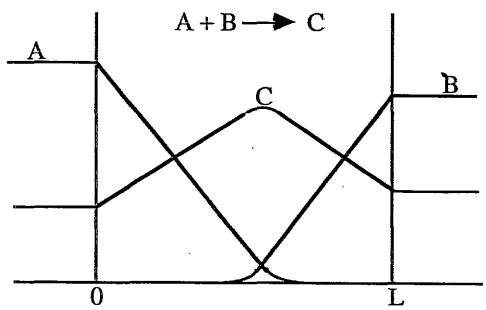

The location of the reaction zone inside the membrane is such that the molar fluxes of the reactants are in stoichiometric ratio. If for some reason the concentration of reactant A in the bulk of the gas increases this will result in an increase of the molar flux of A. This results in an excess

of A at the reaction zone which penetrates further into the membrane so the reaction zone starts shifting towards the side of reactant B. Owing to this shift the distance from the membrane interface to the reaction zone increases for A giving a decrease of the molar flux of A and vice versa for B. The new location of the reaction zone will be such that the molar fluxes of A and B are again in stoichiometric ratio. As a result this membrane reactor operates at stoichiometric molar fluxes of reactants and slip of reactant to the opposite side of the membrane will be prevented by the fast chemical reaction. As the membrane is not used for its separating properties it is attractive to use a rather large pore diameter in order to operate in the continuum regime which gives the highest molar fluxes and therefore the smallest membrane area required.

In the present thesis this new application of the membrane reactor has been studied both theoretically and experimentally using the Claus reaction and the selective catalytic reduction of NO_x by NH_3 (the SCR reaction), presented in equations (1-2), as model reactions.

$$2\,H_2S + SO_2 \longrightarrow \frac{3}{8}S_8 + 2\,H_2O \qquad (1)$$

$$4\,NO + 4\,NH_3 + O_2 \longrightarrow 4\,N_2 + 6\,H_2O \qquad (2)$$

In Chapter 2 a simplified model is presented which describes transport of reactants and products combined with a fast reaction inside the membrane with reactants coming from either side of the membrane. With this model the molar fraction profiles and molar fluxes in and out of the membrane are calculated. In this model the transport of components is described by the combination of viscous flow owing to a pressure difference over the membrane and molecular diffusion described by Fick's law. The reaction is reversible and is assumed to be instantaneous compared to the transport rates of the components. Experimental data using the Claus reaction, presented in equation (1), are also given. This model has been presented at ISCRE 11, Toronto (Sloot et. al., 1990).

In Chapter 3 an experimental study concerning surface diffusion phenomena is presented using steady state diffusion measurements of hydrogen sulfide and sulfur dioxide. Despite the large pore diameter of the membranes of 350 nm, surface diffusion appears to contribute up to 40 % of the total diffusive transport of hydrogen sulfide and sulfur dioxide through the membrane. In the continuum regime the effective diffusion coefficient describing diffusion through the gas phase in the pores of the membrane is inversely proportional to the pressure P. Provided that the fraction of the adsorption sites covered by hydrogen sulfide or sulfur dioxide remains low, the effective surface diffusion coefficient is independent of the pressure P. This difference in pressure dependence has been used to distinguish between both transport mechanisms.

In Chapter 4 an extended, more complete transport model based on the so-called 'Dusty-Gas Model' (Mason and Malinauskas, 1983) is presented in which also surface diffusion has been incorporated. This model is used to verify the simplified transport model presented in Chapter 2. Also some new effects i.e. the development of a pressure profile inside the membrane, owing to the chemical reaction, in the absence of an overall pressure difference over the membrane are

presented. It appears that for the prediction of the development of a maximum or a minimum in the pressure profile inside the membrane it is not sufficient to look only at the stoichiometry of the reaction, i.e. the change in the number of gas molecules by the reaction, but the mobility of the different species owing to the different transport mechanisms must also be taken into account.

In Chapter 5 the membrane reactor is studied experimentally using the Claus reaction as a model reaction. The experimentally determined molar fluxes are compared to the molar fluxes predicted by the transport model described in Chapter 4. It is demonstrated experimentally that the principle of a shifting reaction zone inside the membrane works and that slip of reactant can be prevented by the chemical reaction provided the conditions chosen are not too severe.

In Chapter 6 the applicability of this membrane reactor for de catalytic reduction of nitric oxide with ammonia giving nitrogen and water using alumina membranes impregnated with a vanadium oxide catalyst is studied. It is demonstrated that this membrane reactor is very suitable for this reaction.

References

Armor J.N., 1989, Catalysis with permselective inorganic membranes, Appl. Catal. **49**, 1 - 25

Asaeda A. and L.D. Du, 1986, Separation of alcohol/water gaseous mixtures by thin ceramic membranes, J. Chem. Eng. Jpn. **19**(1), 72 - 77

Champagnie A.M., T.T. Tsotsis and R.G. Minet, 1990, A high temperature catalytic membrane reactor for ethane dehydrogenation, Chem. Eng. Sci. **45**(8), 2423 - 2429

Di Cosimo R., J.D. Burrington and R. K. Graselli, 1986, Oxidative dehydrodimerization of propylene over a Bi_2O_3 - La_2O_3 oxide ion-conductive catalyst, J. Catal. **102**, 234 - 239

Gavalas G.R., C.E. Megiris and S.W. Nam, 1989, Deposition of H_2-permselective SiO_2 films, Chem. Eng. Sci. **44**(9), 1829 - 1835

Gryaznov V.M., V.I. Vedernikov and S.G. Gul'yanova, 1986, Participation of oxygen, having diffused through a silver membrane catalyst, in heterogeneous oxidation processes, Kinet. and Catal. **27**(1), 129 - 133

Gryaznov V.M., 1986, Surface catalytic properties and hydrogen diffusion in palladium alloy membranes, Zeitschr. Phys. Chemie Neue Folge **147**, 123 - 132

Gur'yanova O.S., Yu.M. Serov, S.G. Gul'yanova and V.M. Gryaznov, 1988, Conversion of carbon monoxide on membrane catalysts of palladium alloy. I. Reaction between CO and H_2 on binary palladium alloys with ruthenium and nickel, Kinet. and Catal. **29**(2), 728 - 731

Hsieh H.P., 1988, Inorganic membranes, AIChE Symp. Ser. **261**(84), 1 - 18

Ito N., Y. Shindo, T. Hakuta and H. Yoshitome, 1984, Enhanced catalytic decomposition of HI by using a microporous membrane, Int. J. Hydr. En. **9**(10), 835 - 839

Ito N., Y. Shindo, K. Haraya, K. Obata, T. Hakuta and H. Yoshitome, 1985, Simulation of a reaction accompanied by separation, Int. Chem. Eng. **25**(1), 138 - 142

Kameyama T., M. Dokiya, M. Fujishige, H. Yokokawa and K. Fukuda, 1983, Production of hydrogen from hydrogen sulfide by means of selective diffusion membranes, Int. J. Hydr. En. **8**(1), 5 - 13

Mason E.A. and A.P. Malinauskas, 1983, Gas transport in porous media: The Dusty-Gas Model, Chemical Engineering Monographs 17, Elsevier, Amsterdam

Matson S.L. and J.A. Quinn, 1986, Membrane reactors in bioprocessing, Annals of the New York Academy of Sciences, 152 - 165

Mikhalenko N.N., E.V. Khrapova and V.M. Gryazvov, 1986, Influence of hydrogen on the dehydrogenation of isopropyl alcohol in the presence of a palladium membrane catalyst, Kinet. and Catal. **27**(1), 125 - 128

Mohan K. and R. Govind, 1988a, Analysis of equilibrium shift in isothermal reactors with a permselective wall, AIChE J. **34**(9), 1493 - 1503

Mohan K. and R. Govind, 1988b, Studies on a membrane reactor, Sep. Sci. Tech. **23** (12&13), 1715 - 1733

Nagamoto H. and H. Inoue, 1985, A reactor with catalytic membrane permeated by hydrogen, Chem. Eng. Com. **34**, 315 - 323

Raymont M.E.D., 1975, Make hydrogen from hydrogen sulfide, Hydr. Proc. **54**(7), 139 - 142

Sloot H.J., G.F. Versteeg and W.P.M. van Swaaij, 1990, A non-permselective membrane reactor for chemical processes normally requiring strict stoichiometric feed rates of reactants, Chem. Eng. Sci. **45**(8), 2415 - 2421

Sun Y.M. and S.J. Khang, 1988, Catalytic membrane for simultaneous chemical reaction and separation applied to a dehydrogenation reaction, Ind. Eng. Chem. Res. **27**, 1136 - 1142

Uhlhorn R.J.R., K. Keizer and A.J. Burggraaf, 1989, Gas and surface diffusion in modified γ-alumina systems, J. Membr. Sci. **46**, 225 - 241

Wood B.J., 1968, Dehydrogenation of cyclohexane on a hydrogen-porous membrane, J. Catal. **11**, 30 - 34

Chapter 2

A NON-PERMSELECTIVE MEMBRANE REACTOR FOR CHEMICAL PROCESSES NORMALLY REQUIRING STRICT STOICHIOMETRIC FEED RATES OF REACTANTS

Abstract

A novel type of membrane reactor with feeding of the reactants ifrom opposite sides is presented for chemical processes normally requiring strict stoichiometric feed rates of premixed reactants. The reactants are fed into the reactor at different sides of a porous membrane which is impregnated with a catalyst for a heterogeneously catalyzed reaction. If the reaction rate is fast compared to the diffusion rates of the reactants, a small reaction zone inside the membrane occurs and slip of the reactants to the opposite side of the membrane is prevented. The location of this reaction zone will be such that the molar fluxes of the reactants are always in stoichiometric ratio. The features of this reactor are shown by means of mathematical modelling of molecular diffusion and viscous flow combined with an instantaneous, reversible reaction inside the membrane. As a model reaction the Claus reaction was selected and by conversion measurements the principle of a shifting reaction plane inside a porous membrane is demonstrated.

1. Introduction

Considerable research effort has recently been devoted to membrane reactors. The studies involving membrane reactors presented in literature can be divided in two classes; biological systems and systems where the membrane is used to shift the equilibrium of a reversible reaction (Mohand and Govind, 1988). In the present investigation, a new type of membrane reactor is presented in which the reaction takes place inside the catalytically active membrane and, contrary to usual applications, the permselectivity of the membrane is not important. In Figure 1 a schematic representation of this membrane reactor is given.

Figure 1: Schematic representation of the membrane reactor.

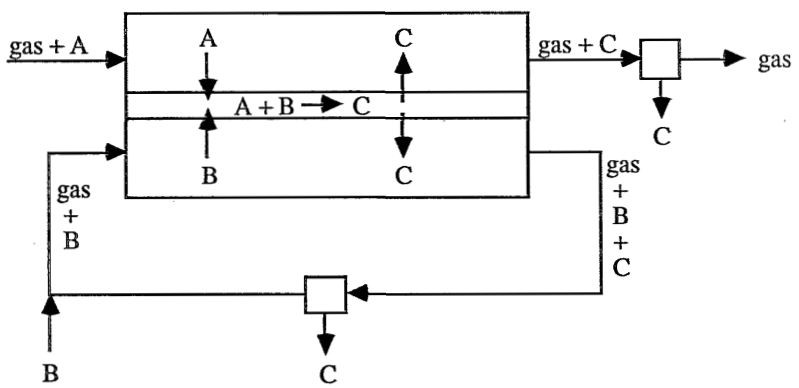

The reactants are fed at different sides of a porous membrane which is impregnated with a catalyst for a heterogeneous chemical reaction. Inside the membrane the reaction takes place. The products diffuse out of the membrane to both sides. If the rate of the reaction is fast compared to the diffusion rates of the reactants in the membrane, a small reaction zone will be present in the membrane, ultimately leading to a reaction plane for instantaneous, irreversible reactions. At this reaction zone or plane the molar fractions of both reactants will be very low. The molar fluxes of the reactants are, in the absence of a pressure difference over the membrane, determined by their concentrations in the bulk of the gas, their diffusion coefficients and the distance to the reaction zone. If for some reason these molar fluxes are temporary not in stoichiometric ratio, there will be an excess of one of the reactants at the reaction zone which will penetrate deeper into the membrane to react with the other reactant. As a result, the location of the reaction zone shifts toward the side of the reactant with the molar flux below stoichiometry. As the distance to the reaction zone decreases for the last mentioned reactant its molar flux increases and the molar flux of the other reactant decreases. Finally, the location of the reaction zone or plane will be such that the molar fluxes of the reactants are always in stoichiometric ratio and slip of the reactants to the opposite side of the membrane is prevented. The membrane reactor operated as described above can therefore be regarded as a very suitable reactor for processes normally requiring strict

stoichiometric feed rates of reactants.

In this work the Claus reaction (Mark H.F. et. al., 1983) has been selected as a model reaction to study the proposed membrane reactor.

$$2\,H_2S + SO_2 \longrightarrow \frac{3}{8}S_8 + 2\,H_2O$$

The membrane used was made of α-Al_2O_3 with a mean porediameter of 350 nm, impregnated with γ-Al_2O_3, the catalyst for the Claus reaction. The Claus reaction however, cannot be regarded as irreversible but is actually an equilibrium reaction instead and therefore the influence of reversibility on the reactor performance has to be determined. Another effect that may have a pronounced effect on the reactor performanee is the occurrence of a pressure difference over the membrane. In order to study both the influence of reversibility and a pressure difference, a mathematical model has been developed which describes the transport and reaction in this membrane reactor. In the model, the transport of reactants and products takes place by simultaneous viscous flow and molecular diffusion while the reaction is assumed to be instantaneous and reversible.

2. Model description

The model developed in the present study is a flux model reflecting the experimental set up used to study the Claus reaction in the membrane reactor which consisted of two well mixed chambers. For simulation of a practical application of the membrane reactor, this flux model has to be incorporated into a reactor model which takes the operation mode (co- or countercurrent) into account.

The instantaneous, reversible reaction can be presented generally by equation (1):

$$\nu_A A + \nu_B B \overset{K_{ev}}{\rightleftharpoons} \nu_C C + \nu_D D \qquad (1)$$

In the mathematical model mass transfer is described into one dimension, the direction perpendicular to the membrane and for steady state conditions. The model has to calculate the molar fractions of the reactants and products, x_A, x_B, x_C, x_D and, if present, of the inert component x_{inert}, and the pressure P as a function of the position in the membrane. As there are six variables to be determined six equations are required to describe mass transfer accompanied by a reversible, instantaneous reaction in the membrane.

The mass balance for component i in the stationary state is given by equation (2); the change of the molar flux of component i with the position in the membrane must be equal to the reaction rate at that position.

$$\frac{dJ_i}{dz} = R_i(z) \tag{2}$$

with $R_i < 0$ for reactants and $R_i > 0$ for products

The mass balances for all components are presented by equations (3-7).

$$\frac{dJ_A}{dz} = R_A \tag{3}$$

$$\frac{dJ_B}{dz} = R_B = \frac{\nu_B}{\nu_A} R_A \tag{4}$$

$$\frac{dJ_C}{dz} = R_C = -\frac{\nu_C}{\nu_A} R_A \tag{5}$$

$$\frac{dJ_D}{dz} = R_D = -\frac{\nu_D}{\nu_A} R_A \tag{6}$$

$$\frac{dJ_{inert}}{dz} = 0 \tag{7}$$

As reaction (1) is regarded as an instantaneous equilibrium reaction compared to mass transfer, R_A is indefinite. Therefore R_A is eliminated by means of adding and subtracting among the equations (3-7) resulting in four independent equations (8-11):

$$\frac{1}{\nu_A}\frac{dJ_A}{dz} - \frac{1}{\nu_B}\frac{dJ_B}{dz} = 0 \tag{8}$$

$$\frac{1}{\nu_A}\frac{dJ_A}{dz} + \frac{1}{\nu_C}\frac{dJ_C}{dz} = 0 \tag{9}$$

$$\frac{1}{\nu_A}\frac{dJ_A}{dz} + \frac{1}{\nu_D}\frac{dJ_D}{dz} = 0 \tag{10}$$

$$\frac{dJ_{inert}}{dz} = 0 \tag{11}$$

In order to solve this set of equations uniquely two additional relations are required. The equilibrium condition is the fifth equation and is assumed to be valid through the entire membrane:

$$K_{ev} = \frac{x_C^{\nu_C} x_D^{\nu_D}}{x_A^{\nu_A} x_B^{\nu_B}} P^{-\nu_A-\nu_B+\nu_C+\nu_D} \tag{12}$$

The sum of the molar fractions must be equal to one which is the sixth and final equation:

$$\sum_{i=1}^{i=nc} x_i = 1 \tag{13}$$

Before the set of equations (8-13) can be solved, the molar flux of each component has to be specified. In the present study it is assumed that there are two mechanisms of transport, viscous flow and molecular diffusion according to Fick's law. These mechanisms are additive owing to the fact that they are independent.

$$J_i = x_i J_{visc} + J_{i,dif} \tag{14}$$

$$\text{with } J_{visc} = -\frac{1}{RT}\left(D_{inert,K} + \frac{B_o P}{\eta}\right)\frac{dP}{dz} \tag{15}$$

$$\text{and } J_{i,dif} = -D_{i,eff}\frac{1}{RT}\frac{d(x_i P)}{dz} \tag{16}$$

The occurrence of the pressure in the driving force in equation (16) is necessary to take pressure diffusion into account (Mason and Malinauskas, 1983). Pressure diffusion is a diffusive transport mechanism, with a pressure gradient as a driving force, which has separating properties, this in contrast to viscous flow. The viscous flow is represented by the equation for the flow of a compressible fluid through a porous medium. The parameter B_o is a membrane specific parameter defined according to equation (17).

$$B_o = \frac{\varepsilon}{\tau}\frac{d_p^2}{32} \tag{17}$$

with ε the porosity, τ the tortuosity and d_p the mean pore diameter of the membrane

The effective diffusion coefficients $D_{i,eff}$ in the membrane are calculated according to resistances in series as given by equation (18).

$$D_{i,eff} = \frac{1}{\frac{1}{\frac{\varepsilon}{\tau} D^{o}_{i,K}} + \frac{1}{\frac{\varepsilon}{\tau} D^{o}_{i,inert}}} \tag{18}$$

The gaseous diffusion coefficients $D^{o}_{i,K}$ and $D^{o}_{i,inert}$ are estimated from gas kinetic theory (Reid et. al., 1977).

To solve the set of equations (8-18), twelve boundary conditions are required. At the membrane interfaces the equilibrium condition must be fulfilled (see equation (12)). Also the sum of the molar fractions must be equal to one at the interfaces (see equation (13)). The pressure at the membrane interfaces must be the same as the pressure in the bulk of the gas at that side of the membrane. The additional six boundary conditions required are obtained from mass balances coupling the molar fluxes from the bulk of the gas to the membrane interface, $J_{i,\,b\text{-}i}$, with the molar fluxes at the interface, $J_{i,\,int}$. Owing to the fact that the reaction is assumed to be instantaneous the molar fluxes from the bulk of the gas to the membrane interface, $J_{i,\,b\text{-}i}$, and the molar fluxes inside the membrane at the interface, $J_{i,\,int}$, do not have to be equal to one another but are coupled by the stoichiometry of the reaction (see equations (19a-19d)).

$$\frac{1}{\nu_B}\left(J_{B,b\text{-}i} - J_{B,\,int}\right) - \frac{1}{\nu_A}\left(J_{A,b\text{-}i} - J_{A,\,int}\right) = 0 \tag{19a}$$

$$\frac{1}{\nu_C}\left(J_{C,b\text{-}i} - J_{C,\,int}\right) + \frac{1}{\nu_A}\left(J_{A,b\text{-}i} - J_{A,\,int}\right) = 0 \tag{19b}$$

$$\frac{1}{\nu_D}\left(J_{D,b\text{-}i} - J_{D,\,int}\right) + \frac{1}{\nu_A}\left(J_{A,b\text{-}i} - J_{A,\,int}\right) = 0 \tag{19c}$$

$$J_{inert,\,b\text{-}i} = J_{inert,\,int} \tag{19d}$$

both at z=0 and z=L

There are eight mass balances at the membrane interfaces, however only six boundary conditions are required and therefore two mass balances must be left out. Equations (19d) are dropped as boundary conditions, however they will be necessary later on.

The molar fluxes inside the membrane at the interface $J_{i,\,int}$ in equations (19) are calculated by equations (14-16). The molar flux of component i from the bulk of the gas to the membrane interface $J_{i,\,b\text{-}i}$ consists of a viscous part and a diffusive part, see equation (20).

$$J_{i,\,b\text{-}i} = x_{i,\,b}\, J_{visc} - D^{o}_{i,\,inert} \frac{P_{bulk}}{RT} \frac{dx_i}{dz}\Big/_{b\text{-}i} \tag{20}$$

In equation (20) b-i stands for $z = -\delta$ or $z = L + \delta$ for the two interfaces of the gas bulk with the gas film. The viscous molar flux in equation (20) J_{visc} is the same flux as inside the membrane and is given by equation (15) and is almost the same as the molar flux of inert. In fact equations (19d) that had to be dropped previously are used at this point. The derivative of the molar fraction at the interface of the gas bulk with the gas film in which the mass transfer resistance in the gas phase is situated, $(dx_i/dz)_{b-i}$ is however still unknown. This variable is determined by integration of the steady state mass balance of component i in the gas film given in equation (21).

$$\frac{D_i^o P}{RT}\frac{d^2 x_i}{dz^2} - J_{visc}\frac{dx_i}{dz} = 0 \qquad (21)$$

for $-\delta < z < 0$ and for $L < z < L + \delta$

The molar fractions x_i in the gas bulk, $x_{i,bulk}$, and at the membrane interface, $x_{i,int}$ where int stands for $z = 0$ or $z = L$, are used as boundary conditions to solve equation (21). The derivative of the molar fraction at the interface of the gas bulk with the gas film $(dx_i/dz)_{b-i}$, required in equation (20), is represented by equation (22).

$$\left.\frac{dx_i}{dz}\right|_{b-i} = (x_{i,int} - x_{i,bulk}) * \frac{J_{visc}}{\mathbb{D}_i^o} * \frac{RT}{P_{bulk}} * \frac{1}{\exp\left(\frac{J_{visc}}{\mathbb{D}_i^o}\frac{RT\,\delta}{P_{bulk}}\right) - 1} \qquad (22)$$

with δ the thickness of the stagnant gas film

At x=0, the membrane interface at the side where A is fed to the reactor, and at x=L, the membrane interface at the B side, equations (19) are applied. Boundary conditions at both sides of the membrane required to solve the set of equations are the molar fractions of all components and the pressure in the bulk of the gas at both sides.

The mass transfer model consisting of this set of equations can only be solved numerically. The method used is a relaxation technique (Press et. al., 1986). In the relaxation method the set of N coupled differential equations is replaced by a set of N finite difference equations on a grid consisting of M mesh points. The discretization scheme is given in equations (23).

$$\frac{dx_i}{dz} = \frac{x_{i,k+1} - x_{i,k-1}}{2h} \qquad (23a)$$

$$\frac{d^2 x_i}{dz^2} = \frac{x_{i,k+1} - 2x_{i,k} + x_{i,k-1}}{h^2} \qquad (23b)$$

The first and second derivative of the pressure to the location in the membrane are also discretisized according to equations (23). A solution of the set of equations to be solved consists of values for the N dependent variables at each of the M meshpoints, therefore a total number of N*M variables. The method produces a matrix equation of size N*M as presented in equation (24).

$$\begin{bmatrix} \frac{\partial E_{1,k=1}}{\partial v_{1,k=1}} & \cdots & \frac{\partial E_{1,k=1}}{\partial v_{N,k=M}} \\ \vdots & & \vdots \\ \frac{\partial E_{N,k=M}}{\partial v_{1,k=1}} & \cdots & \frac{\partial E_{N,k=M}}{\partial v_{N,k=M}} \end{bmatrix} * \begin{bmatrix} d v_{1,k=1} \\ \vdots \\ d v_{N,k=1} \\ d v_{1,k=2} \\ \vdots \\ d v_{N,k=M} \end{bmatrix} = \begin{bmatrix} d E_{1,k=1} \\ \vdots \\ d E_{N,k=1} \\ d E_{1,k=2} \\ \vdots \\ d E_{N,k=M} \end{bmatrix} \qquad (24)$$

with E_{ij} the deviation of equation number i on grid point number j

$d v_{ij} = v_{ij,old} - v_{ij,new}$ where v_{ij} is the present value of variable v_i at k=j

$d E_{ij} = E_{ij,old} - E_{ij,new} = E_{ij,old}$

Owing to the fact that the discretization of the derivatives of a variable $v_{i,k}$ only involves its values at the gridpoints k-1, k and k+1 the matrix with the partial derivatives consists of 3 grid points times 6 equations on each grid point so 18 diagonals in all. Solving equation (24) by inverting the matrix with partial derivatives gives new values of all variables simultaneously. By continuously improving the initial guessed solution the method is said to relax to the true solution (Press et. al., 1986).

3. Numerical results

Two sets of simulations were performed in order to study the influence of reversibility and of a pressure difference over the membrane. As base case, a simulation at a temperature of 473 K in the absence of a pressure difference over the membrane was carried out. Owing to the fact that one of the products of the Claus reaction, elemental sulfur, has a melting point of about 392 K, a temperature of at least 470 K is required in order to be able to remove this product out of the membrane by diffusion through the gas phase. Parameters used in the simulation of the base case are given in Table 1, the molar fluxes calculated in Table 2.

Table 1: Parameters used in Figures 2, 3 and 4.

bulk conditions

	H_2S side	SO_2 side
x_{H_2S}	$1 * 10^{-2}$	$1 * 10^{-10}$
x_{SO_2}	$1 * 10^{-10}$	$1 * 10^{-2}$
x_{S_8}	$1 * 10^{-5}$	$1 * 10^{-5}$
x_{H_2O}	$1 * 10^{-2}$	$1 * 10^{-2}$
P (bara)	1.0 (Fig. 2 and 3)	1.0
	1.5 (Fig. 4)	

hydrodynamic parameter

$$k_g = \frac{\mathbb{D}^o_{i,\,inert}}{\delta} = 1 * 10^{-2}\ m/s$$

membrane parameters

$B_o = 3 * 10^{-15}\ m^2$ ($d_p \approx 1\ \mu m$)

$\frac{\varepsilon}{\tau} = 0.10$

membrane thickness 3 mm

Equilibrium constant (Gamson and Elkins, 1953)

$$K_{ev} = \frac{x_{S_8}^{3/8}\, x_{H_2O}^{2}}{x_{H_2S}^{2}\, x_{SO_2}}$$

$$= 0.924 * 10^{-6} * \exp\left(1.274 * 10^{4} / T\right) * P^{5/8}$$

with P in bar

Table 2: Molar fluxes calculated for Figures 2 and 3.

	T = 473 K		T = 573 K	
	H_2S side	SO_2 side	H_2S side	SO_2 side
J_{H_2S}	$5.68*10^{-4}$	$4.38*10^{-6}$	$5.70*10^{-4}$	$4.31*10^{-5}$
J_{SO_2}	$-8.61*10^{-8}$	$-2.82*10^{-4}$	$-1.15*10^{-5}$	$-2.75*10^{-4}$
J_{S_8}	$-6.68*10^{-5}$	$3.89*10^{-5}$	$-6.68*10^{-5}$	$3.20*10^{-5}$
J_{H_2O}	$-3.44*10^{-4}$	$2.20*10^{-4}$	$-3.33*10^{-4}$	$1.94*10^{-4}$
J_{inert}	$1.99*10^{-5}$	$1.99*10^{-5}$	$2.86*10^{-5}$	$2.86*10^{-5}$

In Figure 2 the calculated molar fraction profiles of this simulation are presented.

Figure 2: Molar fraction profiles at 473 K in absence of a pressure difference over the membrane

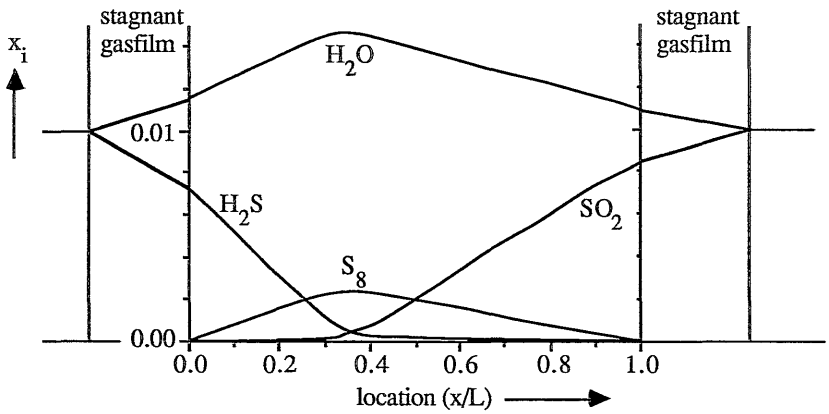

In Figure 2 it can be seen that there is a considerable decrease of the molar fraction of H_2S and SO_2 from the bulk of the gas to the membrane interface and therefore mass transfer resistances in the gas phase are significant and cannot be neglected. As the reaction zone is very small in Figure 2, the Claus reaction can be considered as almost irreversible at these conditions. From Table 2 it can be calculated that the slip of the reactants to the opposing side is less than 1% of the molar flux of the reactants into the membrane.

The influence of reversibility was investigated by means of a simulation, carried out at a temperature of 573 K also in the absence of a pressure difference over the membrane. Parameters used in this simulation are similar to the base case and are given in Table 1. The calculated molar fraction profiles are presented in Figure 3.

Figure 3: Molar fraction profiles at 573 K in absence of a pressure difference over the membrane

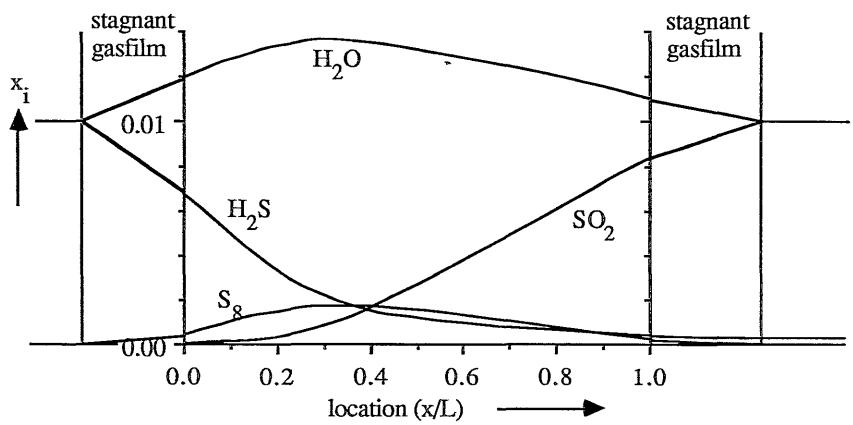

Molar fluxes calculated are given in Table 2. In Figure 3 it can be seen that at 573 K a broad reaction zone exists compared to the situation at 473 K owing to the fact that the value of the equilibrium constant of the Claus reaction is much lower and therefore reversibility becomes more important. The effect of reversibility is also reflected by the slip of H_2S which is 8% of the H_2S molar flux into the membrane as can be calculated from Table 2, compared to less than 1% in the simulation at 473 K. Drawing the tangents of the molar fraction profiles of H_2S and SO_2 at the membrane interfaces at the H_2S and SO_2 side respectively, it appears that the decrease of the gradients of the molar fraction profiles, and therefore the reduction of the molar fluxes, by the reversibility of the reaction is only moderate. So despite the fact that reversibility affects the molar fraction profiles and the slip of reactant substantially, the molar fluxes of the reactants into the membrane are hardly influenced.

In order to study the influence of a pressure difference over the membrane a simulation was carried out at a temperature of 473 K and a pressure difference over the membrane of 0.5 bar with the highest pressure at the H_2S side. The molar fraction profiles are presented in Figure 4.

Figure 4: Molar fraction profiles at 473 K in the presence of a pressure difference of 0.5 bar

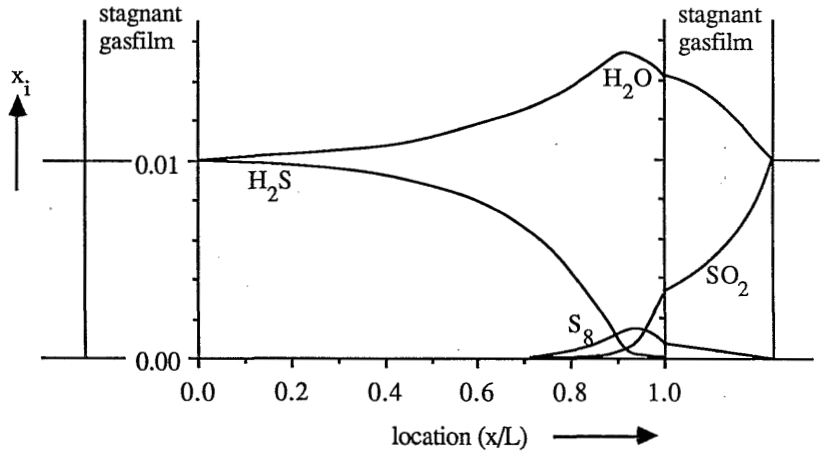

Parameters used are the same as in the base case, and are given in Table 1. In Figure 4 it can be seen that owing to the pressure difference over the membrane, the reaction zone is shifted towards the low pressure side, the profiles become curved and the molar fraction of the low pressure side reactant SO_2 at the membrane interface drops compared to the situation without pressure difference. The curvature of the molar fraction profiles can be attributed to the fact that two transport mechanisms occur, viscous flow and molecular diffusion. As all H_2S reacts at the reaction zone, the total H_2S molar flux left of the reaction zone is constant. The H_2S flux consists of a viscous contribution and a diffusive contribution, which have a linear dependence on the molar fraction of H_2S and on the molar fraction gradient of H_2S respectively. As the molar fraction of H_2S decreases from the interface to the reaction zone, the viscous contribution decreases. To

maintain a constant total molar flux of H_2S, the diffusive contribution must increase, resulting in an increase of the absolute value of the molar fraction gradient of H_2S leading to curved profiles. Owing to the fact that, when a pressure difference is applied, the presence of a viscous flow through the membrane from the H_2S side to the SO_2 side facilitates H_2S transport and reduces SO_2 transport, resulting in a decrease of the interface molar fraction of SO_2, the reaction zone is shifted toward the low pressure side in order to maintain stoichiometry between the H_2S and SO_2 molar fluxes. From these calculations, with parameters as given in Table 1, it can be concluded that despite the pressure difference of 0.5 bar over the membrane with a mean pore diameter of 1 μm, the reaction zone remains in the membrane and therefore the performance of the membrane reactor is not affected.

The quantitative effect of a pressure difference over the membrane on the molar fluxes was also investigated and therefore simulations were carried out at a temperature of 473 K for various pressure differences. In Figure 5 the molar flux of H_2S into the membrane at 473 K is presented as a function of the pressure difference over the membrane.

Figure 5: Molar flux of H_2S into the membrane as a function of the pressure difference

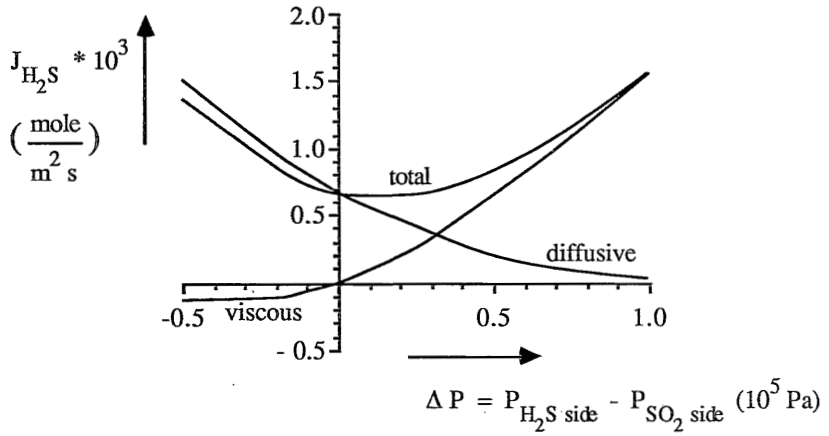

Parameters used are given in Table 1. In this figure besides the total molar flux of H_2S into the membrane also its different contributions, viscous and diffusive, are given. Figure 5 shows a minimum for the total molar flux of H_2S into the membrane. The occurrence of this minimum can be understood if the following assymptotic situations are considered. In case of a much higher pressure on the H_2S side, the H_2S molar flux is mainly determined by viscous flow resulting in a high transport rate of H_2S. As long as the pressure difference is not that high that complete mass transfer limitation of SO_2 from the bulk of the gas to the membrane interface occurs, the H_2S and SO_2 molar fluxes will be in stoichiometric ratio and therefore the transport rate of SO_2 is also high. For the same reason the transport rates of H_2S and SO_2 will be high in case of the highest pressure on the SO_2 side and a minimum will exist at a moderate pressure difference over the membrane.

It seems attractive to use a fixed pressure difference over the membrane as the molar fluxes increase substantially, as can be seen in Figure 5, resulting in smaller membrane area required. A problem in this case is however the transport of inert gas through the membrane which results in the necessity of a bleed stream which will be contaminated with one of the reactants. Therefore it is questionable to conclude that a pressure difference over the membrane in order to reduce the membrane area required would be attractive.

In Figure 6 the molar flux of elemental sulfur out of the membrane at the H_2S side membrane interface is presented as a function of the pressure difference over the membrane.

Figure 6: Molar flux of S_8 out of the membrane at the H_2S side as a function of the pressure difference over the membrane

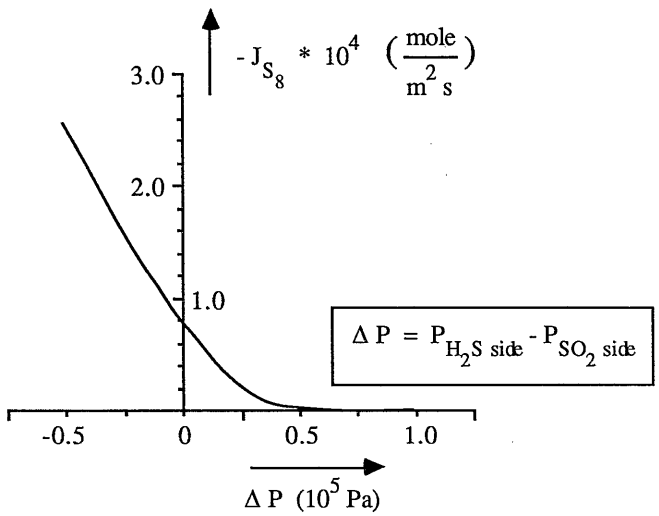

Although it is possible to transport the elemental sulfur preferentially to one side of the membrane, the pressure difference required is quite high, which may result in large amounts of inerts transported through the membrane with the problem described above.

4. Experimental verification

Conversions of H_2S and SO_2 have been measured at a temperature of 549 K and a pressure of 1.5 bar in absence of a pressure difference over the membrane. The membrane used was obtained from the Netherlands Energy Research Foundation ECN and was made of α-Al_2O_3 with a mean pore diameter of 350 nm, a porosity of 41 % and a thickness of 4.5 mm, impregnated with γ-Al_2O_3. By varying the ratio of the flow of H_2S/N_2 and SO_2/N_2 into the compartments of the membrane reactor, the ratio of the bulk concentrations of H_2S and SO_2 was varied. According to the principle of this reactor, this should result in a shift of the reaction plane in the membrane as the

ratio between the driving forces for diffusion of the reactants is varied.

Although the Claus reaction generally cannot be considered irreversible at 549 K, the molar fluxes calculated using this assumption do not deviate substantially from the results taking reversibility into account as was shown by the numerical work studying the influence of reversibility. From the calculations it was also shown that very small pressure differences over the membrane that may occur in the experiments (less than 10 mm H_2O in practice) can be neglected completely. Therefore for the interpretation of this particular system an instantaneous, irreversible reaction in the absence of a pressure difference over the membrane can be assumed, for which the molar flux of H_2S is predicted by equation (25).

$$J_{H_2S} = \frac{2\, D_{SO_2\,eff}\, c_{SO_2} + D_{H_2S\,eff}\, c_{H_2S}}{L + \frac{D_{H_2S\,eff}}{D_{H_2S}}\,\delta_1 + \frac{D_{SO_2\,eff}}{D_{SO_2}}\,\delta_2} \qquad (25)$$

with δ_1 and δ_2 the thickness of the stagnant gas film at the membrane interfaces

and c_{H_2S} and c_{SO_2} the concentrations in the bulk of the gas

Because the aim of the present experimental investigation is to demonstrate the operation principle of this membrane reactor and not to obtain exact values of the effective diffusion coefficients, mass transfer resistances in the gas phase, represented in equation (25) by the denominator, were neglected for convenience of interpretation although their total contribution is estimated to be between 25 and 30% of the total resistance. The denominator in equation (25) is therefore set equal to L and dividing by the bulk concentration of H_2S then results in equation (26).

$$\frac{J_{H_2S}}{c_{H_2S}} = \frac{D_{H_2S\,eff}}{L} + \frac{2\, D_{SO_2\,eff}}{L} * \frac{c_{SO_2}}{c_{H_2S}} \qquad (26)$$

When the molar flux of H_2S, divided by the bulk concentration of H_2S, is plotted as a function of the ratio of the bulk concentrations of SO_2 and H_2S, a straight line should result. From the slope and the intercept of this line the effective diffusion coefficients of SO_2 and H_2S can be calculated respectively.

In Figure 7 the molar flux of H_2S divided by the bulk concentration of H_2S is plotted as a function of the ratio of the bulk concentrations of SO_2 and H_2S. To check the results obtained, the molar flux of H_2S divided by the bulk concentration of SO_2 is plotted as a function of the ratio of the bulk concentrations of H_2S and SO_2. The agreement between the effective diffusion coefficients obtained from these two methods of plotting is within 4%.

Figure 7: Conversion measurements at 549 K

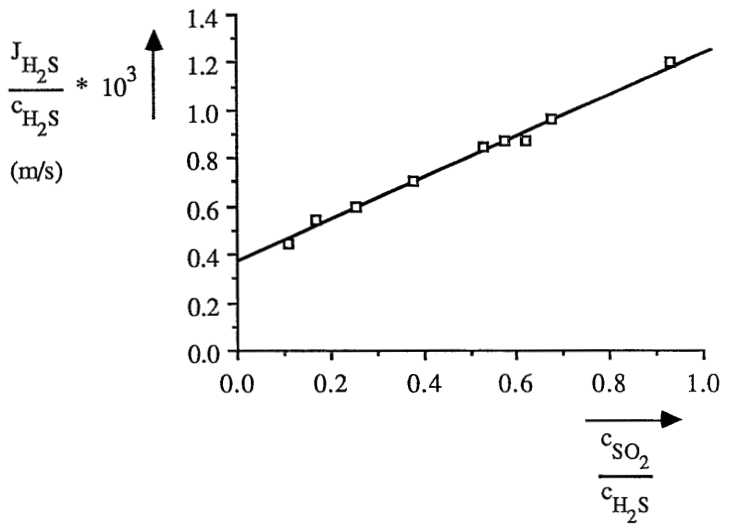

The values of the effective diffusion coefficients obtained are:

$$D_{H_2S\ eff} = 1.77 * 10^{-6}\ m^2/s$$

$$D_{SO_2\ eff} = 2.13 * 10^{-6}\ m^2/s$$

From the straight lines obtained combined with reasonable values for the effective diffusion coefficients for H_2S and SO_2 it is concluded that the reaction plane shifts through the membrane depending on the driving forces for diffusion of H_2S and SO_2 as foreseen by the theory.

5. Conclusions

A new type of membrane reactor with feeding of reactants from opposite sides is presented for processes normally requiring strict stoichiometric feed rates of premixed reactants. The features of this membrane reactor are shown by means of mathematical modelling of molecular diffusion and viscous flow of gases in the membrane, combined with an instantaneous, reversible reaction inside the membrane. It is concluded that mass transfer resistances in the gas phase may be important especially when a pressure difference over the membrane is present. It is demonstrated that a moderate pressure difference over the membrane does not affect the fundamental operation of this reactor.

As a model reaction the Claus reaction was selected and by conversion measurements the principle of a reaction plane inside the membrane, shifting as a function of the driving forces of the reactants, is demonstrated.

Notation

B_o	membrane specific parameter	(m^2)
c	concentration	(mole / m^3)
D_i	diffusion coefficient of component i	(m^2 / s)
$D_{i,K}$	Knudsen diffusion coefficient	(m^2 / s)
d_p	mean pore diameter	(m)
E_{ij}	equation number i on grid point number j	
h	distance between two grid points	(m)
J_i	molar flux of component i	(mole / m^2 s)
K_{ev}	equilibrium constant	
k_g	mass transfer parameter in the gas phase (D_i / δ)	(m / s)
L	membrane thickness	(m)
nc	number of components	(-)
P	pressure	(Pa)
R	gas constant	(J / mole K)
R_i	reaction rate of component i	(mole / m^3 s)
T	temperature	(K)
v_i	variable number i	
x_i	molar fraction of component i	(-)
z	coordinate perpendicular to the membrane	(m)
δ	thickness of the stagnant gas film	(m)
ε	porosity of the membrane	(-)
η	viscosity of the gas	(Pa s)
υ	stoichiometric coefficient	(-)
τ	tortuosity of the membrane	(-)

indices

A	component
B	component
bulk	bulk of the gas
C	component
D	component
dif	diffusive
eff	effective
int	membrane interface
k	number of grid point
visc	viscous

References

Gamson B.W. and R.H. Elkins, 1953, Sulfur from hydrogensulfide, Chem. Eng. Progr., **49**(4), 203-215.

Mark H.F., D.F. Othmer, C.G. Overberger and G.T. Seaborg, 1983, Kirk-Othmer, Encyclopedia of chemical technology, vol. 22, 276-282, John Wiley & Son, New York

Mason E.A. and A.P. Malinauskas, 1983, Gas Transport in Porous Media: The Dusty-Gas Model, Chemical Engineering Monographs 17, pp 42-46 and 96-97, Elsevier, Amsterdam.

Mohan K. and R. Govind, 1988, Analysis of equilibrium shift in isothermal reactors with a permselective wall, AIChE J., **34**(9), 1493-1503.

Press W.H., B.P. Flannery, S.A. Teukolsky and W.T. Vetterling, 1986, Numerical Recipes: the art of scientific computing, pp 578-614, Cambridge University Press, Cambridge.

Reid R.C., J.M. Prausnitz and T.K. Sherwood, 1977, The properties of gases and liquids, 3rd edition, McGraw-Hill, New York.

Chapter 3

SURFACE DIFFUSION OF HYDROGEN SULFIDE AND SULFUR DIOXIDE IN ALUMINA MEMBRANES IN THE CONTINUUM REGIME

Abstract

Surface diffusion of H_2S and SO_2 in alumina membranes with an average pore diameter of about 350 nm, impregnated with γ-Al_2O_3, is studied as a function of pressure at temperatures between 446 and 557 K. Diffusion through the gas phase in the pores of the membrane almost entirely takes place in the continuum regime. The pressure dependence of transport by diffusion through the gas phase and by surface diffusion is different, a fact which is used for the interpretation of the steady state diffusion measurements. It is observed that the contribution of surface diffusion to the total diffusion through the membrane can be as high as about 40%. The surface diffusion data obtained are interpreted by a theoretical surface diffusion model using two parameters to be fitted, the product of the effective surface diffusion coefficient, the concentration of the adsorption sites and the adsorption parameter as well as the adsorption parameter itself. The parameters fitted for SO_2 show a remarkable change between 498 and 525 K which probably may be attributed to a change in the adsorbed species also reported in literature. The parameters fitted for H_2S at different temperatures show a maximum, however, the product of the effective surface diffusion coefficient and the concentration of the adsorption sites increases with temperature.

1. Introduction

A novel type of membrane reactor has been developed in which the membrane is not used to separate components but to keep reactants separated from eachother (Sloot et. al., 1990). The reactants are fed to opposite sides of a porous membrane and diffuse into the membrane from either side. Therefore in principle no pressure difference is applied over the membrane contrary to the usual application of membranes. The membrane contains a catalyst, or is catalytically active by itself, for a heterogeneously catalyzed chemical reaction between the reactants. Provided that the rate of the reaction is fast compared to the diffusion rates of the reactants the process will be diffusion limited. A reaction zone which is small compared to the membrane thickness will occur inside the membrane leading to a reaction plane in case of an instantaneous irreversible reaction. The location of the reaction zone inside the membrane will be such that the molar fluxes of the reactants are in stoichiometric ratio. If the concentration of one of the reactants for some reason changes this will automatically result in a shift of the location of the reaction zone until the molar fluxes of both reactants are in stoichiometric ratio again. Finally the products will diffuse out of the membrane to both sides.

As a model reaction the Claus reaction (Mark et. al., 1983) is used to study this membrane reactor.

$$2\,H_2S + SO_2 \rightleftharpoons \frac{3}{8}\,S_8 + 2\,H_2O \qquad (1)$$

The membrane used is made of α-Al_2O_3 with a mean pore diameter of about 350 nm impregnated with γ-Al_2O_3, a well known catalyst for the Claus reaction.

The molar fluxes of the reactants into the membrane can be calculated assuming an instantaneous irreversible reaction inside the membrane and neglecting mass transfer resistances in the gas phase outside the membrane. The transport is based on the combination of Knudsen and continuum diffusion through the gas phase in the pores of the membrane. The calculation of the molar fluxes requires knowledge of the mean pore diameter and the porosity-tortuosity factor of the membrane. As a result of the assumptions the molar fluxes calculated are the highest possible provided that diffusion through the gas phase in the pores of the membrane is the only transport mechanism. Conversion measurements at a temperature of 549 K in the absence of a pressure difference over the membrane, however, resulted in effective diffusion coefficients of H_2S and SO_2 that seemed to be high compared to the continuum diffusion coefficients calculated from gas kinetic theory (Sloot et. al., 1990). Possibly an additional transport mechanism takes place probably being surface diffusion. In order to verify the occurrence of surface diffusion of H_2S and SO_2 in the membrane steady state diffusion measurements, in the absence of a pressure difference over the membrane, were carried out that are discussed in the present study.

2. Theory

Transport owing to the combination of diffusion through the gas phase in the pores of the membrane and surface diffusion is studied in the steady state using ceramic membranes with a flat sheet geometry. The total transport in the absence of a pressure difference over the membrane of component i owing to the combination of diffusion through the gas phase in the pores of the membrane and surface diffusion is described by equation (2) assuming cylindrically shaped pores.

$$J_{i,\,tot} = J_{i,\,gas} + \frac{4}{d_p} J_{i,\,surf} \tag{2}$$

The geometric factor $4/d_p$ in equation (2) arises from the fact that transport owing to diffusion through the gas phase in the pores is proportional to the cross area of the pores, therefore proportional to d_p^2, whereas transport owing to surface diffusion is proportional to the circumference of the pores, therefore proportional to d_p. The molar flux of component i through the gas phase in the pores of the membrane is described by Fick's law (equation (3)) using the Bosanquet formula for the combination of Knudsen and continuum diffusion by the principle of resistances in series.

$$J_{i,\,gas} = - D^{eff}_{i,\,gas} \frac{P}{RT} \frac{dx_i}{dz} \tag{3}$$

$$\text{with} \quad \frac{1}{D^{eff}_{i,\,gas}} = \frac{1}{\frac{\varepsilon}{\tau} D^{o}_{i,\,K}} + \frac{1}{\frac{\varepsilon}{\tau} D^{o}_{i,\,inert}}$$

The Knudsen and continuum diffusion coefficients $D^o_{i,K}$ and $D^o_{i,\,inert}$ are calculated from the gas kinetic theory (Reid et. al., 1977). The porosity-tortuosity factor ε/τ of the membrane is determined by permeation measurements with a pure gas.

Surface diffusion is also described by Fick's law as presented by equation (4).

$$J_{i,\,surf} = - D^{eff}_{i,\,surf} c_S \frac{d\theta_i}{dz} \tag{4}$$

In equation (4) c_S is the total concentration of adsorption sites on the surface (mole/m^2) and θ_i the fraction of the adsorption sites occupied by component i. Assuming that the adsorption and desorption kinetics are fast compared to the transport rates of component i through the pore and assuming a Langmuir adsorption isotherm, θ_i can be calculated by equation (5) in which b_i is the adsorption parameter.

$$\theta_i = \frac{b_i P x_i}{1 + b_i P x_i} \tag{5}$$

Substitution of equation (5) in equation (4) yields the expression for the molar flux owing to surface diffusion as a function of the driving force in the gas phase in the pores presented in equation (6).

$$J_{i,\,surf} = - D^{eff}_{i,\,surf} c_S \frac{b_i P}{(1 + b_i P x_i)^2} \frac{d x_i}{d z} \tag{6}$$

From literature (Smith and Metzner, 1964, Gilliland et. al., 1974) it is known that the adsorption parameter b_i as well as the surface diffusion coefficient $D_{i,\,surf}$ depends on the fraction of the adsorption sites occupied by component i, θ_i, owing to the fact that there usually is a distribution function of the heat of adsorption instead of a single value. As the adsorption sites with a high heat of adsorption are occupied preferentially, an increase of θ_i results in a decrease of the average heat of adsorption of the remaining not-occupied adsorption sites. This results in a decrease of the adsorption parameter b_i for these sites but at the same time in an increase of the mobility represented by $D_{i,\,surf}$ for these sites. Therefore the product of $b_i D_{i,\,surf}$ is rexpected to be relatively independent of the fraction of the adsorption sites occupied by component i, θ_i.

Substitution of equations (3) and (6) in equation (2) results in the final expression for combined diffusion.

$$J_{i,\,tot} = - \left(D^{eff}_{i,\,gas} \frac{P}{RT} + \frac{4}{d_p} D^{eff}_{i,\,surf} b_i c_S \frac{P}{(1 + b_i P x_i)^2} \right) \frac{d x_i}{d z} \tag{7}$$

Integration of equation (7) results in equation (8) which can be used for the interpretation of experimental data.

$$\frac{J_{i,\,tot} L}{x_{i,\,int\,0} - x_{i,\,int\,L}} = D^{eff}_{i,\,gas} \frac{P}{RT} + \frac{4}{d_p} D^{eff}_{i,\,surf} b_i c_S \frac{P}{(1 + b_i P x_{i,\,int\,0})(1 + b_i P x_{i,\,int\,L})} \tag{8}$$

In equation (8) $x_{i,\,int\,0}$ and $x_{i,\,int\,L}$ represent the molar fractions of component i at the membrane interface at z=0 and z=L respectively. Mass transfer resistances in the gas phase outside the membrane, coupling the molar fractions at the membrane interfaces to the molar fractions in the bulk of the gas, are taken into account by equations (9).

$$J_{i,\,tot} = k_g \frac{P}{RT} \left(x_{i,\,bulk\,o} - x_{i,\,int\,0} \right) \tag{9a}$$

$$J_{i,\,tot} = k_g \frac{P}{RT} \left(x_{i,\,int\,L} - x_{i,\,bulk\,L} \right) \tag{9b}$$

If the pore diameter of the membrane is sufficiently large and the pressure is sufficiently high, diffusion through the gas phase is taking place in the continuum regime. The effective diffusion coefficient $D_{i,\,gas,\,eff}$ is therefore equal to the effective continuum diffusion coefficient which is inversely proportional to the pressure and so the first term in the right hand side of equation (8) is independent of pressure. The second term in the right hand side of equation (8), representing transport owing to surface diffusion, however, is linearly dependent on the pressure, provided that the fraction of the adsorption sites covered by component i is relatively low. This difference in pressure dependence can be used to discriminate between both transport mechanisms.

Rearrangement of equation (8) results in equation (10).

$$\frac{J_{i,\,tot}\,L}{x_{i,\,int\,0} - x_{i,\,int\,L}} - D_{i,\,gas}^{eff} \frac{P}{RT} = \frac{\frac{4}{d_p} D_{i,\,surf}^{eff}\, b_i\, c_S}{(1 + b_i\, P\, x_{i,\,int\,0})\,(1 + b_i\, P\, x_{i,\,int\,L})} * P \tag{10}$$

The left hand side of equation (10) is plotted as a function of pressure. This should result in a straight line through the origin, the slope being equal to $(4/d_p)\, D_{i,\,surf}\, b_i\, c_S$ provided that the fraction of the adsorption sites covered by component i is relatively low. If the product in the denominator of equation (10), $(1 + b_i P x_{i,\,int\,0})\,(1 + b_i P x_{i,\,int\,L})$, is not close to unity this will result in a downward deviation of the straight surface diffusion line at higher pressures.

In porous media usually a distribution function of the pore diameter of the membrane is present. It has to be determined whether this distribution has an influence on the overall molar fluxes that will be determined by experiments. According to literature (Cui et. al., 1990) the standard Johnson and Steward effective diffusion coefficient from steady state diffusion measurements must be calculated from equation (11).

$$\bar{D}_i^{eff} = \int_{d_p=0}^{d_p=\infty} D_i^{eff}(d_p) \frac{d\, f(d_p)}{d\, d_p}\, d\, d_p \tag{11}$$

In equation (11) $f(d_p)$ represents the volume fraction of pores with a diameter equal to d_p. In the derivation of equation (11), using the parrallel pore model, it is assumed that the tortuosity of the pores is independent of the pore diameter. Using the parrallel pore model results in the maximal possible influence of the pore size distribution on the molar fluxes and this therefore can be

regarded as a conservative approximation.

The distribution function of the pore diameter of the impregnated membrane was measured using mercury porosimetry and is presented in Figure 1.

Figure 1: Distribution function of the pore diameter of the impregnated membrane

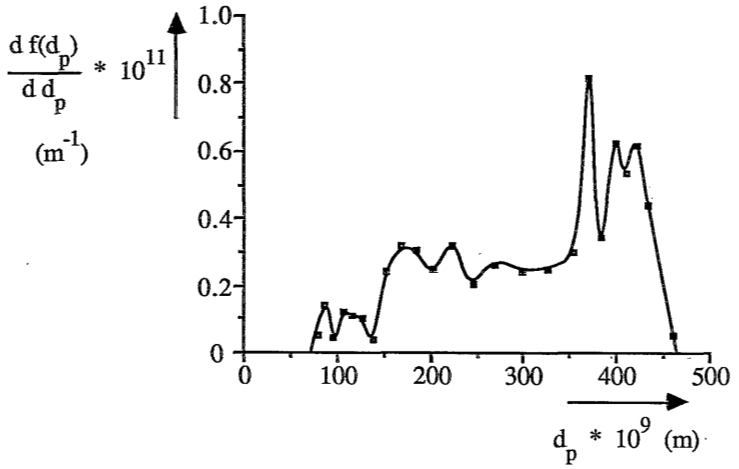

As the determination of the distribution function of the pore diameter takes place with only a small part of the membrane as a sample, it was checked whether this distribution function is constant over the entire membrane. Therefore this measurement was also carried out with another sample of the same membrane. The agreement of the average pore diameters calculated from both distribution functions was within 3%. The average pore diameter of the membrane based on the pore area is 309 nm and based on the pore volume it is 322 nm, calculated by equations (12).

$$\text{volume averaged: } (\bar{d}_p)^2 = \int_{d_p=0}^{d_p=\infty} d_p^2 \frac{d\,f(d_p)}{d\,d_p}\, d\,d_p \tag{12a}$$

$$\text{area averaged: } \bar{d}_p = \int_{d_p=0}^{d_p=\infty} d_p \frac{d\,f(d_p)}{d\,d_p}\, d\,d_p \tag{12b}$$

In the continuum regime in the presence of surface diffusion the overall effective diffusion coefficient as a function of the pore diameter can, according to equation (7), be presented by equation (13).

$$D_i^{eff}(d_p) = C_1 + \frac{C_2}{d_p} \tag{13}$$

Substitution of equation (13) into equation (11) results in the expression that must be used to calculate the average pore diameter for the combination of continuum diffusion and surface diffusion.

$$\frac{1}{\bar{d}_p} = \int_{d_p=0}^{d_p=\infty} \frac{1}{d_p} \frac{d\, f(d_p)}{d\, d_p} d\, d_p \qquad (14)$$

From equation (14) an average pore diameter of 256 nm is calculated. This average pore diameter has to be used in the factor $4/d_p$ in equation (10).

3. Experimental setup

The experimental setup used to measure molar fluxes through the membrane is presented schematically in Figure 2.

Figure 2: Experimental set up

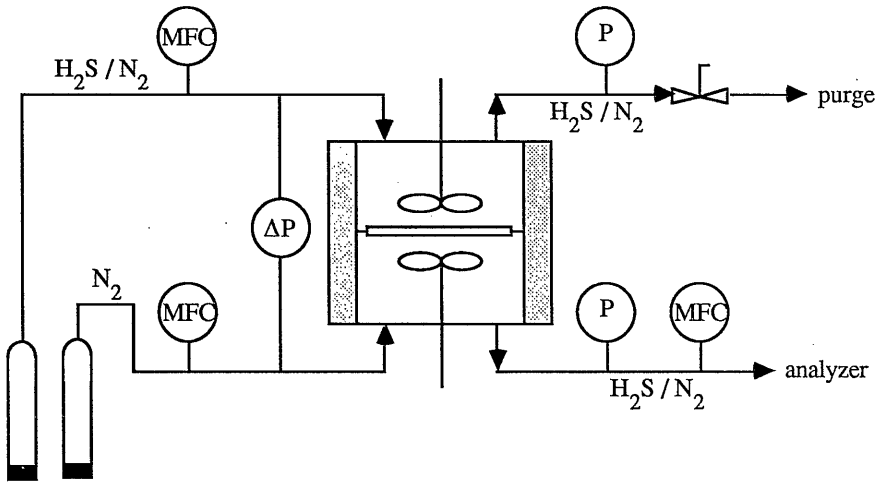

Hydrogen sulfide in nitrogen or sulfur dioxide in nitrogen is fed by a mass flow controller to the membrane reactor to one side of the membrane and nitrogen is fed by a mass flow controller to the other side of the membrane. The reactor is made of stainless steel and consists of three parts, the upper chamber, a membrane holder and the lower chamber kept together by bolts. Both reactor chambers are well stirred and considered to be ideally mixed to simplify the interpretation. The reactor is heated by an electric oven and the temperature in the reactor is controlled. The exit stream of the reactor at the nitrogen side of the membrane contains a mass flow controller. This mass flow controller is used to keep the flow at the nitrogen side of the membrane constant which results in a pressure difference over the membrane of zero. In order to check the pressure difference over the

membrane a U-tube containing coloured water connects the two inlet streams just before the reactor. The pressure in the reactor is controlled by a flow regulator in the exit stream at the hydrogen sulfide in nitrogen side of the membrane. The exit stream at the nitrogen side of the membrane containing hydrogen sulfide is analyzed by gas chromatografy using a flame photometric detector. The column used is a Chromosil column operated at a temperature of 323 K.

In Figure 3 the sealing of the membrane in the stainless steel holder is presented schematically.

Figure 3: Sealing of the membrane in the holder.

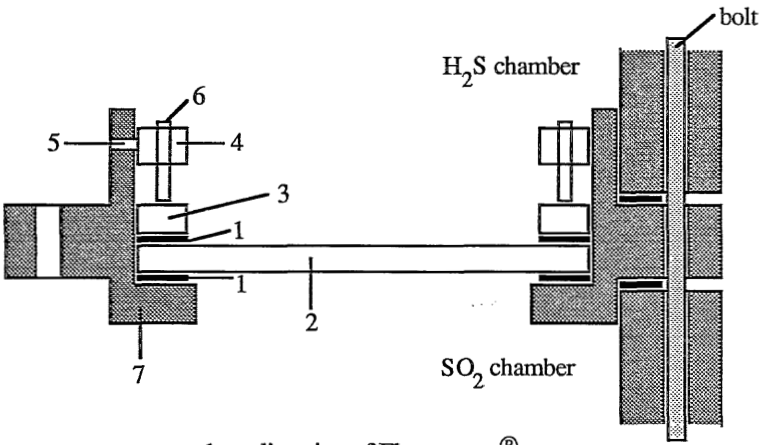

1 sealing ring of Fluorescent®
2 membrane
3 pressure distribution ring
4 ring with 3 bayonet catches
5 bayonet catch
6 screws pressing on 3
7 stainless steel holder

The membrane holder contains successively a sealing ring made of Fluorescent®, a mica reinforced teflon®, the membrane, a second sealing ring, a pressure ring and a ring containing three bayonet catches by which it is connected to the stainless steel holder. This ring contains six 2 mm screws that, after turned on are pressing on the pressure ring which is used to distribute the pressure exercised over the sealing ring. The membrane holder is connected to the H_2S and SO_2 chambers by bolts on the outside, for the sealing between these compartments Fluorescent® rings are used again.

The membranes used were obtained from ECN, Petten and were made of α-Al_2O_3 and had a flat sheet geometry with a diameter of 55 mm and a thickness of about 5 mm. These membranes were impregnated with a saturated solution of aluminum nitrate with ureum in water. After drying and calcining at 700 K for 2 hours γ-Al_2O_3 was obtained, the amount impregnated was of the order of 4.5 %-wt.

Measurements were carried out in the steady state and the time required to obtain the steady state was of the order of 1 to 1.5 hours, the first measurement of each day requiring 3 to 4 hours to

stabilize the system.

From the analysis the bulk concentration of hydrogen sulfide at the nitrogen side, which has diffused through the membrane, is determined and with the flow of nitrogen the molar flux of hydrogen sulfide times the membrane area is calculated. The bulk concentration of hydrogen sulfide at the high concentration side of the membrane is calculated from an overall mass balance. This balance was checked by analysing both exit streams together and the agreement was always within 0.5%. As the molar flux of hydrogen sulfide times the membrane area was at least 20% of the flow of hydrogen sulfide into the reactor the accuracy of the molar flux of hydrogen sulfide or sulfur dioxide measured, based on the agreement of the overall mass balance, was always within 2.5%. The reproducibility of the measurements was always within a few percent.

4. Determination of the porosity-tortuosity factor, ε/τ, of the membrane

In order to be able to subtract the molar flux through the gas phase in the pores of the membrane from the experimentally determined molar fluxes the porosity-tortuosity factor, ε/τ, of the membrane has to be determined. The porosity-tortuosity factor of the membrane is measured by permeation measurements with a pure, non-adsorbing gas. These permeation measurements consisted of forcing a pure gas through the membrane and measuring the pressure drop over the membrane as a function of the flow through the membrane and the average pressure.

The transport through the membrane is in this case caused by the combination of Knudsen diffusion and viscous flow and is presented by equation (15) (see e.g., Mason and Malinauskas, 1983).

$$J_i = -\frac{1}{RT}\left(D_{i,K}^{eff} + \frac{B_o P}{\eta}\right)\frac{dP}{dz} \qquad (15)$$

$$\text{with } B_o = \frac{\varepsilon}{\tau}\frac{d_p^2}{32} \text{ and } D_{i,K}^{eff} = \frac{\varepsilon}{\tau} D_{i,K}^{o} = \frac{\varepsilon}{\tau}\frac{d_p}{3}\sqrt{\frac{8RT}{\pi M_i}}$$

Integration of equation (15) results in equation (16).

$$\frac{J_i}{\Delta P} = \frac{1}{RTL}\frac{\varepsilon}{\tau} D_{i,K}^{o} + \frac{B_o}{RT\eta L}\bar{P} \qquad (16)$$

The average pressure in equation (16) follows directly from the integration and therefore it is not necessary to have a pressure drop over the membrane that is small compared to the pressure itself.

Plotting $J_i / \Delta P$ as a function of the average pressure should result in a straight line. Both from the intercept and from the slope of this line the porosity-tortuosity factor of the membrane can be calculated. In order to check this experimental technique permeation measurements were performed both with nitrogen and with helium at a temperature of 533 K and using the impregnated membrane. In Figure 4 the results of nitrogen and helium are plotted according to equation (16).

Figure 4: Permeation measurements with N_2 and He at a temperature of 533 K.

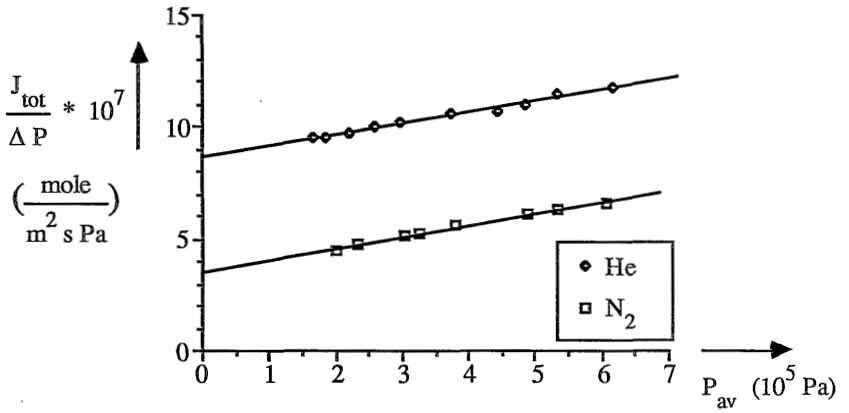

From the intercept and the slope of the lines in Figure 4 the effective Knudsen diffusion coefficient $D_{i,K,eff}$ and the membrane parameter B_0 are calculated respectively, both for helium and for nitrogen. Viscosity data required in the calculation were obtained from literature (Landolt Börnstein, 1969). In Table 1 the results for the parameters are given for helium and for nitrogen.

Table 1: Parameters determined from the permeation measurements at 533 K.

	He	N_2
$D_{i,K}^{eff}$ (m^2/s)	$1.734 * 10^{-5}$	$7.011 * 10^{-6}$
B_0 (m^2)	$2.87 * 10^{-16}$	$2.79 * 10^{-16}$

Before calculating the porosity tortuosity factors from the data in Table 1 the results obtained for He are compared with those obtained for N_2. The values of B_0, being a membrane specific parameter, see equation (15), determined with helium and nitrogen should be identical. From Table 1 it can be concluded that the values agree within 3%. The ratio of the effective Knudsen diffusion coefficients determined for helium and nitrogen should be equal to the inverse of the square root of the ratio of the molar masses of helium and nitrogen as can be seen from equation (15). Comparing the experimentally determined ratio of the effective Knudsen diffusion coefficients of 2.473 with the theoretical ratio of 2.645 the agreement appears to be good as the deviation is about 6.5%. Therefore from the results of the measurements with helium and nitrogen it can be concluded that this technique can be used to determine the characteristic membrane parameters.

From the effective Knudsen diffusion coeficient and from the value of B_0 the porosity-tortuosity factor of the membrane ε/τ can be calculated, see equation (15). As viscous flow is proportional to d_p^2 the average pore diameter to be used in the calculation of ε/τ from B_0 is the volume averaged pore diameter, 322 nm. However in the calculation of ε/τ from the effective Knudsen diffusion

coefficient the area averaged pore diameter, 309 nm, must be used as Knudsen flow is proportional to d_p. The values of the porosity-tortuosity factor ε/τ calculated are given in Table 2.

Table 2: Porosity-tortuosity factor ε/τ of the membrane.

	He	N_2	average
$\frac{\varepsilon}{\tau}$ (from $D_{i,K}^{eff}$)	0.092	0.099	0.096
$\frac{\varepsilon}{\tau}$ (from B_0)	0.074	0.072	0.073

From Table 2 it can be concluded that the porosity-tortuosity factor, ε/τ, of the membrane determined from the viscous flow parameter B_0 is about 24% lower compared to the value determined from the effective Knudsen diffusion coefficient. A possible explanation is the use of the parallel pore model whereas in practice the distribution of the pore diameter can very well be located in the individual pores. As the membrane parameter B_0 is proportional to d_p^2 whereas the effective Knudsen diffusion coefficient is proportional to d_p an obstruction inside the pore having a smaller pore diameter reduces viscous flow more effectively than Knudsen diffusion. So the porosity-tortuosity factor, ε/τ, of the membrane calculated from B_0 is reduced more by the occurrence of an obstruction inside the pore compared to the porosity-tortuosity factor calculated from the effective Knudsen diffusion coefficient.

Because in the diffusion measurements transport is caused by diffusion processes and not by viscous flow, as there is no pressure difference over the membrane, the porosity-tortuosity factor ε/τ determined from the effective Knudsen diffusion coefficient will be used in the interpretation of the diffusion measurements.

5. Determination of the mass transfer parameter in the gas phase k_g

For the interpretation of diffusion data, the difference in the pressure dependence of diffusion through the gas phase in the pores of the membrane and surface diffusion is used. Therefore it is important to interpret the measured data using the correct pressure dependence of the mass transfer parameter in the gas phase, k_g, outside the membrane. The mass transfer parameter, k_g, as a function of pressure and temperature can usually be described by a Sherwood (Re, Sc) relation as presented in equation (17).

$$Sh = C_1 + C_2\, Re^m\, Sc^n \qquad (17)$$

$$\text{with } Sh = \frac{k_g\, d}{D_i^0}\ ,\ Re = \frac{\rho\, N\, d^2}{\eta} \text{ and } Sc = \frac{\eta}{\rho\, D_i^0}$$

Values of m and n in equation (17) as reported in literature, determined in gas-liquid systems in stirred cells with a smooth interface, are m=2/3 and n=1/2 (Versteeg et. al., 1987). For these

gas-liquid systems it appeared that constant C_1 is negligible. From equation (17) and these values of m and n the dependency given in equation (18) is calculated.

$$k_g \sim (P)^{-1/3} (\eta T)^{-0.17} (D_i^o)^{1/2} \qquad (18)$$

with D_i^o the diffusion coefficient at a pressure of 10^5 Pa

Since the difference between the continuum diffusion coefficients at atmosferic pressure of H_2S and SO_2 in N_2 is about 30%, the k_g values for H_2S and SO_2 will differ only about 15%. The influence of the temperature on k_g in the range of 450 Kto 550 K where diffusion measurements were performed, is limited to about 5%, according to equation (18). The difference of the k_g value between a pressure of 10^5 and $6*10^5$ Pa, however, is about 50 % according to equation (18). Therefore, and to determine the value of the constant C_2 in equation (17), k_g measurements were performed as a function of pressure in the experimental setup used for diffusion measurements.

The mass transfer parameter in the gas phase outside the membrane, k_g, was measured by performing conversion measurements with H_2S and SO_2 at a temperature of 534 K. H_2S in N_2, with a H_2S molar fraction of 0.03, and SO_2 in N_2, with a molar fraction of SO_2 of 1500 ppm, are fed to opposite sides of the porous membrane. Both reactants diffuse through the stagnant gas film outside the membrane into the membrane and react very fast resulting in a very small reaction zone as was pointed out in the introduction. Owing to the high molar fraction of H_2S the location of this reaction zone is entirely shifted towards the membrane interface at the SO_2 side and mass transfer limitation of SO_2 in the gas phase outside the membrane occurs. In this situation slip of H_2S to the opposite side of the membrane occurs. From the determination of the conversion of SO_2 the mass transfer parameter k_g is calculated as a function of pressure. To check whether the k_g values obtained are independent of the flow rate of the mixture of SO_2 and N_2, this flow rate was varied. No influence on the k_g values calculated was observed. In Figure 5 the mass transfer parameter k_g is given as a function of pressure. During these experiments the stirrer speed was kept constant at the same value as used in the diffusion measurements.

Figure 5: Mass transfer in the gas phase outside the membrane as a function of pressure

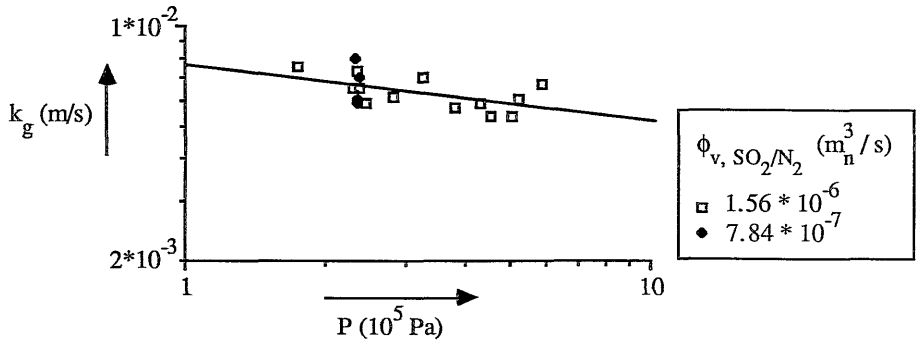

The mass transfer parameter k_g as a function of the pressure P can be described by equation (19).

$$k_g = 7.53 * 10^{-3} * P^{-0.16} \qquad (19)$$

with P in 10^5 Pa

Except for two data all experimentally determined k_g-values can be described according to equation (19) within 15%. The agreement between the pressure dependence of k_g determined, -0.16, and literature data (Versteeg et. al., 1987), - 1/3, is reasonable. The k_g data given by equation (19) are used in the interpretation of the diffusion measurements.

6. Results from diffusion measurements

Diffusion measurements as a function of pressure were performed both with H_2S and with SO_2 at temperatures between 450 K and 550 K. The interpretation of the diffusion data was performed according to equation (10). An example of the figures obtained is given in Figure 6 for SO_2 at a temperature of 548 K.

Figure 6: Diffusion data of SO_2 as a function of pressure at a temperature of 548 K.

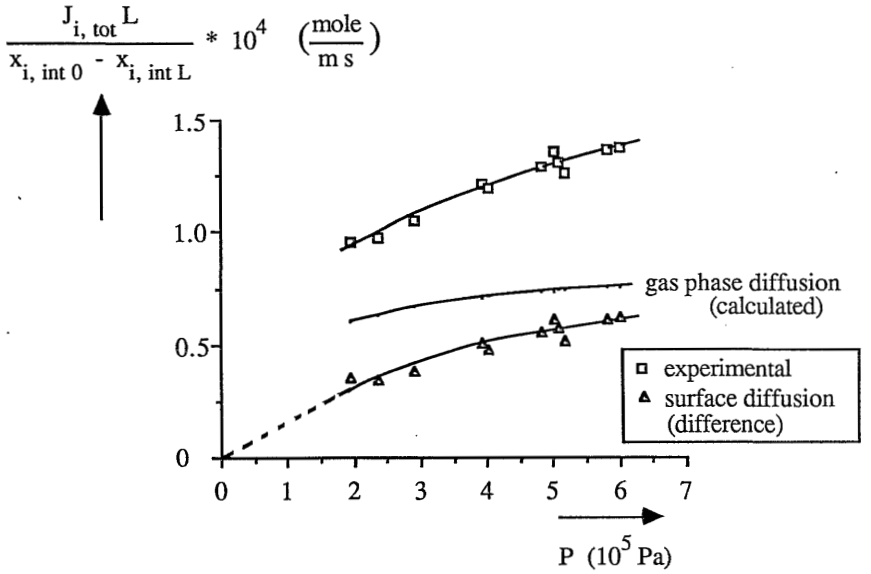

From Figure 6 it can be seen that there is a substantial difference between the transport expected on the basis of only diffusion through the gas phase in the pores of the membrane and the experimentally observed transport; the difference amounts to 60 to 80% based on gas phase diffusion. From the fact that the line representing gas phase diffusion is not entirely independent of

the pressure it can be concluded that the experiments performed at these lower pressures are not yet completely in the continuum regime. Subtraction of the transport through the gas phase in the membrane from the experimentally determined transport gives the contribution of surface diffusion (see equation (10)). The line representing surface diffusion, which according to equation (10) should pass through the origin, is not straight but curved. Apparently the denominator in the surface diffusion term in equation (10) plays a role meaning that at the highest pressures the fraction of the adsorption sites covered by SO_2 is not negligibly small. As the curvature is caused by the adsorption parameter b_i the data can be used to determine both the product $D_{i,S}\, b_i\, c_S$ and b_i by a two-parameter fit of the experimental data. Chosing values for the product $D_{i,S}\, b_i\, c_S$ and b_i, theoretical values of the surface diffusion contribution term of equation (10), $SDC_{theor.}$, can be calculated as a function of pressure from equation (20) and compared with the experimental values, $SDC_{exp.}$, presented by equation (21).

$$SDC_{theor} = \frac{4}{d_p} D^{eff}_{i,S}\, b_i\, c_S\, \frac{P}{(1 + b_i P x_{i,\,int\,0})(1 + b_i P x_{i,\,int\,L})} \tag{20}$$

$$SDC_{exp} = \frac{J_{i,\,tot}\, L}{x_{i,\,int\,0} - x_{i,\,int\,L}} - D^{eff}_{i,gas} \frac{P}{RT} \tag{21}$$

The parameters $D_{i,S}\, b_i\, c_S$ and b_i are fitted minimizing the cumulative relative deviation function, CD, between the surface diffusion model and the experimental data by the expression given in equation (22).

$$CD = \sum_{j=1}^{j=N} \left(\frac{SDC_{theor,\,j} - SDC_{exp,\,j}}{SDC_{av,\,j}} \right)^2 \tag{22}$$

with N the number of experimental data and $SDC_{av,\,j} = \frac{SDC_{theor,\,j} + SDC_{exp,\,j}}{2}$

Successively now the data obtained for SO_2 and H_2S are discussed.

6.1. Surface diffusion data of SO_2 on γ-Al_2O_3

In Table 3 the fitted parameters for SO_2 are presented at different temperatures, also the calculated value of the product $D_{i,S}\, c_S$ and the average relative deviation between the theoretical surface diffusion model and the experimental data are given. A graphical comparison of the experimental surface diffusion data and the theoretically fitted data as a function of pressure at different temperatures is given in the appendix.

Table 3: Surface diffusion parameters of SO_2 at different temperatures

T (K)	$D_{i,S}^{eff} b_i c_S * 10^{17}$ $(\frac{mole}{Pa\,s})$	$b_i * 10^3$ (Pa^{-1})	$D_{i,S}^{eff} c_S * 10^{14}$ $(\frac{mole}{s})$	average relative deviation $\sqrt{\frac{CD}{N}}$
447	0.58	-0.01	-	0.033
473	0.65	-0.01	-	0.088
498	0.74	0.11	-	0.022
525	1.50	1.36	1.10	0.062
548	1.31	0.90	1.46	0.058

From Table 3 it can be seen that the parameters $D_{i,S} b_i c_S$ and b_i fitted can be divided into two groups, the data at temperatures of 447, 473 and 498 K and the data at 525 and 548 K. The surface diffusion data within these two groups of temperatures are reasonably constant but there is a remarkable difference between the two groups of data. From a change of the temperature of 498 to 525 K the fitted adsorption parameter, b_i, increases suddenly by about a factor of 10 whereas the value of the product $D_{i,S} b_i c_S$ increases by about a factor of 2. The values of the product $D_{i,S} c_S$ are only presented at the two highest temperatures as only in that situation an acceptable accuracy of the adsorption parameter b_i is present.

Studies in literature concerning the adsorption of SO_2 on γ-Al_2O_3 reveal that there are different adsorbed species, physically adsorbed SO_2 and a weakly chemisorbed SO_2^- anion (Deo and Dalla Lana, 1971, Ono et. al., 1977, Karge et. al., 1984, Chang, 1978). Ono et. al. (1977) studied the formation of SO_2^- anions on γ-Al_2O_3 as a function of temperature using electrospin resonance and found a maximum in the amount of SO_2^- anions at a temperature of 513 K of approximately 10 percent of the SO_2 adsorbed. Karge et. al. (1984) reported also a sudden decrease of the relative amount of SO_2^- anions, however, at a higher temperature between 550 and 650 K. Chang (1978) measured adsorption isotherms of SO_2 on γ-Al_2O_3 and found a gradual decrease in the amount of SO_2 adsorbed in a temperature region of 298 to 773 K which is in contradiction to the increase of the adsorption parameter b_i between 498 and 525 K as presented in Table 3. Deo and Dalla Lana (1971) studied the adsorption of SO_2 on γ-Al_2O_3 using infrared spectroscopy and reported a remarkable change in the infrared absorption spectra between 473 and 573 K. The absorption band at 1685 cm^{-1}, observed at temperatures up to 473 K, has disappeared at 573 K and absorption bands at 1440 and 1570 cm^{-1}, that hardly occur up to 473 K, are much stronger at 573 K. This indicates that at 573 K a species is present which was not present at lower temperatures.

Although the change in surface diffusion behaviour of SO_2 reported in Table 3 cannot be explained with the results from literature concerning the nature of adsorbed SO_2 it is likely connected to the change in the relative amount of some chemisorbed species.

From the adsorption isotherms measured by Chang (1978) the adsorption parameter can be calculated. Chang distinguishes two types of adsorbed SO_2, a chemisorbed species and a physically adsorbed species. From the total amount of SO_2 adsorbed, consisting of both physically adsorbed and chemisorbed SO_2, an adsorption parameter b_i of $1.1*10^{-3}$ Pa^{-1} can be calculated from his data at 473 K for a partial pressure of SO_2 of 133 Pa whereas from the amount of physically adsorbed SO_2 only a value of $8*10^{-5}$ Pa^{-1} can be calculated. These values are in reasonable agreement with the data presented in Table 3 and indicate that the chemisorbed species in the present situation is only present at higher temperatures. Gilliland et. al. (1974) reported surface diffusion coefficients of SO_2 in porous glass and porous carbon. At a temperature of 288 K they reported values of the surface diffusion coefficient of SO_2 between $5*10^{-9}$ and $2*10^{-8}$ m^2/s depending on the heat of adsorption. The activation energy of surface diffusion they found was 27 kJ/mole. To calculate the surface diffusion coefficient of SO_2 from the data presented in Table 3, the total concentration of adsorption sites, c_S, is estimated by equation (23) which is based on monolayer coverage (Gilliland et. al., 1974).

$$\text{area/molecule} = 1.09\ (m/\rho)^{2/3} \tag{23}$$

In equation (23) m is the molar mass and ρ the density of the adsorbate as a saturated liquid. From equation (23) a value of c_S of $9.5*10^{-6}$ mole/m^2 is calculated. From Table 3 an effective surface diffusion coefficient of SO_2 of about $1*10^{-9}$ m^2/s results. Using the porosity-tortuosity factor of the membrane of 0.096 a surface diffusion coefficient of SO_2 of $1*10^{-8}$ m^2/s results which is of the same order compared to the values reported in literature by Gilliland et. al. (1974).

To determine the influence of the mass transfer parameter in the gas phase outside the membrane, k_g, on the interpretation of the diffusion measurements, equation (18), two additional fits were performed. One fit uses values for k_g that are increased by 50% and the other fit uses a dependence of k_g of the pressure P of the power -1/3 as found in literature (Versteeg et. al., 1987). In the last case the constant was adjusted to give the same k_g values at an average pressure of 0.5 MPa. In the first situation, using a 50% higher k_g, the parameters $D_{i,S}$ b_i c_S and b_i fitted were only 4 to 8 % lower. Lower values are expected as the decrease of the mass transfer resistance in the gas phase outside the membrane results in an increase of the driving force over the membrane itself and as a result a larger part of the experimentally observed molar flux is ascribed to diffusion through the gas phase in the pores of the membrane. In the second situation, a different pressure dependence of k_g, the surface diffusion parameters fitted deviated less than 1% compared to those presented in Table 3. Therefore the exact relationship giving k_g as a function of pressure is not very important for the interpretation of surface diffusion data in the system used.

6.2 Surface diffusion data of H_2S on γ-Al_2O_3

Diffusion measurements of H_2S through the membrane as a function of pressure were carried out at temperatures between 446 and 557 K. The contribution of surface diffusion was calculated

in the same way as described before. The surface diffusion parameters $D_{i,S}\, c_S\, b_i$ and b_i were fitted from the data and the results are presented in Table 4.

Table 4: Surface diffusion parameters of H_2S at different temperatures

T (K)	$D^{eff}_{i,S}\, b_i\, c_S * 10^{17}$ $(\frac{mole}{Pa\, s})$	$b_i * 10^3$ (Pa^{-1})	$D^{eff}_{i,S}\, c_S * 10^{14}$ $(\frac{mole}{s})$	average relative deviation $\sqrt{\frac{CD}{N}}$
446	0.93	0.75	1.24	0.074
484	1.28	1.25	1.02	0.058
521	1.60	1.00	1.60	0.123
557	0.94	0.51	1.84	0.081

From Table 4 it seems that both the product $D_{i,S}\, c_S\, b_i$ and the adsorption constant b_i show a maximum as a function of temperature whereas the product $D_{i,S}\, c_S$ increases with temperature. A graphical comparison of the experimental data and the theoretical data predicted using the fitted parameters is given in the appendix.

7. Conclusions

It is demonstrated experimentally that surface diffusion of H_2S and SO_2 in an alumina membrane with an average pore diameter of 322 nm, impregnated with γ-Al_2O_3, can contribute substantially to the transport rate. Moreover, for this system it is of almost the same order of magnitude as the transport caused by ordinary diffusion through the gas phase in the pores. Owing to the large pore diameter diffusion through the gas phase in the pores of the membrane is determined almost completely by continuum diffusion and the molar flux is therefore independent of pressure. Surface diffusion however is linearly proportional to the pressure provided the fraction of the adsorption sites covered is very low. It is demonstrated that the resulting difference in pressure dependence of both transport mechanisms can be used to distinguish between diffusion through the gas phase in the pores and surface diffusion.

As the fraction of the adsorption sites covered with H_2S or SO_2 appears to be considerable, it was necessary to use a two parameter fit, the product $D_{i,S}\, c_S\, b_i$ and the adsorption parameter b_i itself, to interpret the surface diffusion data. For SO_2 the fitted surface diffusion parameters show a remarkable change between 498 and 525 K which probably can be attributed to the change of some chemisorbed species as has been reported in literature. The order of magnitude of the data found are in reasonable agreement with literature data. For H_2S the parameters fitted show a maximum with temperature, but the product of the effective surface diffusion coefficient and the concentration of adsorption sites increases with temperature.

Notation

b_i	adsorption constant	Pa^{-1}
B_o	membrane specific parameter defined in equation (15)	m^2
c_S	concentration of adsorption sites	mole / m^2
CD	cumulative relative deviation function between SDC_{exp} and SDC_{theor} (see equation (20-22))	-
d_p	average pore diameter	m
$D^o_{i,\,inert}$	continuum diffusion coefficient	m^2 / s
$D^o_{i,\,K}$	Knudsen diffusion coefficient	m^2 / s
$D_{i,\,gas}$	diffusion coefficient in the gas phase in the pores	m^2 / s
$D_{i,\,surf}$	surface diffusion coefficient	m^2 / s
$f(d_p)$	volume fraction of the pores with diameter d_p	-
k_g	mass transfer parameter in the gas phase outside the membrane	m / s
$J_{i,\,gas}$	molar flux owing to diffusion through the gas phase in the pores	mole / m^2 s
$J_{i,\,tot}$	total molar flux owing to both transport mechanisms	mole / m^2 s
$J_{i,\,surf}$	molar flux owing to surface diffusion	mole / m s
L	membrane thickness	m
M_i	molar mass of component i	kg / mole
m	exponent in equation (17)	-
n	exponent in equation (17)	-
P	pressure	Pa
R	gas constant	J / mole K
Re	Reynolds number defined in equation (17)	-
Sc	Schmidt number defined in equation (17)	-
Sh	Sherwood number defined in equation (17)	-
T	temperature	K
SDC_{exp}	experimental surface diffusion contribution (see equation (20))	mole / m s
SDC_{theor}	theoretical surface diffusion contribution (see equation (21))	mole / m s
x_i	molar fraction of component i	-
z	location inside the membrane	m
ε	porosity of the membrane	-
η	viscosity of the gas	Pa s
ρ	density of the gas	kg / m^3
τ	tortuosity of the membrane	-
θ_i	fraction of the adsorption sites covered by component i	-

subscripts

bulk 0	in the well stirred bulk of the gas at the side of z=0
bulk L	in the well stirred bulk of the gas at the side of z=L
eff	effective, corrected for the porosity-tortuosity of the membrane
int 0	at the membrane interface at z=0
int L	at the membrane interface at z=L

References

Butt J.B. and R.N. Foster, 1969, Surface transport effects on catalytic activity, Ind. Eng. Chem. Fund. **8**(1), 171 - 172

Chang C.C., 1978, Infrared studies of SO_2 on γ-Alumina, J. Catal. **53**, 374 - 385

Cui C.L., J.R. Authelin, D. Schweich and J. Villermaux, 1990, Consequence of distributed properties on effective diffusivities in porous solids, Chem. Eng. Sci. **45**(8), 2611 - 2617.

Deo A.V. and I.G. Dalla Lana, 1971, Infrared studies of the adsorption and surface reactions of hydrogen sulfide and sulfur dioxide on some aluminas and zeolites, J. Catal. **21**, 270 - 281

Gilliland E.R., R.F. Baddour, G.P. Perkinson and K.J. Sladek, 1974, Diffusion on surfaces. I. Effect of concentration on the diffusivity of physically adsorbed gases, Ind. Eng. Chem. Fund. **13**(2), 95 - 105

Karge H.G., S. Trevizan de Suarez and I.G. Dalla Lana, 1984, A new cell for combined IR and ESR investigations on solid catalysts, J. Phys. Chem. **88**, 1782 - 1784

Landolt Börnstein, 1969, Zahlenwerte und funktionen aus physik, chemie , astronomie, geophysik und technik, 6^{e} Auflage, II Band, 5^{e} Teil, Bandteil a, 26, Springer Verlag, Berlin

Mark H.F., D.F. Othmer, C.G. Overberger and G.T. Seaborg, 1983, Kirk-Othmer, Encyclopedia of chemical technology, vol. 22, pp 276-282, John Wiley & Son, New York

Mason E.A. and A.P. Malinauskas, 1983, Gas transport in porous media: The Dusty-Gas Model, Chemical Engineering Monographs 17, Elsevier, Amsterdam

Ono Y., H. Takagiwa and S. Fukuzumi, 1977, Formation of sulfur dioxide anions on Aaumina, J. Catal. **50**, 181 - 183

Reid R.C., J.M. Prausnitz and Sherwood T.K., 1977, The properties of gases and liquids, 3rd edition, McGraw-Hill

Sloot H.J., G.F. Versteeg and W.P.M. van Swaaij, 1990, A non-permselective membrane reactor for chemical processes normally requiring strict stoichiometric feed rates of reactants, Chem. Eng. Sci. **45**(8), 2415 - 2421, chapter 2 in this thesis

Smith R.K. and A.B. Metzner, 1964, Rates of surface migration of physically adsorbed gases, J. Phys. Chem. **68**(10), 2741 - 2747

Versteeg G.F., P.M.M. Blauwhoff and W.P.M. van Swaaij, 1987, The effect of diffusivity on gas-liquid mass transfer in stirred vessels. Experiments at atmospheric and alevated pressures, Chem. Eng. Sci. **42**, 1103 - 1119

Appendix: Experimental and theoretically calculated surface diffusion data.

1. Surface diffusion data of SO_2 as a function of pressure at different temperatures

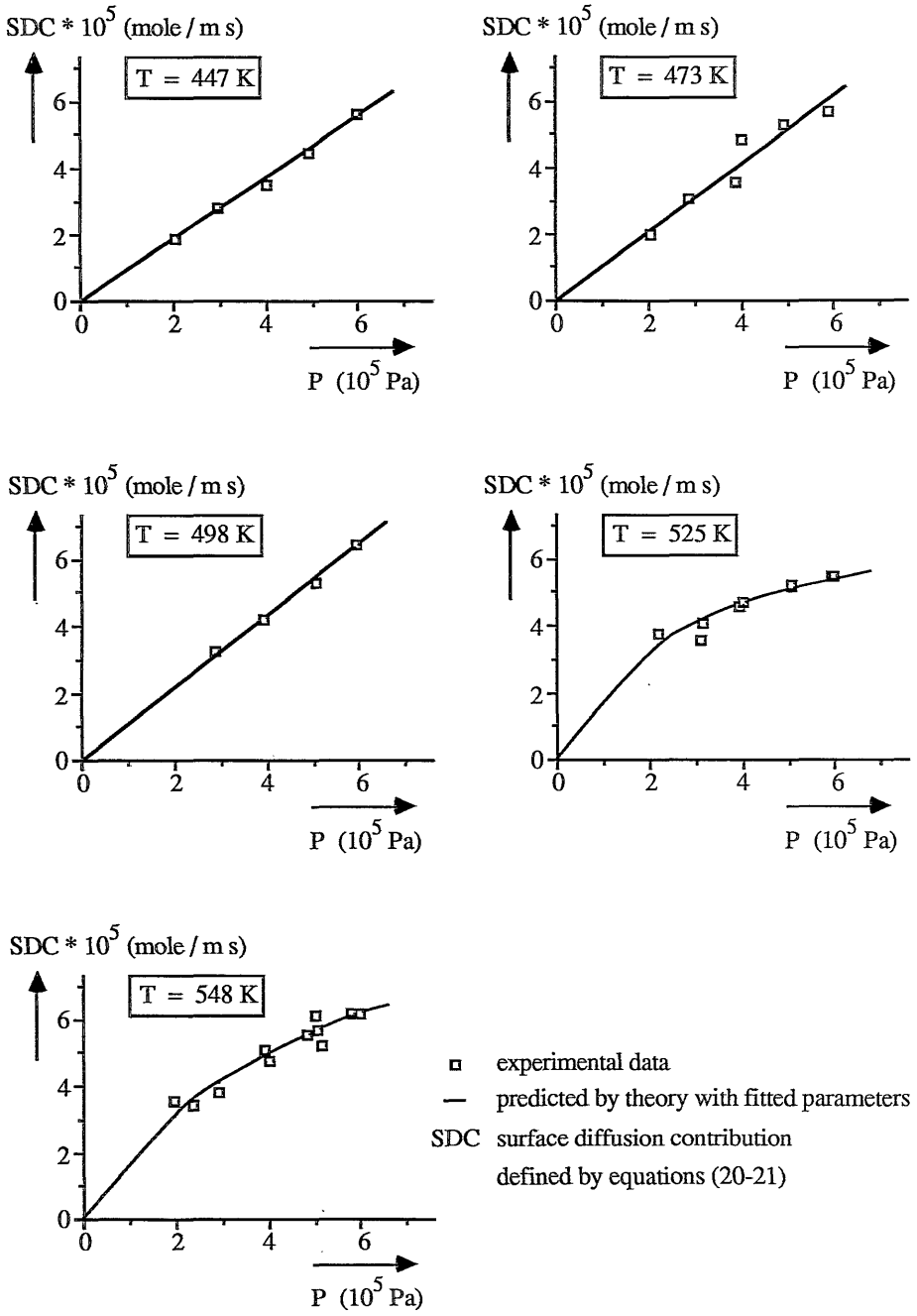

2. Surface diffusion data of H_2S as a function of pressure at different temperatures

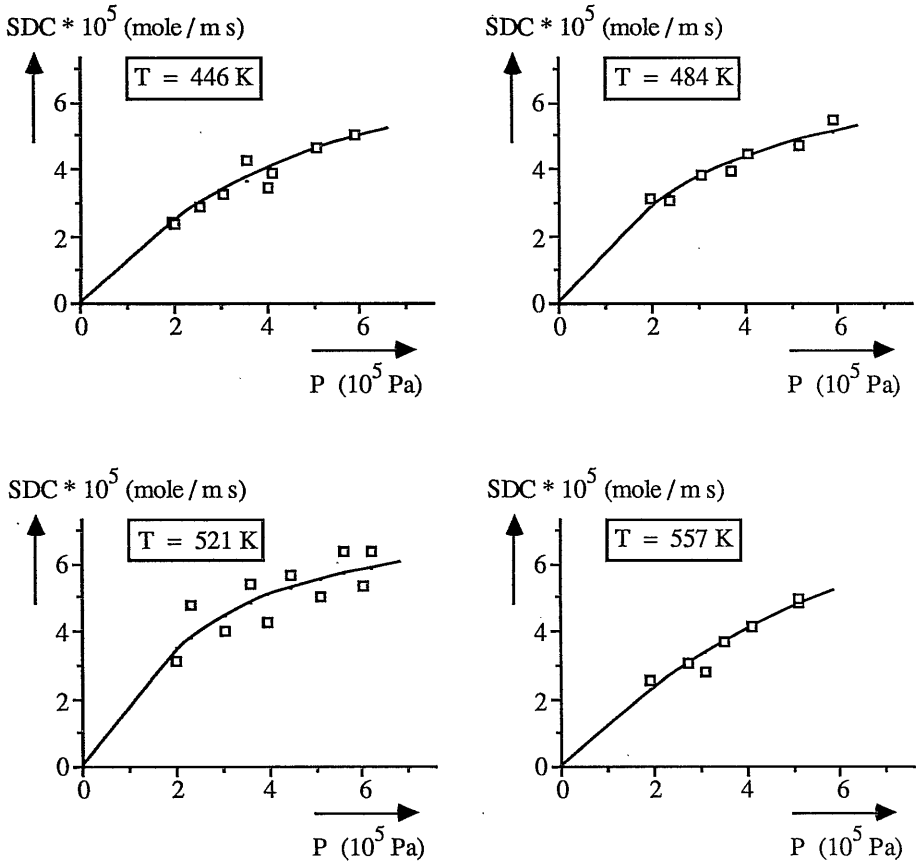

- ◘ experimental data
- — predicted by theory with fitted parameters

SDC surface diffusion contribution
defined by equations (20-21)

Chapter 4

MATHEMATICAL MODELLING OF MASS TRANSPORT COMBINED WITH AN INSTANTANEOUS, REVERSIBLE REACTION INSIDE A MEMBRANE

Abstract

A mathematical model, based on the so-called 'Dusty-Gas Model' extended with surface diffusion, is presented which describes mass transport owing to molecular diffusion and viscous flow combined with an instantaneous reversible reaction inside a membrane with reactants fed to opposite sides of the membrane taking mass transfer resistances in the gas phase outside the membrane into account. As a model reaction the Claus reaction is chosen to study this membrane reactor.

The present model is used to determine the validity of a previously presented simplified model. From the comparison of both models it is concluded that the simplified model predicts the correct molar fluxes provided the system is very diluted and can therefore be considered a pseudo-binary system.

It is concluded also from the model that to determine whether, in absence of an overall pressure difference over the membrane, a maximum or a minimum in the pressure profile inside the membrane is to be expected not only depends on the stoichiometry of the reaction but also on the mobilities of the different species.

1. Introduction

A novel type of membrane reactor has been developed and investigated in which a membrane is used to keep reactants separated from each other and have them come together in a controlled way instead of using the membrane to separate components. In a previous chapter (Sloot et. al., 1990) a simplified transport model for this reactor was presented, now a fundamentally more correct model based on the so called 'Dusty-Gas Model' (Mason and Malinauskas, 1983) is presented which also includes surface diffusion as an additional transport mechanism.

In this reactor the reactants are fed at opposite sides of a porous membrane which contains a catalyst for a heterogeneously catalyzed reaction between the reactants. The reactants diffuse from either side into the membrane and therefore a pressure difference over the membrane is in principle not necessary, this in contrast to the usual applications of membranes. Inside the membrane a reaction between the reactants occurs and the products obtained diffuse out of the membrane to both sides. If the rate of the chemical reaction is fast compared to the diffusion rates of the reactants, a small reaction zone or, in case of an instantaneous irreversible reaction, a reaction plane inside the membrane results. The location of this reaction zone will be such that the molar fluxes of the reactants are in stoichiometric ratio. If for some reason the concentration of one of the reactants increases this will evolve in a higher molar flux of this reactant into the membrane. At the reaction zone an excess of this reactant will be present and therefore this component will penetrate further into the membrane before the reaction takes place. This results in a shift of the reaction zone towards the side of the reactant whose molar flux is below stoichiometry. Owing to this shift, the distance from the membrane interface to the reaction zone decreases for this reactant resulting in an increase of its molar flux and vice versa for the other reactant. The new location of the reaction zone will be such that the molar fluxes of both reactants are in stoichiometric ratio again.

Owing to the fast reaction inside the membrane, slip of the reactants to the opposite side of the membrane is not possible provided the reaction is irreversible. Because of the stoichiometric molar fluxes and the impossibility of slip of the reactants to the opposite side of the membrane, this reactor could be very suitable for chemical processes requiring strict stoichiometric feed rates of reactants.

In order to study this membrane reactor and to determine the influence of reversibility of the reaction and of the effect of a pressure difference over the membrane which can possibly occur in practice, a mathematical model is developed. This model describes mass transport owing to molecular diffusion and viscous flow through the membrane in combination with an instantaneous, reversible reaction inside the membrane. As a fundamental transport model in porous media, the so called 'Dusty-Gas Model' (Mason and Malinauskas, 1983), extended with surface diffusion has been used. A simplified transport model describing transport combined with an instantaneous reversible reaction inside a membrane was presented earlier (Sloot et. al., 1990). This simplified model uses Fick's diffusion equations for describing the diffusion of all components and uses effective binary diffusion coefficients. The use of Fick's diffusion equation in describing multi-component diffusion however is only valid in very diluted, pseudo binary, systems. The present model is based on a fundamentally more correct and more widely valid transport model and

can therefore be used to determine the validity of the simplified model. Also a number of new effects are predicted by the present model.

2. Model description

The model presented here is a flux model describing mass transport in a membrane in combination with an instantaneous, reversible reaction inside the membrane with reactants coming from different sides of the membrane. Transport is described in the stationary state in the direction perpendicular to a membrane with a flat sheet geometry, reflecting the experimental setup used. To simulate a practical application using porous membranes this flux model must be modified to cylindrical coordinates and be incorporated into a reactor model taking the operation mode (co- or countercurrent) into account.

The instantaneous, reversible reaction is presented by equation (1).

$$\nu_A A + \nu_B B \underset{}{\overset{K_{eq}}{\rightleftharpoons}} \nu_C C + \nu_D D \qquad (1)$$

The basic variables to be calculated as a function of the position in the membrane are the pressure P and the molar fractions of the components A, B, C, D and, if present, of the inert components. As in the present model one inert component is taken into account there are six variables to be calculated as a function of the position in the membrane and therefore also six equations are required. The differential mass balance for a component i is presented by equation (2).

$$\frac{dJ_i}{dz} = R_i(z) \qquad (2)$$

with $R_i < 0$ for reactants and $R_i > 0$ for products

The mass balances for all components A, B, C, D and inert are given by equations (3-7).

$$\frac{dJ_A}{dz} = R_A(z) \qquad (3)$$

$$\frac{dJ_B}{dz} = R_B(z) = \frac{\nu_B}{\nu_A} R_A(z) \qquad (4)$$

$$\frac{dJ_C}{dz} = R_C(z) = -\frac{\nu_C}{\nu_A} R_A(z) \qquad (5)$$

$$\frac{dJ_D}{dz} = R_D(z) = -\frac{\nu_D}{\nu_A} R_A(z) \qquad (6)$$

$$\frac{dJ_{inert}}{dz} = 0 \tag{7}$$

As the rate of the reaction presented by equation (1) is considered instantaneous compared to mass transport, the reaction rate R_A is indefinite. Therefore R_A is eliminated by adding and subtracting among the equations (3-6) resulting in four independent equations (8-11).

$$\frac{1}{\nu_A}\frac{dJ_A}{dz} - \frac{1}{\nu_B}\frac{dJ_B}{dz} = 0 \tag{8}$$

$$\frac{1}{\nu_A}\frac{dJ_A}{dz} + \frac{1}{\nu_C}\frac{dJ_C}{dz} = 0 \tag{9}$$

$$\frac{1}{\nu_A}\frac{dJ_A}{dz} + \frac{1}{\nu_D}\frac{dJ_D}{dz} = 0 \tag{10}$$

$$\frac{dJ_{inert}}{dz} = 0 \tag{11}$$

The fifth equation required is the equilibrium condition which is assumed to be valid through the entire membrane.

$$K_{eq} = \frac{x_C^{\nu_C} x_D^{\nu_D}}{x_A^{\nu_A} x_B^{\nu_B}} P^{\nu_C + \nu_D - \nu_A - \nu_B} \tag{12}$$

The sum of the molar fractions must be equal to one which is the sixth and final equation:

$$\sum_{i=1}^{i=nc} x_i = 1 \tag{13}$$

To solve the set of equations (8-13) additional equations are required specifying the molar fluxes, J_i, as a function of the driving forces. As mentioned before the 'Dusty-Gas Model' (Mason and Malinauskas , 1983) extended with surface diffusion is used to obtain the expressions for J_i. The total molar flux J_i of a component i through the pores of the membrane with a mean pore diameter d_p is calculated according to equation (14) assuming cylindrically shaped pores.

$$J_i = J_{i,\,gas} + \frac{4}{d_p} J_{i,\,surf} \qquad i = 1, \ldots, nc \tag{14}$$

Equation (14) reflects the fact that transport through the gas phase in the pores of the membrane is proportional to the cross area of the pores and therefore proportional to d_p^2 whereas transport owing to surface diffusion is proportional to the circumference of the pores and therefore proportional to d_p.

The molar flux of a component i through the gas phase in the pores is calculated by the 'Dusty Gas Model' equations (15) (Mason and Malinauskas, 1983) omitting thermo diffusion and external forces e.g., gravitation fields in fast rotating systems. The gas phase is assumed to behave as an ideal gas.

$$\sum_{j=1}^{j=nc} \left(\frac{x_j J_{i,gas} - x_i J_{j,gas}}{P D_{ij}} \right) + \frac{J_{i,gas}}{P D_{iK}} = -\frac{x_i}{RT} \left(\frac{1}{P} + \frac{B_o}{\eta D_{iK}} \right) \frac{dP}{dz} - \frac{1}{RT} \frac{dx_i}{dz}$$

$$i = 1, ..., nc \qquad (15)$$

The first term on the left hand side in equation (15) represents continuum diffusion written in the Stefan Maxwell formulation of diffusion and the second term represents Knudsen diffusion. The first term on the right hand side reflects transport caused by a pressure gradient and consists of a pressure diffusion term and a viscous flow contribution. The second term on the right hand side gives the transport owing to a molar fraction gradient. The effective continuum and Knudsen diffusion coefficients used in equation (15) are determined by equations (16).

$$D_{ij} = \frac{\varepsilon}{\tau} D_{ij}^o \quad \text{and} \quad D_{iK} = \frac{\varepsilon}{\tau} D_{iK}^o \qquad (16)$$

The continuum binary diffusion coefficients D_{ij}^o are calculated by gas kinetic theory (Reid et. al., 1977) and the Knudsen diffusion coefficients D_{iK}^o by equation (17).

$$D_{iK}^o = \frac{d_p}{3} \sqrt{\frac{8RT}{\pi M_i}} \qquad (17)$$

Equations (15-17) contain only two variables that have to be specified; the porosity-tortuosity factor ε/τ and the average pore diameter d_p. The membrane specific parameter B_o is related to ε/τ and d_p according to equation (18) (see e.g., Mason and Malinauskas, 1983).

$$B_o = \frac{\varepsilon}{\tau} \frac{d_p^2}{32} \qquad (18)$$

Surface diffusion is described by Fick's law as presented by equation (19).

$$J_{i,\,surf} = - D_{i,s}\, c_s \frac{d\theta_i}{dz} \qquad i = 1, ..., nc \qquad (19)$$

In equation (19) $D_{i,S}$ is the effective diffusion coefficient of surface diffusion of component i, c_S is the concentration of adsorption sites (moles/m^2) and θ_i the fraction of the adsorption sites covered by component i. The rates of adsorption and desorption are assumed to be fast compared to the transport rate through the membrane and therefore an instantaneous adsorption-desorption equilibrium is obtained. It is assumed that the fraction of the adsorption sites covered by component i, θ_i, can be described by a Langmuir isotherm as presented in equation (20).

$$\theta_i = \frac{b_i x_i P}{1 + P \sum_{j=1}^{j=nc} b_j x_j} \qquad i = 1,..., nc \qquad (20)$$

Equations (19-20) contain nc effective diffusion coefficients, D_{iS}, nc adsorption constants, b_i, and the total concentration of adsorption sites, c_S, whose values have to be specified on beforehand in the calculations.

To solve the set of equations (8-20) uniquely twelve boundary conditions are required. At the membrane interfaces the equilibrium condition (equation 12) must be fulfilled and also the sum of the molar fractions has to be equal to one (equation 13). The pressure at the membrane interfaces must be equal to the pressure in the bulk of the gas at that side of the membrane (equation 21).

$$P_{int} = P_{bulk} \qquad z=0 \text{ and } z=L \qquad (21)$$

There are still six additional boundary conditions required.

Mass transfer resistances outside the membrane are taken into account. Because outside of the membrane no reaction takes place and inside the membrane the reaction is assumed to be instantaneous, the molar fluxes from the bulk of the gas to the membrane interface $J_{i,\,b\text{-}i}$ and the molar fluxes in the membrane at the interface $J_{i,\,int}$ do not have to be equal to eachother but are coupled by the stoichiometry of the reaction. Owing to the assumption of an instantaneous reaction, continuity of both the molar fluxes and the molar fractions at the membrane interface cannot be fulfilled. As the condition of continuity of the molar fractions must always be satisfied continuity of the molar fluxes at the membrane interfaces is not possible. Equations (22 - 25) represent the coupling of the molar fluxes $J_{i,\,b\text{-}i}$ and $J_{i,\,int}$ by the stoichiometry of the reaction.

$$\frac{1}{\nu_B}\left(J_{B,\,b\text{-}i} - J_{B,\,int}\right) - \frac{1}{\nu_A}\left(J_{A,\,b\text{-}i} - J_{A,\,int}\right) = 0 \qquad z=0 \text{ and } z=L \qquad (22)$$

$$\frac{1}{\nu_C}\left(J_{C,\,b\text{-}i} - J_{C,\,int}\right) + \frac{1}{\nu_A}\left(J_{A,\,b\text{-}i} - J_{A,\,int}\right) = 0 \qquad z=0 \text{ and } z=L \qquad (23)$$

$$\frac{1}{\nu_D}\left(J_{D,\,b\text{-}i} - J_{D,\,int}\right) + \frac{1}{\nu_A}\left(J_{A,\,b\text{-}i} - J_{A,\,int}\right) = 0 \qquad z=0 \text{ and } z=L \qquad (24)$$

$$J_{inert,\,b\text{-}i} = J_{inert,\,int} \qquad z=0 \text{ and } z=L \qquad (25)$$

There are eight mass balances at the membrane interfaces to be fulfilled and only six boundary conditions required to solve the set of equations (8-20) uniquely and therefore two mass balances seem to be superfluous.

Equations (22-25) introduce five new variables, $J_{A,\,b\text{-}i}$, $J_{B,\,b\text{-}i}$, $J_{C,\,b\text{-}i}$, $J_{D,\,b\text{-}i}$ and $J_{inert,\,b\text{-}i}$ at z=0 and at z=L and therefore ten additional equations specifying these molar fluxes from the bulk of the gas to the membrane interface are required. In order to describe the combination of flow and diffusion outside the membrane the film model is used. To specify the molar fluxes in the stagnant gas film caused by diffusion the Stefan Maxwell diffusion equation (26) is applied.

$$\sum_{j=1}^{j=nc} \frac{x_j J_{i,\,dif} - x_i J_{j,\,dif}}{P D_{ij}^{o}} = -\frac{1}{RT}\frac{dx_i}{dz} \qquad i = 1,\ldots,\,nc\text{-}1 \qquad (26)$$

The reason for the use of the Stefan Maxwell diffusion equation instead of Fick's law is that these equations are fundamentally to be preferred above Fick's diffusion equation in describing multi-component diffusion especially for the diffusion of the inert component that is present in large amounts.

Equations (26) give the diffusion fluxes of the components relative to eachother. In case of a pressure difference over the membrane, a part of the transport through the membrane is caused by viscous flow (see equation (15)) and this flow through the membrane also should pass the stagnant gas films representing mass transfer resistances in the gas phase outside the membrane. Owing to the fact that this is a flow through free space the pressure drop in the stagnant gas film is negligible. The combination of flow with diffusion is represented by equation (27).

$$J_{i,\,tot} = J_{i,\,dif} + x_i J_{flow} \qquad i = 1,\ldots,nc \qquad (27)$$

Using equations (27) to eliminate the diffusive fluxes in equations (26) results in equations (26) again for the total molar fluxes as the terms containing the molar flux caused by flow exactly cancel.

As equations (26) predict molar fluxes relative to eachother, only nc-1 independent equations

can be obtained for a system containing nc species and therefore equations (26) applied to both z=0 and z=L gives only eight equations. Therefore still two additional equations are required to solve the molar fluxes $J_{i,\,b\text{-}i}$, one at z=0 and one at z=L, specifying either an additional relation between the fluxes or specifying one of the molar fluxes. By these additional equations the molar fluxes are given relative to a fixed position, i.e. the membrane. The two mass balances at the membrane interfaces that seemed to be superfluous, owing to the number of boundary conditions at the membrane interfaces required, turn out to be necessary as fixing equations. Therefore equations (22-24) are used as boundary conditions at the membrane interfaces at z=0 and z=L and equations (25) are used as fixing equations at z=0 and z=L for the equations (26).

Because equations (26) introduce new derivatives, eight additional boundary conditions are required to solve equations (26). Boundary conditions used with equations (26) are four molar fractions $x_{A,\,bulk}$, $x_{B,\,bulk}$, $x_{C,\,bulk}$ and $x_{D,\,bulk}$, in the bulk of the gas at both sides of the membrane. The pressure P in the bulk of the gas at both sides of the membrane must also be specified because of equation (18) at z=0 and z=L. Finally the molar fraction of inert in the bulk of the gas at both sides is determined by the condition that the sum of the molar fractions in the bulk must be equal to one (equation (13)).

3. Solution method

The set of equations (8-26) can only be solved numerically. The numerical method used to solve the equations is a relaxation method (Press et. al., 1986). In the relaxation method the set of N differential equations is replaced by a set of N finite difference equations on a grid consisting of M grid points by using a chosen discretisation scheme. An initial solution of the set of N*M equations is obtained by specifying all N*M variables by an estimated guess. With these variables the deviation from the set of N*M equations is calculated and by a multi-dimensional Newton Raphson method new values of all variables are calculated. This iteration proces continues until the deviation of all equations is less then a specified value.

The numerical technique produces a matrix equation presented in equation (28).

$$\begin{bmatrix} \frac{\partial E_{1,\,k=1}}{\partial v_{1,\,k=1}} & \cdots & \frac{\partial E_{1,\,k=1}}{\partial v_{N,\,k=M}} \\ \vdots & & \vdots \\ \frac{\partial E_{N,\,k=M}}{\partial v_{1,\,k=1}} & \cdots & \frac{\partial E_{N,\,k=M}}{\partial v_{N,\,k=M}} \end{bmatrix} * \begin{bmatrix} dv_{1,\,k=1} \\ \vdots \\ dv_{N,\,k=1} \\ dv_{1,\,k=2} \\ \vdots \\ dv_{N,\,k=M} \end{bmatrix} = \begin{bmatrix} dE_{1,\,k=1} \\ \vdots \\ dE_{N,\,k=1} \\ dE_{1,\,k=2} \\ \vdots \\ dE_{N,\,k=M} \end{bmatrix} \qquad (28)$$

with $E_{i,j}$ the deviation of equation number i on grid point number j

$$d v_{i,j} = v_{i,j\,old} - v_{i,j\,new} \quad \text{where } v_{i,j\,old} \text{ is the present value of variable } v_i \text{ at } k=j$$

$$d E_{i,j} = E_{i,j\,old} - E_{i,j\,new} = E_{i,j\,old}$$

The discretisation of the first and second order derivatives of a variable v to the location in the membrane are based on the discretisation scheme given in equation (29).

$$\frac{d v}{d z}\Big|_k = \frac{v_{k+1} - v_{k-1}}{2 h} \quad \text{and} \quad \frac{d^2 v}{d z^2}\Big|_k = \frac{v_{k+1} - 2 v_k + v_{k-1}}{h^2} \tag{29}$$

As a Newton Raphson iteration is used, partial derivatives of the N*M equations to all N*M variables are required. To obtain a fast convergence behaviour of the numerical method, analytical expressions for the partial derivatives are preferred. Analytical expressions for all partial derivatives of the derivative of the molar fluxes to the location in the membrane used in equations (8 - 11), were derived from equations (15) by rearranging these equations to give explicit expressions for the molar fluxes (see equation 30 in vector notation).

$$\bar{J} = A^{-1} \bar{P} \tag{30}$$

$$\text{with } A_{ij} = - \frac{x_i}{P D_{ij}} \qquad i \neq j$$

$$A_{ij} = \sum_{\substack{l=1 \\ l \neq i}}^{nc} \frac{x_l}{P D_{il}} + \frac{1}{P D_{iK}} \qquad i = j$$

$$P_i = - \frac{x_i}{RT} \left(\frac{B_o}{\eta D_{iK}} + \frac{1}{P} \right) \frac{d P}{d z} - \frac{1}{RT} \frac{d x_i}{d z} \qquad i = 1, \ldots, nc$$

By differentiation of equation (30) to the location in the membrane z, analytical expressions for the derivatives of the molar fluxes are obtained (see equation 31 in vector notation).

$$\frac{d}{d z} \left(\bar{J} \right) = A^{-1} \bar{Q} \tag{31}$$

$$\text{with } Q_i = \sum_{j=1}^{nc} \frac{J_j \frac{dx_i}{dz} - J_i \frac{dx_j}{dz}}{P D_{ij}} + \frac{J_i}{P^2 D_{iK}} \frac{dP}{dz} + \frac{x_i}{P^2 RT} \left(\frac{dP}{dz} \right)^2 -$$

$$\frac{x_i}{RT} \left(\frac{B_o}{\eta D_{iK}} + \frac{1}{P} \right) \frac{d^2 P}{dz^2} - \frac{1}{RT} \left(\frac{B_o}{\eta D_{iK}} + \frac{1}{P} \right) \frac{dx_i}{dz} \frac{dP}{dz}$$

$$- \frac{1}{RT} \frac{d^2 x_i}{dz^2}$$

The matrix A in equation (31) is the same matrix as in equation (30). In the solution method partial derivatives of equation (31) to all variables v at all grid points are required. Calculation of these partial derivatives requires partial derivatives of the inverted matrix A. Before calculating the partial derivatives by hand, equations (30) and (31) are rearranged finally resulting in equations (32).

$$\frac{\partial}{\partial v_k} \left(\frac{d\bar{J}}{dz} \right) = A^{-1} \left\{ \frac{\partial}{\partial v_k} (\bar{Q}) - \left(\frac{\partial}{\partial v_k} (A) \right) \left(\frac{d\bar{J}}{dz} \right) \right\} \qquad (32)$$

$$\text{with } \frac{\partial}{\partial v_k} (\bar{J}) = A^{-1} \left\{ \frac{\partial}{\partial v_k} (\bar{P}) - \left(\frac{\partial}{\partial v_k} (A) \right) \bar{J} \right\}$$

The matrix inversion of A required at each grid point is calculated numerically.

Determination of the partial derivatives of the surface diffusion fluxes is straightforward as these molar fluxes are already written in an explicit form (see equations 19-20). Although writing out the partial derivatives requires a lot of work, the advantage is that numerical convergence can be expected to be faster than using approximated values for the partial derivatives.

Special attention must be paid to the discretisation of the boundary conditions given by equations (22-25). These equations require molar fluxes at the membrane interface which cannot be calculated according to the discretisation scheme given by equation (29) owing to the fact that the discretisation uses values of the molar fractions and pressures one grid point backward and also one grid point forward and one of the two is not available at the membrane interfaces. Using an alternative discretisation scheme at the interfaces is dangerous because of different break off errors introduced possibly resulting in numerical convergence without satisfying overall mass balances. As the reaction zone is normally located somewhere inside the membrane and not very close to one of the interfaces, the molar fluxes at the interfaces are replaced by the molar fluxes one grid point into the membrane giving equations (33-36).

$$\frac{1}{\nu_B} (J_{B,\,b\text{-}i} - J_{B,\,k}) - \frac{1}{\nu_A} (J_{A,\,b\text{-}i} - J_{A,\,k}) = 0 \qquad k=2 \text{ and } k=m\text{-}1 \qquad (33)$$

$$\frac{1}{\nu_C}\left(J_{C,\,b\text{-}i} - J_{C,\,k}\right) + \frac{1}{\nu_A}\left(J_{A,\,b\text{-}i} - J_{A,\,k}\right) = 0 \qquad k=2 \text{ and } k=m\text{-}1 \qquad (34)$$

$$\frac{1}{\nu_D}\left(J_{D,\,b\text{-}i} - J_{D,\,k}\right) + \frac{1}{\nu_A}\left(J_{A,\,b\text{-}i} - J_{A,\,k}\right) = 0 \qquad k=2 \text{ and } k=m\text{-}1 \qquad (35)$$

$$J_{inert,\,b\text{-}i} = J_{inert,\,k} \qquad k=2 \text{ and } k=m\text{-}1 \qquad (36)$$

Although physically it is possible that the reaction zone becomes located entirely at the membrane interface this will result in severe slip of reactant. The model is not able to predict the correct molar fluxes in this case.

Another point requiring attention is the calculation of the molar fluxes from the bulk of the gas to the membrane $J_{i,\,b\text{-}i}$ which should be obtained by solving the set of differential equations (26). Instead of solving these differential equations (26) they are linearized giving equations (37).

$$\sum_{j=1}^{nc} \frac{\bar{x}_j J_{i,\,b\text{-}i} - \bar{x}_i J_{j,\,b\text{-}i}}{D_{ij}^{o}} = -\frac{P}{RT}\frac{x_{i,\,int} - x_{i,\,bulk}}{\delta} \qquad (37)$$

$$\text{with } \bar{x}_i = \frac{x_{i,\,bulk} + x_{i,\,int}}{2}$$

It can be calculated that the deviation of the molar fluxes obtained from the linearized equations compared to the molar fluxes obtained from solving the differential equations is always less than 2 % provided the system is very diluted and the molar masses of the components do not differ much.

The matrix of size N*M with the partial derivatives of all equations to all variables consists of M*M block elements of size N*N, reflecting the M gridpoints, of the structure given in equation (38).

$$\begin{array}{c} k=1 \\ \\ \\ \\ \\ \\ \\ \\ \\ k=m \\ \\ k=1 \end{array} \begin{bmatrix} H & R_1 & R_2 & & & & & & \\ L_1 & H & R_1 & & & & & & \\ & L_1 & H & R_1 & & & & & \\ & & * & & & & & & \\ & & & * & & & & & \\ & & & & * & & & & \\ & & & & L_1 & H & R_1 & & \\ & & & & & L_1 & H & R_1 & \\ & & & & & L_2 & L_1 & H & \end{bmatrix} \begin{array}{c} \\ \\ \\ \\ \\ \\ \\ \\ \\ \\ k=m \end{array} \qquad (38)$$

H: block element on main diagonal

R: block element on right hand side diagonal

L: block element on left hand side diagonal

The discretization of the internal equations, from k=2 to k=m-1, at gridpoint k results in partial derivatives unequal to zero at the gridpoints k, k-1 and k+1 and therefore only the block elements H, L_1 and R_1 exist in equation (38). Owing to the fact that the equations at the membrane interfaces use molar fluxes at k=2 and at k=m-1 for respectively the left and right hand side boundary conditions, different blocks with partial derivatives exist in equation (38), i.e. two right hand blocks at k=1 and two left hand blocks at k=m besides the main diagonal element H.

To obtain the set of variables that are supposed to be better fulfilling the set of equations, the matrix in equation (38) is reduced to the identity matrix. This reduction takes place by successively reducing a block element on the main diagonal to the identity matrix and eliminating the left hand block one row below going from k=1 to k=m-1. Then L_2 and L_1 at k=m are eliminated using the main diagonal element, reduced to the identity matrix, at k=m-2 and k=m-1 respectively. From k=m-1 to k=2 the right hand blocks are then eliminated using the main diagonal blocks one row below. Finally R_1 and R_2 at k=1 are eliminated using the main diagonal element at k=2 and k=3 respectively.

To start the iteration proces initial values of all variables have to be specified. The molar fractions at the membrane interfaces are set equal to the given molar fractions in the bulk of the gas whereas molar fractions at all grid points inside the membrane are calculated taking linear molar fraction profiles between the membrane interfaces. The pressure profile is initiated in the same way.

Simulations were performed on a AT compatible computer provided with a mathematical coprocessor. The number of grid points used varied between 50 and 300 depending on the situation simulated. The number of grid points used was increased until overall mass balances were satisfied within 0.5%.

4. Numerical verification

For a number of asymptotic cases of the model developed in the present study analytical or approximate analytical solutions can be derived. Therefore it is possible to compare the results of the simulations of the numerically solved model with those of the analytical or approximate analytical solutions. In this way a verification of the model is obtained. The asymptotic cases studied are an instantaneous, irreversible reaction in the absence and in the presence of a pressure difference over the membrane. The different situations are being studied using the Claus reaction as a model reaction (Mark et. al., 1983).

$$2\,H_2S + SO_2 \rightleftharpoons \frac{3}{8}\,S_8 + 2\,H_2O \qquad (39)$$

Data concerning the Claus equilibrium are obtained from literature (Gamson and Elkins, 1953 and Verver, 1984). The analytical solutions of the asymptotic cases are derived using the Fick diffusion equation to describe multi-component diffusion, which is allowed only in case of very diluted, pseudo-binary systems and therefore the molar fractions of H_2S, SO_2, H_2O and S_8 in the bulk of

the gas phase at both sides of the membrane are fixed at low values (equal to or less than 0.01), the balance being N_2. Surface diffusion has been omitted in these simulations by setting the adsorption parameters b_i equal to zero.

The parameters used in the simulations are given in Table 1:

Table 1: Parameters used in the simulations.

membrane parameters: $L = 3 * 10^{-3}$ m

$\varepsilon/\tau = 0.10$

$d_p = 1$ μm (4.2)

adsorption parameters: $b_i = 0$ Pa^{-1} ($i = H_2S$, SO_2, S_8, H_2O and N_2)

gas composition:

	x_{H_2S}	x_{SO_2}	x_{S_8}	x_{H_2O}	P (bara)
H_2S side:	$2*10^{-3}$	$1*10^{-15}$	$1*10^{-4}$	$2*10^{-3}$	1.0
SO_2 side:	$1*10^{-15}$	$2*10^{-3}$	$1*10^{-4}$	$2*10^{-3}$	1.0

temperature: $T = 473$ K

equilibrium constant: $K_{eq} = 0.924*10^{-6} * \exp(1.274*10^4/T)$ (10^5 Pa)

(Verver, 1984)

number of grid points: 50 (§ 4.1), 300 (§ 4.2)

4.1 An instantaneous, irreversible reaction in the absence of a pressure difference over the membrane

In the case of an instantaneous, irreversible reaction in the absence of a pressure difference over the membrane analytical expressions for the molar fluxes can easily be derived (see appendix). The mass transfer resistances in the gas phase outside the membrane were neglected. The analytically derived molar flux of H_2S into the membrane is given by equation (40) and the molar flux of S_8 to the H_2S side is given by equation (41).

$$J_{H_2S} = \frac{P}{RT} \left(D^{eff}_{H_2S} \bar{x}_{H_2S} + 2 D^{eff}_{SO_2} \bar{x}_{SO_2} \right) \frac{1}{L} \qquad (40)$$

$$\text{with } D^{eff}_i = \frac{\varepsilon}{\tau} * \frac{1}{\frac{1}{D^0_{i/N_2}} + \frac{1}{D^0_{iK}}}$$

$$J_{S_8 L} = \frac{3}{16} \frac{P}{RT} 2 D^{eff}_{SO_2} \bar{x}_{SO_2} \frac{1}{L} \qquad (41)$$

For the comparison with the numerical model simulations were carried out in the absence of a pressure difference over the membrane at a temperature of 473 K and without mass transfer resistances outside the membrane. In Table 2 the molar fluxes of H_2S into the membrane and of S_8 out of the membrane to the H_2S side are given for different pore diameters of the membrane.

Table 2: Analytical and numerical molar fluxes for different pore diameters.

d_p (m)	J_{H_2S} $(\frac{mole}{m^2 s})$		$J_{S_8 L}$ $(\frac{mole}{m^2 s})$	
	analytical	numerical	analytical	numerical
10^{-9}	$7.503 * 10^{-7}$	$7.482 * 10^{-7}$	$8.347 * 10^{-8}$	$8.340 * 10^{-8}$
10^{-8}	$7.207 * 10^{-6}$	$7.186 * 10^{-6}$	$8.023 * 10^{-7}$	$8.017 * 10^{-7}$
10^{-7}	$5.160 * 10^{-5}$	$5.144 * 10^{-5}$	$5.781 * 10^{-6}$	$5.775 * 10^{-6}$
10^{-6}	$1.345 * 10^{-4}$	$1.340 * 10^{-4}$	$1.523 * 10^{-5}$	$1.521 * 10^{-5}$
10^{-5}	$1.602 * 10^{-4}$	$1.596 * 10^{-4}$	$1.821 * 10^{-5}$	$1.818 * 10^{-5}$
10^{-4}	$1.633 * 10^{-4}$	$1.627 * 10^{-4}$	$1.858 * 10^{-5}$	$1.854 * 10^{-5}$

From Table 2 it can be concluded that the molar fluxes calculated by the numerical model agree well with the analytically obtained molar fluxes. The numerically calculated molar fluxes are slightly lower (± 0.3 %) which could be caused by the fact that, in contrast to what is assumed, the Claus reaction is not entirely irreversible at the conditions used in the calculations (Sloot et. al., 1990).

4.2 An instantaneous, irreversible reaction in the presence of a pressure difference over the membrane

It is possible to derive an approximate analytical solution of the molar flux of H_2S into the membrane as a function of the pressure difference over the membrane in the situation of very diluted systems where multi-component diffusion can be described by Fick's law. It is necessary to assume that the reaction is irreversible and the pressure difference over the membrane must be low compared to the pressure level in order to use constant 'effective' diffusion coefficients that are independent of pressure. The molar flux of H_2S is calculated by equation (42) while the factor Y in equation (42) can be calculated from the implicit equation (19) given in the appendix. The constants introduced in equation (42) are defined in the appendix. For the derivation of equation (42) the reader is referred to the appendix.

$$J_{H_2S} = -\bar{x}_{H_2S} \frac{A_{H_2S} J_{visc} E_{H_2S} Y}{J_{visc}(1-Y) + A_{H_2S} Y (1-E_{H_2S})} \qquad (42)$$

The molar fluxes of H_2S into the membrane obtained from the simulations in the presence of a pressure difference over the membrane are compared to the molar fluxes calculated according to equation (42) in Table 3. It should be noted that the pressure difference over the membrane is not small compared to the pressure level which is a condition for the derivation of equation (42). Provided the pressure drop over the membrane is reasonably linear the calculation of effective diffusion coefficients at the average pressure in the analytical solution is however an acceptable approximation. The volumetric flow rate, owing to viscous flow through the membrane, increases with decreasing pressure and thus results in a higher gas velocity and an increase in pressure drop. Therefore non-linear pressure profiles can be expected for viscous flow through the membrane in principle. However, according to the 'Dusty-Gas Model' the molar flux of the inert component, nitrogen, which molar fraction is almost equal to one, is described by equation (43).

$$J_{inert} = -\frac{1}{RT}\left(D^{eff}_{inert,K} + \frac{B_o P}{\eta}\right)\frac{dP}{dz} \qquad (43)$$

The transport of inert is determined by viscous flow and Knudsen flow. When the relative contributions are calculated for a pore diameter of 1 μm and at atmosferic mean pressure, it appears that the viscous flow contribution causes less than 40% of the inert transport. As the Knudsen flow contribution results in a linear pressure profile it is concluded that the approximation of linear pressure profiles inside the membrane is reasonable. Therefore the numerically calculated molar fluxes of H_2S into the membrane can be compared to the analytically obtained values. The results are presented in Table 3.

Table 3: Verification of the molar fluxes in the presence of a pressure difference over the membrane. The parameters used are given in Table 1.

P_{H_2S} side	P_{SO_2} side	J_{H_2S} $(\frac{mole}{m^2 s})$	
(10^5 Pa)	(10^5 Pa)	approximate analytical	numerical
1.50	1.00	$3.172 * 10^{-4}$	$3.041 * 10^{-4}$
1.25	1.00	$1.658 * 10^{-4}$	$1.588 * 10^{-4}$
1.10	1.00	$1.103 * 10^{-4}$	$1.091 * 10^{-4}$
1.00	1.00	$1.109 * 10^{-4}$	$1.108 * 10^{-4}$
1.00	1.10	$1.608 * 10^{-4}$	$1.557 * 10^{-4}$
1.00	1.25	$3.085 * 10^{-4}$	$2.908 * 10^{-4}$

From Table 3 it can be concluded that the agreement between the numerically and analytically calculated molar fluxes of H_2S into the membrane is satisfactory with respect to the approximations necessary for the calculation of the molar fluxes according to the approximate analytical solution.

5. Numerical evaluation of the transport model

First simulations were carried out for conditions without surface diffusion both in the absence (5.1) and in the presence (5.2) of a pressure difference over the membrane. Next simulations were carried out to study the influence of surface diffusion both in the absence (5.3) and in the presence (5.4) of the instantaneous reversible reaction. In the latter simulations no pressure difference over the membrane was present.

5.1 Simulations in the absence of a pressure difference over the membrane

Simulations were performed at a temperature of 473 K in absence of surface diffusion. In Figure 1 the molar fraction profiles and the pressure profile inside the membrane are presented. Parameters used in this simulation are given in Table 1.

Figure 1: Profiles in the absence of surface diffusion and without a pressure difference at a temperature of 473 K

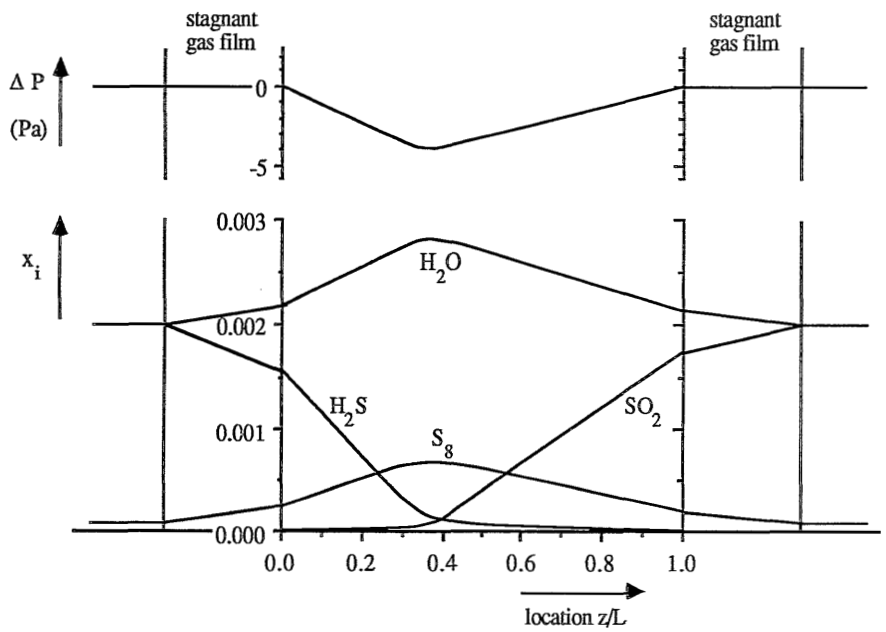

In Figure 1 it can be seen that at 473 K the reaction zone, owing to the high equilibrium constant of the Claus reaction, is small and at these conditions and this temperature the Claus reaction can be

considered to be almost irreversible.

As can be seen from the decrease of the molar fraction of the reactants H_2S and SO_2 and the increase of the molar fraction of the products S_8 and H_2O from the bulk of the gas to the membrane interface, mass transfer resistances in the gas phase are important for the conditions specified in Table 1 and must be taken into account.

The pressure inside the membrane shows a minimum at the location of the reaction zone although there is no overall pressure difference over the membrane. The occurrence of this minimum can be attributed to a higher molar fraction of inert at the reaction zone compared to the bulk of the gas on both sides of the membrane. This is caused by the fact that the number of gas molecules is reduced by the chemical reaction (see equation (39)). This results in a driving force for diffusion of the inert component out of the membrane to both sides. As the net transport of the inert is equal to zero, owing to the fact that there is neither an overall driving force for diffusion of inert or for viscous flow, an additional transport mechanism must be present to compensate for the diffusive transport. The pressure minimum results in viscous flow compensating for the diffusion of inert.

In Figure 2 the dependence of the molar flux of H_2S and of the created pressure difference on the pore diameter of the membrane is presented. As a change of the pore diameter effects the mass transfer resistance in the membrane this also results in a change of the contribution of the mass transfer resistances in the gas phase outside the membrane. Therefore simulations were performed with negligible mass transfer resistances in the gas phase ouside the membrane in order to eliminate this effect. Owing to the fact that the mass transfer resistance in the gas phase is eliminated and the reaction is assumed to be instantaneous, also at the membrane interfaces, the composition of the gas at both sides of the membrane must be set at equilibrium in these simulations. Otherwise a considerable conversion would occur at the interfaces of the gas phase and the membrane. The molar flux of H_2S for the different pore diameters has already been given in Table 2.

Figure 2: Molar flux of H_2S and ΔP at the pressure minimum as a function of the pore diameter

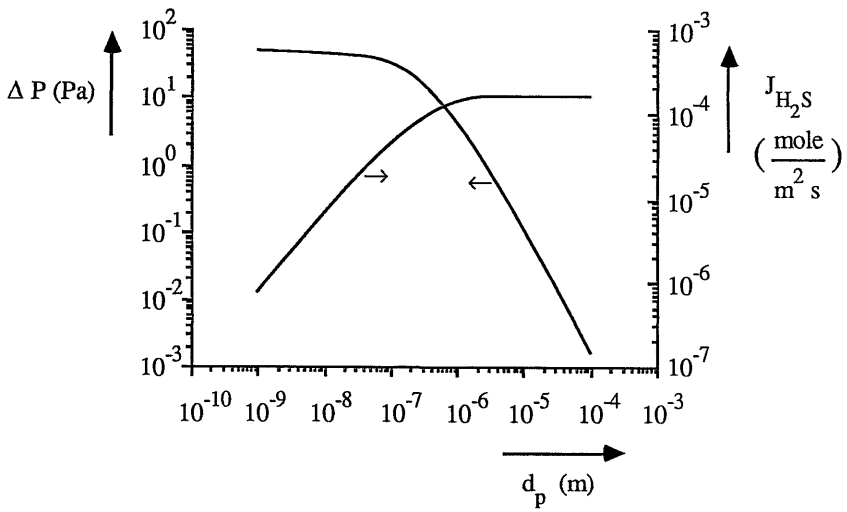

For small pore diameters ($<10^{-8}$ m) transport takes place in the Knudsen regime and as the Knudsen diffusion coefficient is directly proportional to the pore diameter (equation 17), the molar flux of H_2S is directly proportional to the pore diameter.

The molar fraction gradient of inert in the membrane is independent of the pore diameter because the transport of all components is affected identically by the pore diameter. Therefore the difference between the fraction of inerts in the bulk of the gas and at the reaction zone remains constant. As for small pores the transport of inert caused by a pressure gradient is determined by Knudsen diffusion and not by viscous flow both the diffusion owing to a molar fraction gradient of inert and the transport owing to a pressure gradient depend in the same way on the pore diameter of the membrane. Therefore the pressure minimum developed inside the membrane is independent of the pore diameter as can be seen in Figure 2.

For large pore diameters ($>10^{-6}$ m) transport takes place in the continuum regime and the molar flux of H_2S is not influenced by the pore diameter because the continuum diffusion coefficent is independent of the pore diameter of the membrane. Also for large pores the difference between the fraction of inert in the bulk of the gas and at the reaction zone remains constant. Therefore the transport of inert owing to diffusion is also independent of the pore diameter. The transport of inert into the membrane owing to a pressure minimum developed is caused by viscous flow which increases with d_p^2 (equations 15 and 18). In order to compensate for the transport of inert caused by diffusion, the pressure difference being developed must be proportional to d_p^{-2} which is shown in Figure 2.

Also from Figure 2 it can be concluded that in order to obtain high molar fluxes the pore diameter should be about 1 μm by preference. For larger pore diameters the molar fluxes remain constant. However, an increasing amount of viscous flow of inert in case of a pressure difference over the membrane occurs (Sloot et. al., 1990).

5.2 Numerical simulations in the presence of a pressure difference over the membrane

The membrane reactor usually is operated without a pressure difference over the membrane as the reactants must diffuse in stoichiometric ratio from opposite sides into the membrane. In practice a pressure difference over the membrane can occur e.g., in case of different pressure drops along the membrane area on both sides of the membrane. Therefore it is necessary to determine the influence of a pressure difference over the membrane on the reactor performance. These effects have been extensively explained (Sloot et. al., 1990) and from the simulations with the extended model it can be concluded that the occurrence of a pressure difference over the membrane results in similar phenomena as those observed with the simple model. Therefore the reader is referred to Sloot et. al. (1990).

5.3 *Numerical simulations in the presence of surface diffusion in the absence of a chemical reaction*

The transport in the membrane, owing to the combination of diffusion through the gas phase in the pores and surface diffusion has been studied is the absence of a chemical reaction. As in the simulations with a small reaction zone inside the membrane the molar fractions of H_2S and SO_2 are very low at the location of the reaction zone it is especially interesting to study the behaviour of surface diffusion at these low molar fractions. In the simulations the mass transfer resistances in the gas phase outside the membrane were negligible. In Table 4 the conditions used in the simulations are specified. Only H_2S is assumed to adsorb.

Table 4: Conditions used in the simulations of surface diffusion of H_2S through the membrane. The other parameters are given in Table 1.

gas composition:

	x_{H_2S}	x_{SO_2}	x_{S_8}	x_{H_2O}	P (bara)
H_2S side:	$1*10^{-2}$	eq.	$1*10^{-8}$	$1*10^{-2}$	1.0
SO_2 side:	$1*10^{-5}$	eq.	$1*10^{-8}$	$1*10^{-4}$	1.0

surface diffusion coefficient: $D_{i,s}^{eff} = 6 * 10^{-8}$ m^2/s

concentration of adsorption sites: $c_S = 9.5 * 10^{-6}$ (mole/m^2) (Sloot et. al., 1991)

In Figure 3 the molar fraction profiles of H_2S in the membrane are presented for different values of the adsorption parameter b_{H2S} and in Figure 4 the corresponding pressure profiles.

Figure 3: Molar fraction profiles of H_2S for different values of the adsorption parameter b_{H2S} in the absence of a chemical reaction.

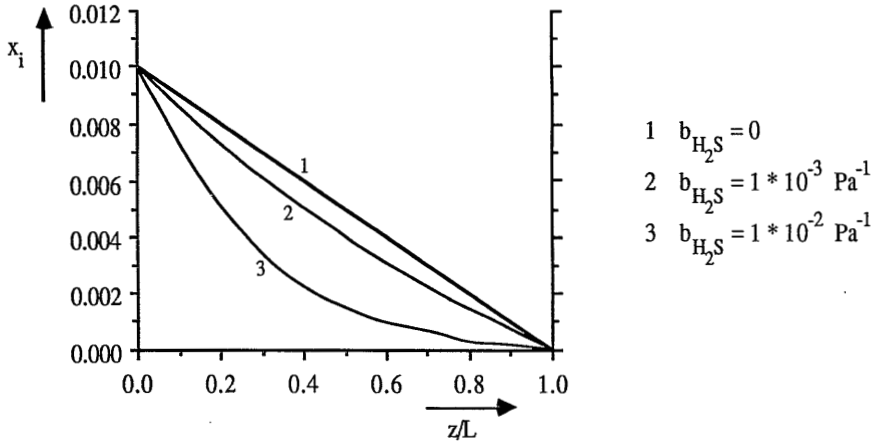

Figure 4: Pressure profiles inside the membrane belonging to the simulations in Figure 3.

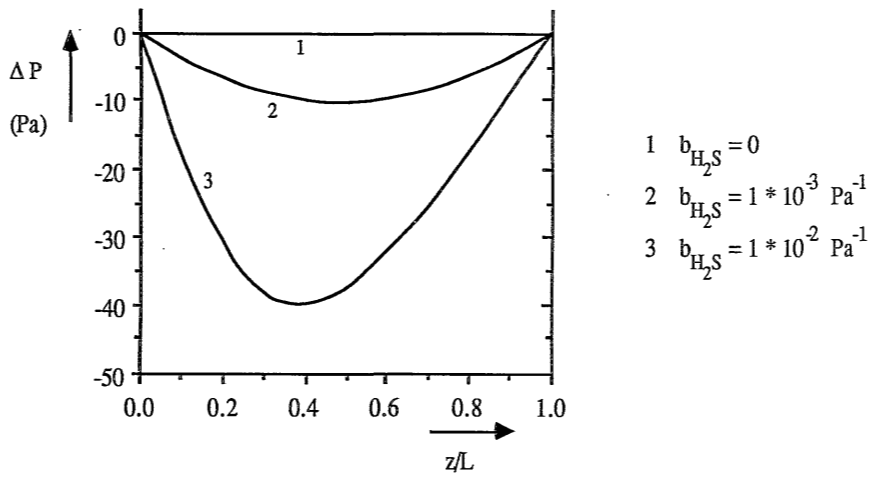

From Figure 3 it can be concluded that in the absence of surface diffusion, $b_{H2S} = 0$ and for low values of the adsorption parameter b_{H2S}, the expected straight molar fraction profile is obtained but for increasing values of the adsorption parameter the profiles become curved and simultaneously a minimum in the pressure is being developed. These effects can be explained by the degrees of coverage of the surface by H_2S. At low values of b_{H2S} the degree of coverage of the surface is relatively small and the gradient in the degree of coverage with the location is linear resulting in a certain constant molar flux of H_2S over the surface besides the transport through the gas phase in the pores of the membrane. Increasing the value of b_{H2S} results in an increasing degree of coverage of the surface and at the membrane side with the highest molar fraction of H_2S the gradient in the degree of coverage is relatively small (equation 20). At the side with the lower molar fraction of H_2S this gradient is steeper resulting in an increase of the molar flux of H_2S owing to surface diffusion. As the total molar flux of H_2S through the membrane is constant the molar flux through the gas phase in the pores of the membrane must decrease. This implicates a decrease of the molar fraction gradient of H_2S in the gas phase in the pores of the membrane resulting in a curved molar fraction profile of H_2S. However, owing to this curvature the molar fraction profile of inert must be curved also giving diffusive transport of inert varying with the position in the membrane. Therefore a pressure profile inside the membrane is developed as the molar flux of inert must remain constant. The existence of pressure profiles inside the membrane despite the absence of a pressure difference over the membrane caused by the change of surface diffusion along the pores of the membrane has been demonstrated by Asaeda et. al. (1981). The basic cause of the occurrence of a minimum in the pressure profile inside the membrane is the profile of the molar fraction of the inert component. The minimum in the profile of the molar fraction of inert can be caused e.g., by a change of the number of gas molecules by a chemical reaction (Figure 1) or the occurrence of surface diffusion in case of strong adsorption of one of the components (Figure 4).

In Table 5 the molar flux of H_2S is given for different values of the adsorption parameter b_{H2S}.

Table 5: Molar flux of H_2S caused by combined transport through a membrane with a pore diameter of 10 nm and 1 μm as a function of the adsorption parameter b_{H2S}

	J_{H_2S} $(\frac{mole}{m^2 s})$	
b_{H_2S} (Pa^{-1})	$d_p = 1 * 10^{-8}$ m	$d_p = 1 * 10^{-6}$ m
0	$1.46 * 10^{-5}$	$2.66 * 10^{-4}$
$1 * 10^{-5}$	$7.24 * 10^{-4}$	$2.73 * 10^{-4}$
$1 * 10^{-4}$	$6.52 * 10^{-3}$	$3.32 * 10^{-4}$
$1 * 10^{-3}$	$3.58 * 10^{-2}$	$6.26 * 10^{-4}$
$1 * 10^{-2}$	$6.49 * 10^{-2}$	$9.14 * 10^{-4}$

From Table 5 it can be concluded that surface diffusion can play an important role even in membranes with a large pore diameter provided the surface concentration is high enough compared to the concentration in the gas phase.

5.4 Numerical simulations in the presence of a chemical reaction in the membrane

A numerical simulation was performed in the presence of the chemical reaction inside the membrane and with an adsorption parameter b_i for H_2S equal to $1*10^{-3}$ Pa^{-1}. Molar fractions in the bulk of the gas are the same as used in the simulation presented in Figure 1 and are given in Table 1. Figure 5 shows the molar fraction profiles and the pressure profile in the membrane.

Figure 5: Profiles in the presence of a chemical reaction and surface diffusion without pressure difference over the membrane ($b_{H2S} = 1 * 10^{-3}$ Pa^{-1}).

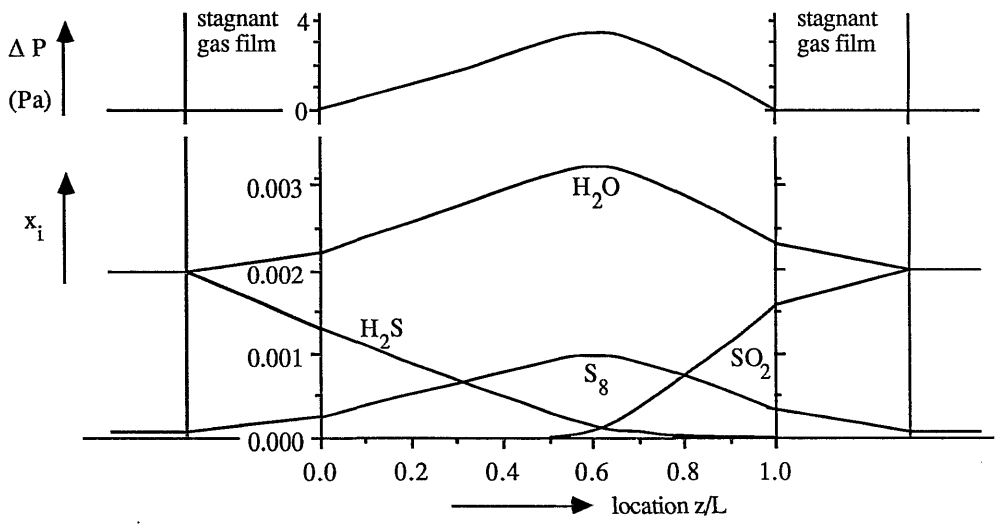

From the comparison between Figures 1 and 5 it can be concluded that a maximum in the pressure profile is developed (Figure 5) instead of a minimum (Figure 1) and the location of the reaction zone is shifted substantially towards the SO_2 side of the membrane. The shift of the reaction zone is caused by the fact that transport of H_2S is increased by surface diffusion in contrast to the transport of SO_2. In order to maintain stoichiometric molar fluxes of H_2S and SO_2 the location of the reaction zone shifts towards the SO_2 side.

Owing to the increased transport of H_2S by surface diffusion the molar fluxes of the reactants into the membrane are increased and therefore at the reaction zone a larger amount of products are formed. Therefore higher molar fluxes of the products out of the membrane are necessary which results in an increase of the maximum in the molar fraction profiles of the products at the reaction zone. It appears that the molar fraction of inert at the reaction zone becomes lower than the molar fraction of inert in the bulk of the gas resulting in a driving force for diffusion of inert into the membrane, contrary to the situation in Figure 1. A maximum in the pressure profile is required to keep the molar flux of inert constant through the membrane. From these simulations it can be concluded that for the determination of whether a maximum or a minimum in the pressure profile is to be expected it is not enough to look at the stoichiometry of the reaction only (whether the number of gaseous molecules increases or decreases by the reaction) but the mobilities of the different species, the molar flux owing to a certain driving force, must also be taken into account.

6. Comparison of the results of the numerical model with those of the previous model

A simplified model predicting molar fluxes and molar fraction profiles in case of an instantaneous reversible reaction inside a membrane with reactants coming from opposite sides of the membrane was presented earlier (Sloot et. al., 1990). In this simplified model transport is described by a combination of viscous flow and molecular diffusion described by Fick's law. By comparison of the results of the present model with the results obtained from the simplified model the validity of the approach in the simplified model to describe multi-component diffusion by Fick's law instead of by Stefan Maxwell diffusion relations can be checked. In 6.1 the situation in the absence of a pressure difference over the membrane and in 6.2 the situation in the presence of a pressure difference over the membrane is studied.

6.1 Comparison of both models in the absence of a pressure difference over the membrane

Simulations were performed at a temperature of 523 K at different molar fractions of H_2S in order to simulate both in the dilute, pseudo-binary regime where multi-component diffusion is adequately described by Fick's law and in the concentrated regime where deviations between the models can be expected. In all simulations the molar fraction of SO_2 in the bulk of the gas has been set at 0.75 times the molar fraction of H_2S in the bulk of the gas at the H_2S side. Molar fractions of the products in the bulk of the gas are fixed at the values given in Table 1. The aim of the simulations is to determine whether the present model and the simplified model predict the same

molar fluxes. For the conditions of high molar fractions of H_2S and SO_2 these simulations are not realistic in the sense that the partial pressure of elemental sulfur at the reaction zone inside the membrane exceeds its saturated vapour pressure at 523 K. The ratio of the molar fluxes predicted by the simplified model and by the present model is plotted as a function of the molar fraction of H_2S in the bulk of the gas at the H_2S side. In Figure 6 the ratio of the molar fluxes of H_2S, Figure 6a, of elemental sulfur towards the H_2S side, Figure 6b, of the slip of SO_2 and H_2S, Figures 6c and 6d respectively, and of the inert component, Figure 6e, is presented.

Figure 6: Comparison of the molar fluxes predicted by both transport models, the Dusty-Gas Model and the simplified model (Sloot et. al., 1990) in absence of a pressure difference over the membrane

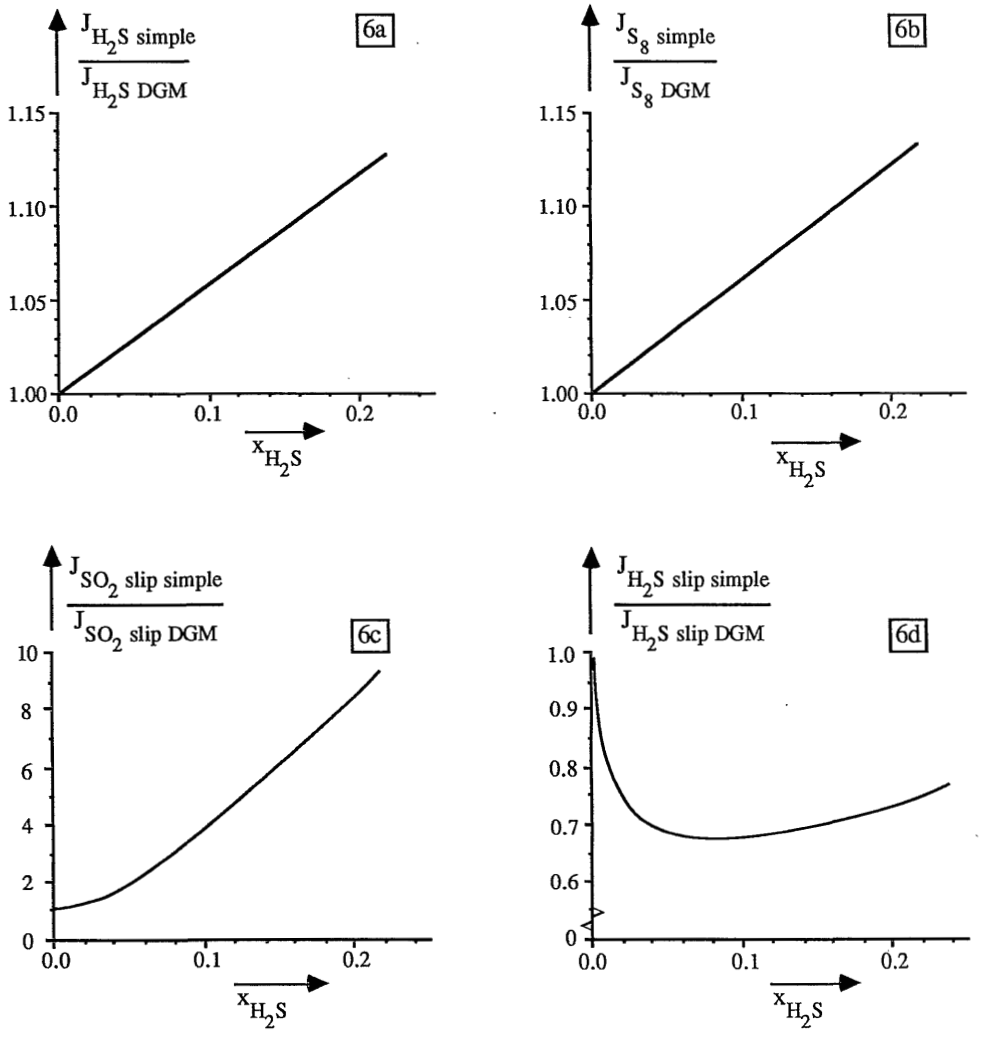

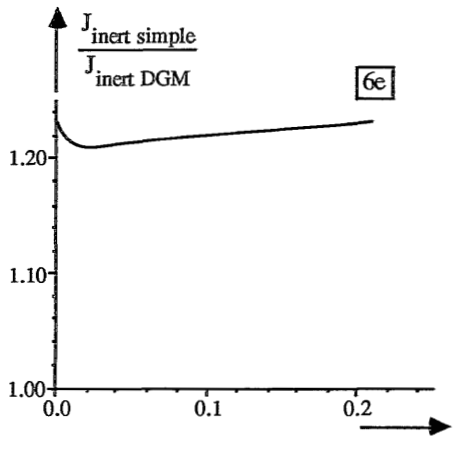

Ratio's of the molar fluxes of:

6a: H_2S into the membrane
6b: S_8 out of the membrane to the H_2S side
6c: SO_2 out of the membrane to the H_2S side
6d: H_2S out of the membrane to the SO_2 side
6e: inert through the membrane

From Figure 6 it can be concluded that in case of a low molar fraction of H_2S, both models predict the same molar fluxes of H_2S, elemental sulfur towards the H_2S side and the slip of H_2S and SO_2 as can be expected in the pseudo-binary regime where multi-component diffusion can adequately be described by Fick's law. However the deviation of the molar flux of inert predicted by both models is about 20%. For the inert component the system cannot be regarded as dilute and therefore the description of the transport of inert by the simplified model using Fick's law is fundamentally not correct. The difference between the molar fluxes of inert calculated by both models is probably caused by the net total molar flux unequal to zero resulting in a drag force on the inert component according to the description of diffusion by Stefan Maxwell as present in the Dusty-Gas Model which is not taken into account by the simplified model.

Looking at the ratio of the molar fluxes predicted by both models at higher molar fractions of H_2S it appears that the agreement between the molar fluxes of H_2S and of elemental sulfur towards the H_2S side predicted by both models is reasonably good (15% difference at maximum). The slip of H_2S and SO_2 predicted by both models however shows large differences, the slip of H_2S predicted by the simplified model being lower than predicted by the present model and the slip of SO_2 being higher. These differences can probably be attributed to the fact that the net molar flux is larger than zero. As a consequence there is a drag force on all components from the H_2S side towards the SO_2 side resulting in a small shift of the reaction zone towards the SO_2 side. Therefore the slip predicted by the present model of H_2S is larger and the slip of SO_2 is smaller compared to those predicted by the simplified model. In order to check the explanation of these phenomena by the fact that the net molar flux is larger than zero a simulation was performed with a reduced molar fraction of SO_2 at the SO_2 side, the molar fraction of H_2S being 0.05, resulting in a net molar flux into the membrane at the H_2S side of about zero. As a result the slip of SO_2 predicted by both models is the same within 0.5%. Surprisingly the H_2S slip predicted by the simplified model is 27% lower compared to the slip calculated by the present model. Although the net molar flux at the SO_2 side is slightly negative, therefore going into the membrane, and therefore it would be expected that the slip of H_2S predicted by the present model is lower compared to the slip of H_2S calculated by the simplified model. Apparently the argument of the net molar flux is a necessary but not sufficient condition.

6.2 Comparison of both models in the presence of a pressure difference over the membrane

To compare the molar fluxes in the presence of a pressure difference over the membrane calculated by both models simulations were carried out at a pressure difference of 0.25 bar over the membrane with the highest pressure at the H_2S side. Mass transfer resistances in the gas phase were made negligible. The molar fractions of H_2S and SO_2 were varied in the same way as described in 5.1. Further conditions were kept the same as in 6.1. In Figure 7 the different molar fluxes calculated by both models are compared by giving their ratio as a function of the molar fraction of H_2S.

Figure 7: Comparison of the molar fluxes predicted by both transport models, the Dusty Gas Model and the simplified model (Sloot et. al., 1990) in presence of a pressure difference of 0.25 bar over the membrane

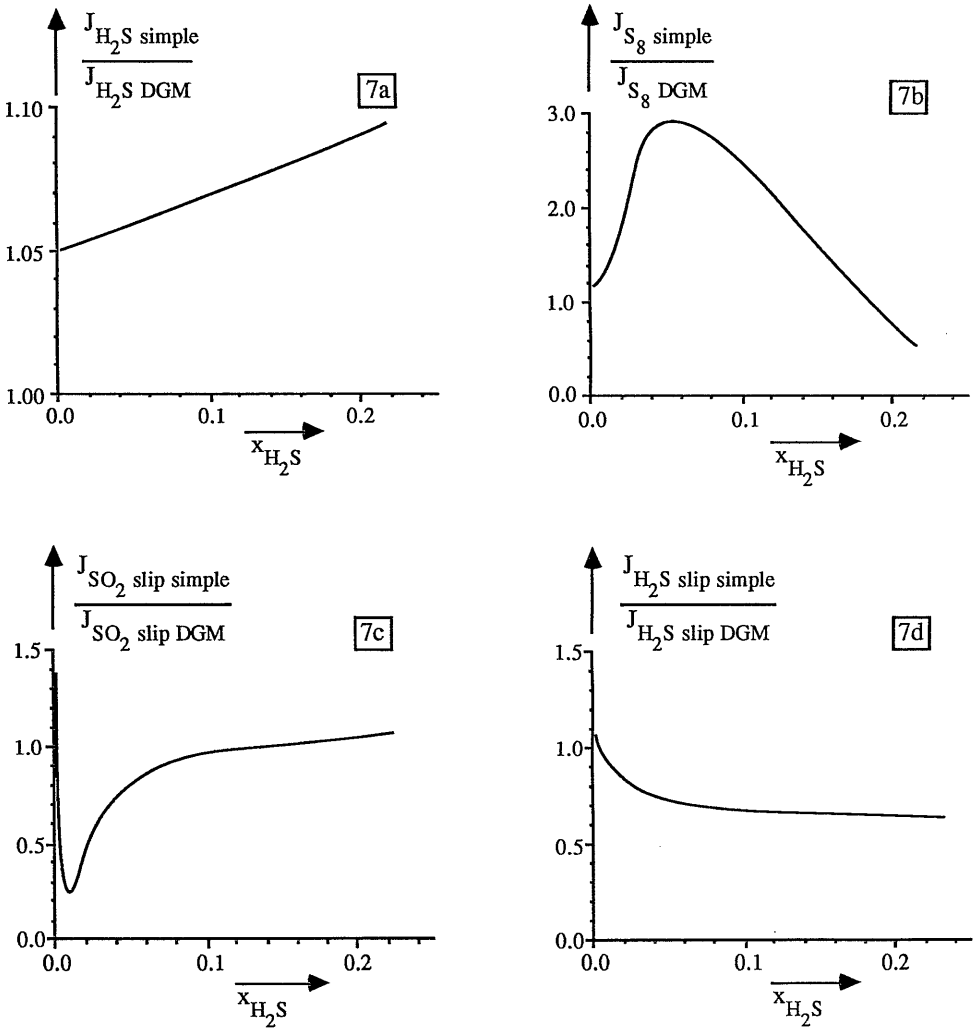

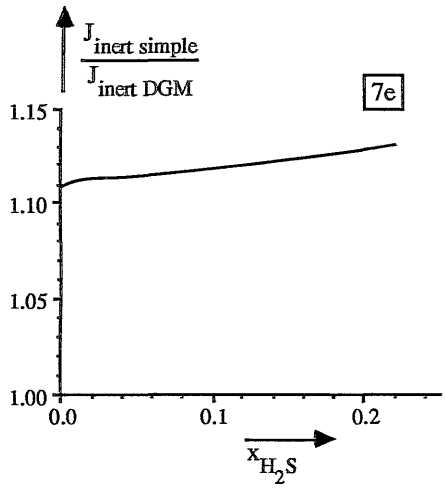

Ratio's of the molar fluxes of:

7a: H_2S into the membrane
7b: S_8 out of the membrane to the H_2S side
7c: SO_2 out of the membrane to the H_2S side
7d: H_2S out of the membrane to the SO_2 side
7e: inert through the membrane

Although convergence was always obtained by the simplified model the agreement of the overall mass balances was relatively bad (deviations up to 6% occurred). Increasing the number of grid points did not reduce these deviations, but the molar fluxes calculated were hardly influenced and are therefore believed to be reliable. In the simulations using the present model this problem did not occur, deviations of the overall mass balances were always less than 0.3% and the molar fluxes calculated did not change with increasing number of grid points.

From Figure 7 it can be seen that the molar fluxes of H_2S into the membrane predicted by both models agrees reasonably, although the molar flux calculated by the simplified model is 5 to 10% higher than the molar flux calculated by the present model. This is probably caused by the fact that the molar fluxes of inert calculated by the simplified model are always higher resulting in a higher viscous contribution of the molar flux of H_2S into the membrane compared to the viscous contribution in the present model. The large deviation in the molar flux of elemental sulfur towards the H_2S side predicted by both models at a molar fraction of H_2S of 6% can be explained in the following way. The molar flux of elemental sulfur towards the H_2S side is determined by two oppositely directed contributions; a viscous one resulting in a molar flux of sulfur into the membrane at the H_2S side and a diffusive one resulting in a molar flux out of the membrane to the H_2S side. The viscous contribution does not depend very much on the molar fraction of H_2S at the conditions studied but the diffusive contribution depends quite a lot on the molar fraction of H_2S as a higher molar fraction of H_2S results in a higher production rate of elemental sulfur inside the membrane which has to be transported out of the membrane. At molar fractions of H_2S up to 1%, the viscous contribution of the transport of elemental sulfur dominates resulting in a appreciable flux of elemental sulfur into the membrane at the H_2S side. At a molar fraction of H_2S of 10% and higher, the diffusive contribution dominates resulting in a appreciable molar flux of sulfur out of the membrane at the H_2S side. In both situations the deviation between the molar fluxes of sulfur to the H_2S side is relatively small. In case of a molar fraction of H_2S between 1 and 10% the diffusive and the viscous contribution are about equal and therefore the resulting fluxes of sulfur are relatively small. As the molar flux of inert predicted by both models differs about 12% this

results in a relatively small difference in the viscous contribution. Owing to the fact that the molar flux of sulfur is caused by two about compensating transport mechanisms, the relative difference in the total molar fluxes of elemental sulfur to the H_2S side predicted by both models is quite substantial.

The slip of H_2S to the SO_2 side and vice versa predicted by both models are of the same order of magnitude although the differences are up to about 70%. It is remarkable that the agreement in the slip of SO_2 calculated by both models is much better compared to the situation without a pressure difference over the membrane.

7. Conclusions

A mathematical model is presented describing mass transport owing to molecular diffusion and viscous flow in combination with an instantaneous reversible reaction in a membrane with the reactants coming from opposite sides of the membrane. The model is based on the so called 'Dusty Gas Model' (Mason and Malinauskas, 1983) extended with surface diffusion. Mass transfer resistances in the gas phase outside the membrane are taken into account. As a model reaction to study the model of this membrane reactor the Claus reaction is chosen.

It is demonstrated that pressure profiles inside the membrane are developed even in the absence of an overall pressure difference over the membrane. To determine whether a maximum or a minimum of the pressure will occur it is not sufficient to just look at the stoichiometry of the reaction but the mobilities of the different species should also be taken into account.

The present model is used to determine the validity of a previously presented simplified model (Sloot et. al., 1990). From this comparison it is concluded that the simplified model qualitatively predicts the correct molar fluxes including the slip of reactants to the opposite side of the membrane both in absence and in the presence of a moderate pressure difference over the membrane provided the molar fractions of the reactants and products remain low compared to the molar fraction of inert (dilute systems).

Notation

A_i	constant defined in the appendix	mole / m^2 s
A_{ij}	matrix element defined in equation (30)	
b_i	adsorption constant of a component	Pa^{-1}
B_i	constant defined in the appendix	
B_o	membrane specific parameter defined by equation 18	m^2
C_i	constant defined in the appendix	
c_S	surface concentration of adsorption sites	mole / m^2
D_{ij}	effective continuum diffusion coefficient of component i in j	m^2 / s
D_{iK}	effective Knudsen diffusion coefficient of component i	m^2 / s
D_{iS}	effective surface diffusion coefficient	m^2 / s
d_p	mean pore diameter	m

E_i	constant defined in the appendix	
E_{ij}	deviation of equation i on grid point number j	-
h	membrane thickness L divided by the number of grid points M	m
$J_{i,\,gas}$	molar flux of component i through the gas phase	mole / m^2 s
$J_{i,\,tot}$	total molar flux of component i	mole / m^2 s
$J_{i,\,surf}$	molar flux of component i over the surface	mole / m s
k	grid point number	-
K_{eq}	equilibrium constant	
L	membrane thickness	m
M	number of grid points	-
M_i	molar mass	kg / mole
m	constant defined in the appendix	-
nc	number of components	-
P	pressure	Pa
P_i	variable defined in equation (30)	
Q_i	variable defined in equation (31)	
R	gas constant	J / mole K
R_i	reaction rate	mole / m^3 s
T	temperature	K
v	general variable used in equation (28)	
x	molar fraction	-
Y	parameter defined in the appendix	
Z	constant defined in the appendix	
z	location inside the membrane	m

Greek symbols:

δ	thickness of the stagnant gas film outside the membrane	m
δ_r	location of the reaction plane, used in the appendix	m
ε	porosity of the membrane	-
η	viscosity	Pa s
ν	stoichiometric coefficient	-
θ_i	fraction of surface covered by component i	-
τ	tortuosity of the membrane	-

indices:

A	reactant
B	reactant
b-i	from the bulk of the gas to the membrane interface
bulk	in the bulk of the gas
C	product
D	product

dif	diffusive
flow	viscous flow
i	general component
inert	component
int	membrane interface
tot	total

References

Asaeda M., J. Watanabe, Y. Matono, K. Kojima and R. Toei, 1981, Combined surface and gas phase diffusion through plugs of porous adsorbents in transition diffusion regime, J. Chem. Eng. Jpn. **14**(1), 13-19

Gamson B.W. and R.H. Elkins, 1953, sulfur from hydrogen sulfide, Chem. Eng. Progr. **49**(4), 203-215

Mark H.F., D.F. Othmer, C.G. Overberger and G.T. Seaborg, 1983, Kirk-Othmer, Encyclopedia of Chemical Technology, vol. 22, John Wiley & Son, New York

Mason E.A. and A.P. Malinauskas, 1983, Gas transport in porous media: The Dusty-Gas Model, Chemical Engineering Monographs 17, Elsevier, Amsterdam

Press W.H., B.P. Flannery, S.A. Teukolsky and W.T. Vetterling, 1986, Numerical Recipes: the art of scientific computing, Cambridge University Press, Cambridge

Reid R.C., J.M. Prausnitz and T.K. Sherwood, 1977, The properties of gases and liquids, 3rd edition, McGraw-Hill, New York

Sloot H.J., G.F. Versteeg and W.P.M. van Swaaij, 1990, A non-permselective membrane reactor for chemical processes normally requiring strict stoichiometric feed rates of reactants, Chem. Eng.Sci. **45**(8), 2415-2421, chapter 2 in this thesis

Sloot H.J., G.F. Versteeg, C.A. Smolders and W.P.M. van Swaaij, 1991, Surface diffusion of hydrogen sulfide and sulfur dioxide in alumina membranes in the continuum regime, to be published, chapter 3 in this thesis

Verver A.B., 1984, The catalytic oxidation of hydrogen sulphide to sulphur in a gas-solid trickleflow reactor, thesis, Twente University, The Netherlands

Appendix: Approximate analytical molar fluxes in limiting situations

Analytical, approximate solutions for the calculation of the molar flux of H_2S have been derived for two specific asymptotic cases. The situations studied are an instantaneous, irreversible reaction in the absence and in the presence of a pressure difference over the membrane. In the first case, an analytical expression for the molar flux of H_2S is derived both with and without mass transfer resistances in the gas phase. In the presence of a pressure difference over the membrane, mass transfer resistances in the gas phase become very important. Therefore in the analytical expression derived for the calculation of the molar flux of H_2S these resistances were taken into account. In the derivation of the analytical solutions, diffusion is described by Fick's law and therefore the expressions obtained can only be expected to be valid in situations where a multi-component system can adequately be described by a pseudo binary system which is the case in dilute systems. These models are set up for the Claus reaction given in equation (1).

$$2\,H_2S + SO_2 \rightleftharpoons \frac{3}{8}\,S_8 + 2\,H_2O \qquad (1)$$

1. An instantaneous, irreversible reaction in the absence of a pressure difference over the membrane:

In this situation a reaction zone is present at the position δ_r in the membrane, which position is such that the molar fluxes of H_2S and SO_2 are in stoichiometric ratio. Because there is no pressure difference over the membrane and the molar fractions of both H_2S and SO_2 are sufficiently low Fick's diffusion law can be applied. The transport of H_2S and SO_2 is determined by ordinary diffusion and the molar fraction profiles are linear. The molar fluxes of H_2S and SO_2 are given in equation (2).

$$J_{H_2S} = D^{eff}_{H_2S}\,\frac{P}{RT}\,\frac{x^{int}_{H_2S}}{\delta_r} \quad \text{and} \quad J_{SO_2} = -\,D^{eff}_{SO_2}\,\frac{P}{RT}\,\frac{x^{int}_{SO_2}}{L-\delta_r} \qquad (2)$$

It should be noted that the molar flux of SO_2 is directed opposite to the molar flux of H_2S. The mass-transfer resistances in the gas phase outside the membrane are represented by equations (3).

$$J_{H_2S} = k_{g,\,H_2S}\,\frac{P}{RT}\left(\bar{x}_{H_2S} - x^{int}_{H_2S}\right) \qquad (3a)$$

$$J_{SO_2} = -\,k_{g,\,SO_2}\,\frac{P}{RT}\left(\bar{x}_{SO_2} - x^{int}_{SO_2}\right) \qquad (3b)$$

The molar fractions of H_2S and SO_2 at the membrane interfaces are eliminated by combining equations (2) and (3) resulting in the molar fluxes presented by equations (4).

$$J_{H_2S} = \frac{P}{RT} \frac{\bar{x}_{H_2S}}{\frac{1}{k_{g,\,H_2S}} + \frac{\delta_r}{D^{eff}_{H_2S}}} \tag{4a}$$

$$J_{SO_2} = -\frac{P}{RT} \frac{\bar{x}_{SO_2}}{\frac{1}{k_{g,\,SO_2}} + \frac{L-\delta_r}{D^{eff}_{SO_2}}} \tag{4b}$$

The location of the reaction plane δ_r is eliminated by the condition of stoichiometry of the molar fluxes of H_2S and SO_2 resulting in the expression for the molar flux of H_2S given in equation (5).

$$J_{H_2S} = \frac{P}{RT} \frac{\bar{x}_{H_2S} D^{eff}_{H_2S} + 2\bar{x}_{SO_2} D^{eff}_{SO_2}}{\frac{D^{eff}_{H_2S}}{k_{g,\,H_2S}} + \frac{D^{eff}_{SO_2}}{k_{g,\,SO_2}} + L} \tag{5}$$

The denominator represents a series of mass transfer resistances; gas phase mass transfer resistances both at the H_2S and at the SO_2 side and the membrane resistance. In case mass transfer resistances in the gas phase are absent the denominator reduces to the membrane thickness L.

The effective diffusion coefficients of H_2S and SO_2 in equation (5) are calculated according to equation (6) taking Knudsen and continuum diffusion into account by the concept of diffusive resistances in series.

$$D^{eff}_i = \frac{1}{\frac{1}{\frac{\varepsilon}{\tau} D^{o}_{i/N_2}} + \frac{1}{\frac{\varepsilon}{\tau} D^{o}_{iK}}} \tag{6}$$

The continuum diffusion coefficients and the Knudsen diffusion coefficients are calculated by gas kinetic theory (Reid et. al., 1977).

2. *An instantaneous, irreversible reaction in the presence of a pressure difference over the membrane:*

Also for this situation a reaction plane exists at position δ_r. The difference with the first situation is the fact that because of the pressure difference over the membrane, a viscous flow through the membrane is present increasing the transport of the high pressure side reactant and decreasing the transport of the low pressure side reactant. In Figure 1 a schematic drawing of the molar fraction profiles is given.

Figure 1: Schematical molar fraction profiles in case of an irreversible, instantaneous reaction in the presence of a pressure difference over the membrane.

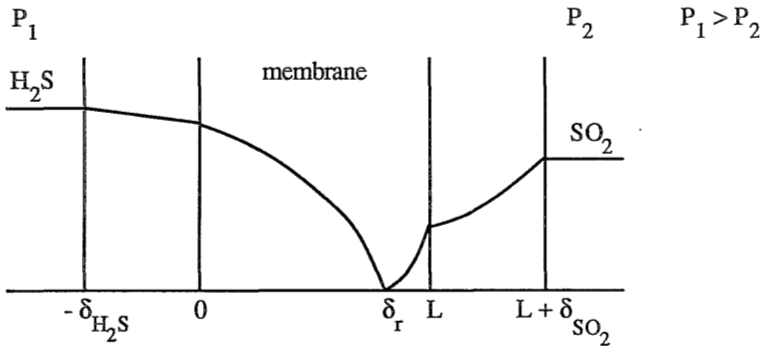

Transport of H_2S and SO_2 through the gas phase outside the membrane at either side is described by a combination of viscous flow and molecular diffusion as presented by equation (7).

$$J_i = x_i J_{visc} - D^o_{i/N_2} \frac{P}{RT} \frac{dx_i}{dz} \tag{7}$$

In the gas phase no pressure gradient is present and diffusion is determined by continuum diffusion. Equation (7) is integrated using the boundary condition that at the interface of the bulk of the gas with the gas film $z = -\delta_{H2S}$ the molar fraction of H_2S is equal to the molar fraction of H_2S in the bulk of the gas. The resulting equation is applied to the membrane interface at $z = 0$ resulting in equation (8) for the molar flux of H_2S.

$$J_{H_2S} = J_{visc} \frac{x^{int}_{H_2S} - \bar{x}_{H_2S} \exp\left(\frac{RT}{P} J_{visc} \frac{\delta_{H_2S}}{D^o_{H_2S}}\right)}{1 - \exp\left(\frac{RT}{P} J_{visc} \frac{\delta_{H_2S}}{D^o_{H_2S}}\right)} \tag{8}$$

The unknown variables in equation (8) are the viscous flow, J_{visc}, and the molar fraction of H_2S at the membrane interface, $x_{H2S,\,int}$.

The molar flux of SO_2 into the membrane is calculated in the same way using the boundary condition that at $z = L + \delta_{SO2}$ the molar fraction of SO_2 is equal to the molar fraction of SO_2 in the bulk of the gas and is given by equation (9).

$$J_{SO_2} = J_{visc} \frac{x^{int}_{SO_2} - \bar{x}_{SO_2} \exp\left(-\frac{RT}{P} J_{visc} \frac{\delta_{SO_2}}{D^o_{SO_2}}\right)}{1 - \exp\left(-\frac{RT}{P} J_{visc} \frac{\delta_{SO_2}}{D^o_{SO_2}}\right)} \tag{9}$$

In case of low molar fractions of the reactants, the transport of reactants inside the membrane can be described by equation (10) according to the 'Dusty-Gas Model' (Mason and Malinauskas, 1983) which takes into account viscous flow, ordinary diffusion and pressure diffusion.

$$J_i = x_i J_{visc} - \frac{D^{eff}_i}{RT} \frac{d(x_i P)}{dz} \tag{10}$$

If the pressure difference over the membrane is small compared to the absolute pressure, the effective diffusion coefficient can be considered independent of the pressure and its value is calculated by equation (6) at the average pressure. The viscous flow is assumed to be equal to the inert flow because of the very dilute system and can be calculated with equation (11).

$$J_{visc} = -\frac{1}{RT}\left(D^{eff}_{N_2 K} + \frac{B_o P}{\eta}\right)\frac{dP}{dz} \tag{11}$$

Since the transport of inert is determined almost entirely by viscous flow J_{visc} is independent of the position in the membrane. If the pressure difference over the membrane is small compared to the pressure level integration of equation (11) results in an almost linear pressure drop through the membrane. Transport of H_2S and SO_2 is then described by equation (12).

$$J_i = x_i(z)\, J_{visc} - \frac{D^{eff}_i}{RT}\left(x_i(z)\frac{P_2 - P_1}{L} + \bar{P}\frac{dx_i}{dz}\right) \tag{12}$$

Boundary conditions required for integrating equations (12) are the molar fractions of H_2S at the membrane interface at the H_2S side and of SO_2 at the SO_2 side for the molar flux of H_2S and SO_2

respectively. The resulting equations are applied at the reaction plane $z=\delta_r$ where the molar fractions of H_2S and SO_2 are equal to zero and the molar fluxes are given by equations (13 - 14).

$$J_{H_2S} = - \frac{x^{int}_{H_2S} \left(J_{visc} - \frac{D^{eff}_{H_2S}}{RT} \frac{P_2 - P_1}{L} \right) \exp\left(\left(\frac{RT}{P_{av}} \frac{J_{visc}}{D^{eff}_{H_2S}} - \frac{P_2 - P_1}{P_{av} L} \right) \delta_r \right)}{1 - \exp\left(\left(\frac{RT}{P_{av}} \frac{J_{visc}}{D^{eff}_{H_2S}} - \frac{P_2 - P_1}{P_{av} L} \right) \delta_r \right)} \tag{13}$$

$$J_{SO_2} = - \frac{x^{int}_{SO_2} \left(J_{visc} - \frac{D^{eff}_{SO_2}}{RT} \frac{P_2 - P_1}{L} \right) \exp\left(\left(\frac{RT}{P_{av}} \frac{J_{visc}}{D^{eff}_{SO_2}} - \frac{P_2 - P_1}{P_{av} L} \right) (\delta_r - L) \right)}{1 - \exp\left(\left(\frac{RT}{P_{av}} \frac{J_{visc}}{D^{eff}_{SO_2}} - \frac{P_2 - P_1}{P_{av} L} \right) (\delta_r - L) \right)} \tag{14}$$

In order to simplify the representation of the equations three constants are introduced presented in equations (15a - 15c).

$$A_i = J_{visc} - \frac{D^{eff}_i}{RT} \frac{P_2 - P_1}{L} \tag{15a}$$

$$B_i = \frac{D^{eff}_i}{RT} P_{av} \tag{15b}$$

$$C_i = \frac{D^{o}_i}{RT} P_{av} \tag{15c}$$

The molar fractions of H_2S and SO_2 at the membrane interfaces are eliminated by combining equations (8) and (13) for H_2S and equations (9) and (14) for SO_2 using the condition of continuity of the molar fluxes resulting in equations (16 - 17).

$$J_{H_2S} = \frac{- \bar{x}_{H_2S} J_{visc} \exp\left(\frac{\delta_{H_2S} J_{visc}}{C_{H_2S}} \right) \exp\left(\frac{A_{H_2S} \delta_r}{B_{H_2S}} \right)}{J_{visc} \left(1 - \exp\left(\frac{A_{H_2S} \delta_r}{B_{H_2S}} \right) \right) + A_{H_2S} \exp\left(\frac{A_{H_2S} \delta_r}{B_{H_2S}} \right) \left(1 - \exp\left(\frac{\delta_{H_2S} J_{visc}}{C_{H_2S}} \right) \right)} \tag{16}$$

$$J_{SO_2} = \frac{-\bar{x}_{SO_2} J_{visc} \exp\left(-\frac{J_{visc}\,\delta_{SO_2}}{C_{SO_2}}\right) \exp\left(\frac{A_{SO_2}(\delta_r - L)}{B_{SO_2}}\right)}{J_{visc}\left(1-\exp\left(\frac{A_{SO_2}(\delta_r - L)}{B_{SO_2}}\right)\right) + A_{SO_2} \exp\left(\frac{A_{SO_2}(\delta_r - L)}{B_{SO_2}}\right)\left(1-\exp\left(-\frac{J_{visc}\,\delta_{SO_2}}{C_{SO_2}}\right)\right)} \tag{17}$$

To further simplify the representation of the resulting equation for the molar flux of H_2S a number of constants and variables are introduced given in equations (18).

$$E_{H_2S} = \exp\left(\frac{\delta_{H_2S} J_{visc}}{C_{H_2S}}\right)$$

$$E_{SO_2} = \exp\left(-\frac{\delta_{SO_2} J_{visc}}{C_{SO_2}}\right)$$

$$Y = \exp\left(\frac{A_{H_2S}\,\delta_r}{B_{H_2S}}\right)$$

$$Z = \exp\left(-\frac{A_{SO_2}\,L}{B_{SO_2}}\right)$$

$$m = \frac{A_{SO_2}}{A_{H_2S}} \frac{B_{H_2S}}{B_{SO_2}} \tag{18}$$

Finally the location of the reaction plane δ_r is eliminated by the condition of stoichiometric molar fluxes of H_2S and SO_2 resulting in the expression given in equation (19).

$$\left(2\bar{x}_{SO_2} A_{SO_2} E_{SO_2} Z\left(A_{H_2S}(1-E_{H_2S}) - J_{visc}\right) + \bar{x}_{H_2S} A_{H_2S} E_{H_2S} Z\left(A_{SO_2}(1-E_{SO_2}) - J_{visc}\right)\right)*$$

$$Y^m + 2\bar{x}_{SO_2} A_{SO_2} E_{SO_2} Z J_{visc}\, Y^{m-1} + \bar{x}_{H_2S} A_{H_2S} E_{H_2S} J_{visc} = 0 \tag{19}$$

The only variable present in equation (19) is Y which is calculated from equation (19) numerically by a root finding procedure. The molar flux of H_2S is then calculated by equation (20).

$$J_{H_2S} = -\bar{x}_{H_2S} \frac{A_{H_2S} J_{visc} E_{H_2S} Y}{J_{visc}(1-Y) + A_{H_2S} Y (1-E_{H_2S})} \tag{20}$$

In the absence of a pressure difference over the membrane equations (19 - 20) should give the expression presented in equation (5). When the pressure difference is going to zero J_{visc} and A_i become zero whereas E_i, Z and Y become 1. As these values cannot be substituted directly in equation (20) the factors 1-Y and 1-E_{H2S} in the denominator of equation (20) are obtained from a first order Taylor expansion resulting after some rearrangement in equation (21).

$$J_{H_2S} = \bar{x}_{H_2S} \frac{E_{H_2S} Y}{\frac{\delta_r}{B_{H_2S}} + Y \frac{\delta_{H_2S}}{C_{H_2S}}} \tag{21}$$

By taking the limit of the pressure difference over the membrane going to zero, and substituting the variable Y and the constants B, C and E by their expressions (see equations (15) and (18)) equation (22) is obtained.

$$J_{H_2S} = \frac{P_{av}}{RT} \frac{\bar{x}_{H_2S}}{\frac{\delta_{H_2S}}{D^{o}_{H_2S}} + \frac{\delta_r}{D^{eff}_{H_2S}}} \tag{22}$$

The location of the reaction plane δ_r must be obtained from equation (19). Equation (19) can be presented for convenience by equation (23). The definition of the constants T_1, T_2 and T_3 is obvious comparing equations (19) and (23).

$$T_1 Y^m + T_2 Y^{m-1} + T_3 = 0 \tag{23}$$

Substitution of the expressions for Y and m from equations (18) in equation (23) results after rearrangement in equation (24).

$$T_1 \exp\left(\frac{A_{SO_2} \delta_r}{B_{SO_2}}\right) + T_2 \exp\left(\frac{A_{SO_2} \delta_r}{B_{SO_2}}\right) \exp\left(-\frac{A_{H_2S} \delta_r}{B_{H_2S}}\right) + T_3 = 0 \tag{24}$$

In order to obtain a linear equation in δ_r the exponential factors, all going to 1 in the absence of a pressure difference over the membrane, are worked out using first order Taylor expansion. Writing out the result and neglecting the second order term in δ_r yields equation (25).

$$\delta_r = -\frac{T_1 + T_2 + T_3}{T_1 \frac{A_{SO_2}}{B_{SO_2}} + T_2 \left(\frac{A_{SO_2}}{B_{SO_2}} - \frac{A_{H_2S}}{B_{H_2S}}\right)} \tag{25}$$

The numerator and the denominator of equation (25) are worked out using first order Taylor expansion for the factors 1-E_i and 1-Z ultimately resulting in equations (26 - 27).

$$T_1+T_2+T_3 = A_{SO_2} A_{H_2S} J_{visc} \left(-2\,\bar{x}_{SO_2} E_{SO_2} Z \frac{\delta_{H_2S}}{C_{H_2S}} + \bar{x}_{H_2S} E_{H_2S} \left(Z \frac{\delta_{SO_2}}{C_{SO_2}} + \frac{L}{B_{SO_2}}\right)\right) \tag{26}$$

$$T_1 \frac{A_{SO_2}}{B_{SO_2}} + T_2 \left(\frac{A_{SO_2}}{B_{SO_2}} - \frac{A_{H_2S}}{B_{H_2S}}\right) = - A_{SO_2} A_{H_2S} J_{visc} \left(2\,\bar{x}_{SO_2} E_{SO_2} Z *$$

$$\left(\frac{1}{B_{H_2S}} + \frac{\delta_{H_2S}}{C_{H_2S}} \frac{A_{SO_2}}{B_{SO_2}}\right) + \bar{x}_{H_2S} E_{H_2S} Z \left(1 - A_{SO_2} \frac{\delta_{SO_2}}{C_{SO_2}}\right) \frac{1}{B_{SO_2}}\Bigg) \tag{27}$$

Combining equations (25 - 27) and substituting the expressions for B_i and C_i yields equation (28).

$$\delta_r = -\frac{D^{eff}_{H_2S} D^{eff}_{SO_2} \left(-2\,\bar{x}_{SO_2} \frac{\delta_{H_2S}}{D^{o}_{H_2S}} + \bar{x}_{H_2S} \frac{\delta_{SO_2}}{D^{o}_{SO_2}} + \bar{x}_{H_2S} \frac{L}{D^{eff}_{SO_2}}\right)}{2\,\bar{x}_{SO_2} D^{eff}_{SO_2} + \bar{x}_{H_2S} D^{eff}_{H_2S}} \tag{28}$$

Substituting equation (28) in equation (22) finally yields the desired expression for the molar flux of H_2S.

$$J_{H_2S} = \frac{P_{av}}{RT} \frac{2\,\bar{x}_{SO_2} D^{eff}_{SO_2} + \bar{x}_{H_2S} D^{eff}_{H_2S}}{D^{eff}_{H_2S} \frac{\delta_{H_2S}}{D^{o}_{H_2S}} + D^{eff}_{SO_2} \frac{\delta_{SO_2}}{D^{o}_{SO_2}} + L} \tag{29}$$

Defining k_g as a continuum diffusion coefficient divided by the thickness of a stagnant layer δ according to the film model we see that equation (29), which has been derived from the model where a pressure difference over the membrane was present but decreased to zero is the same as equation (5) derived in absence of a pressure difference over the membrane and therefore the two models predict the same molar flux of H_2S in the absence of a pressure difference over the membrane.

Chapter 5

A HIGH TEMPERATURE MEMBRANE REACTOR PART 2: AN EXPERIMENTAL STUDY

Abstract

The Claus reaction is used to verify experimentally the previously presented transport model (Sloot et. al., 1991b) in a non-permselective membrane reactor with a mean pore diameter of 350 nm. Both at a temperature of 493 K and at 542 K the experimentally determined molar fluxes are 10 to 20% lower compared to the molar fluxes predicted by the transport model. Conversion measurements performed at pressures of 220 kPa and 500 kPa demonstrate the occurrence of surface diffusion as a transport mechanism despite the large pore diameter of the membrane. In the presence of a pressure difference over the membrane the agreement of the experimentally determined molar fluxes and those calculated by the transport model is reasonable.

1. Introduction

The membrane reactor with separated feeding of reactants, described in detail in the previous part (Sloot et. al., 1991b), is studied experimentally with the Claus reaction as a model reaction (Mark et. al., 1983):

$$2\,H_2S + SO_2 \rightleftharpoons \frac{3}{8}\,S_8 + 2\,H_2O \qquad (1)$$

In part 1 a mathematical model was presented predicting the molar fluxes and the molar fraction profiles that describes transport with an instantaneous, reversible reaction inside a porous membrane. This model is based on the socalled 'Dusty-Gas Model' (Mason and Malinauskas, 1983) extended with surface diffusion. In this part the membrane reactor is studied experimentally and the molar fluxes are compared with the molar fluxes predicted by the mathematical model using parameters that have been measured independently (Sloot et. al., 1991a).

2. Theory

When the above mentioned Claus reaction is assumed to be instantaneous and irreversible the derivation of the molar flux of H_2S as a function of the concentrations of H_2S and SO_2, in the bulk of the gas at the H_2S and SO_2 sides of the membrane respectively, in the absence of a pressure difference over the membrane is straightforward and the result is given in equation (2).

$$J_{H_2S} = \frac{D^{eff}_{H_2S}\, c_{H_2S,\,bulk} + 2\, D^{eff}_{SO_2}\, c_{SO_2,\,bulk}}{N} \qquad (2)$$

$$\text{with } N = L + \frac{D^{eff}_{H_2S}}{D^{o}_{H_2S}} * \delta_{H_2S} + \frac{D^{eff}_{SO_2}}{D^{o}_{SO_2}} * \delta_{SO_2}$$

The denominator in equation (2) represents three mass transfer resistances in series; the resistance of the membrane and the resistances in the gas phase outside the membrane at the H_2S and SO_2 side respectively. The parameters δ_{H2S} and δ_{SO2} represent the thickness of a stagnant gas film by which the mass transfer resistances outside the membrane are described. The mass transfer parameter k_g, which is equal to the continuum diffusion coefficient divided by the thickness of the stagnant gas film, has been measured experimentally in the membrane reactor as a function of pressure (Sloot et. al., 1991a) and can be described by equation (3).

$$k_g = \frac{D^{o}_{i,\,inert}}{\delta_i} = 7.53 * 10^{-3} * P^{-0.159} \qquad \text{with P in } 10^5 \text{ Pa} \qquad (3)$$

The effective diffusion coefficients for H_2S and SO_2 used in equation (2) consist of the contributions of both diffusion through the gas phase in the pores of the membrane and surface diffusion. Assuming cylindrically shaped pores, a Langmuir adsorption isotherm and describing surface diffusion by Fick's law, equation (4) can be derived for the combination of both transport mechanisms (Sloot et. al., 1991a).

$$D_i^{eff} = D_{i,\,gas}^{eff} + \frac{4}{d_p} \frac{D_{i,S}^{eff}\, c_S\, b_i\, RT}{(1 + b_i\, P\, x_{i,\,int\,0})\,(1 + b_i\, P\, x_{i,\,int\,L})} \qquad (4)$$

$$\text{with } \frac{1}{D_{i,\,gas}^{eff}} = \frac{1}{\frac{\varepsilon}{\tau} D_{i,K}^{o}} + \frac{1}{\frac{\varepsilon}{\tau} D_{i,\,inert}^{o}}$$

In equation (4) b_i is the adsorption parameter (Pa^{-1}) and c_S the concentration of adsorption sites on the surface (mole/m^2). The surface diffusion parameters $D_{i,S}\, c_S\, b_i$ and the adsorption parameter b_i have been measured independently (Sloot et. al., 1991a) as a function of temperature and are given in Table 1:

Table 1: Surface diffusion parameters of H_2S and SO_2

	T (K)	b_i (Pa^{-1})	$D_{i,S}\, c_S\, b_i$ (mole / Pa s)
H_2S	484	$1.25 * 10^{-3}$	$1.28 * 10^{-17}$
	521	$1.00 * 10^{-3}$	$1.60 * 10^{-17}$
	557	$5.1 * 10^{-4}$	$9.4 * 10^{-18}$
SO_2	498	$1.1 * 10^{-4}$	$7.4 * 10^{-18}$
	525	$1.36 * 10^{-3}$	$1.50 * 10^{-17}$
	548	$9.0 * 10^{-4}$	$1.31 * 10^{-17}$

The mathematical model described in part 1 (Sloot et. al., 1991b) predicts the molar fluxes as a function of the gas composition at both sides of the membrane using parameters that are measured independently and therefore no parameters to be fitted remain. These calculated molar fluxes are compared to the experimentally determined molar fluxes here.

Equation (2) is rewritten to equation (5) by division by the molar fraction of H_2S in the bulk of the gas.

$$\frac{J_{H_2S}}{x_{H_2S,\,bulk}} = \frac{P}{RT} * \frac{D_{H_2S}^{eff}}{N} + \frac{P}{RT} * \frac{2\, D_{SO_2}^{eff}}{N} * \left(\frac{x_{SO_2,\,bulk}}{x_{H_2S,\,bulk}}\right) \qquad (5)$$

A graphical representation of the experimental data is possible by plotting J_{H2S}/x_{H2S} as a function of x_{SO2}/x_{H2S}. The advantage of this way of plotting, see equation (5), is that this equation contains only two variables, the molar flux of H_2S divided by the molar fraction of H_2S and the ratio of the molar fractions of SO_2 and H_2S. From the molar fractions of H_2S and SO_2 in the bulk of the gas the molar flux of H_2S is calculated from the transport model described in part 1 and the results can be plotted in the same graph as the experimental data for comparison.

3. Experimental setup

The experimental setup used is given schematically in Figure 1.

Figure 1: Experimental setup

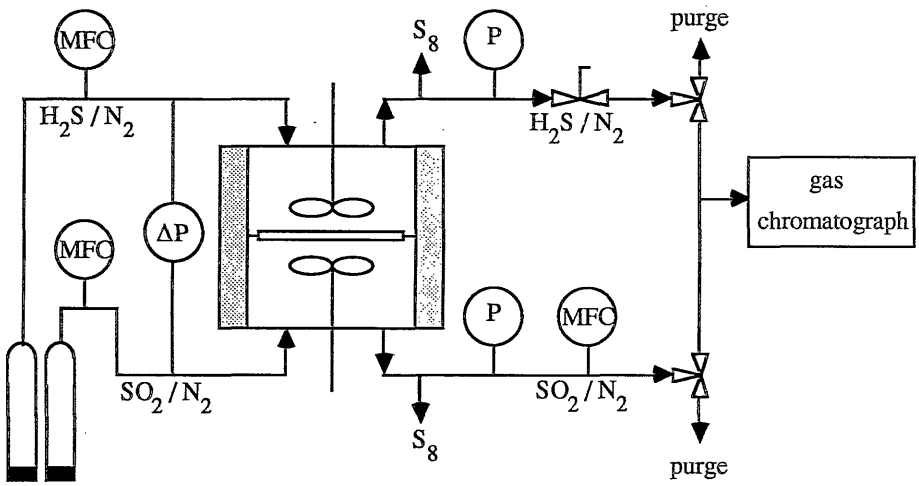

Hydrogen sulfide in nitrogen and sulfur dioxide in nitrogen, with molar fractions of H_2S and SO_2 of about 1500 ppm, are fed to the membrane reactor by mass flow controllers. The outlet of the reactor at the SO_2 side of the membrane contains a manometer and an additional mass flow controller. This mass flow controller is used to adjust the flow out of the reactor at the SO_2 side. In this way the pressure difference over the membrane is fixed at the desired value. Both outlets of the reactor contain a sulfur condensor directly after the reactor to prevent plugging by elemental sulfur produced. The outlet of the reactor at the H_2S side of the membrane contains a manometer and a pressure regulator to fix the pressure in the membrane reactor. Both outlets can either be purged or send to the analyzer in order to be able to measure conversions of H_2S and SO_2 simultaneously or determine the slip of either H_2S or SO_2. In addition there is the possibility of analyzing the inlets of the reactor, not shown in Figure 1. The pressure difference over the membrane is measured by a U-tube filled with water located at the inlet directly in front of the reactor. The reactor is made of stainless steel and consists of three parts; the H_2S chamber, the membrane holder and the SO_2 chamber. The temperature of the reactor is controlled by an Eurotherm. The sealing of the

membrane in the holder is described in detail elsewhere (Sloot et. al., 1991a). Gases were analysed by gas chromatografy using a FPD detector. The column used was a Chromosil column operated at 323 K.

The membrane used is made of α-Al_2O_3 with an average pore diameter of 350 nm and a thickness of 4.5 mm. The membrane has been impregnated with a saturated solution of aluminum nitrate, $Al(NO_3)_3$, and ureum, $CO(NH_2)_2$, in water at a temperature of about 373 K. After drying the impregnated membrane and calcination γ-Al_2O_3 results, the amount impregnated was 0.023 g/m^2. The porosity-tortuosity factor of the membrane ε/τ was determined to be 0.096 (Sloot et. al., 1991a).

4. Experimental results

Conversion measurements have been performed at temperatures of 493 K and 542 K and pressures of 200 and 500 kPa. Conversions were determined based on both H_2S and SO_2, the average conversion of H_2S is calculated using equation (6):

$$\zeta_{H_2S,\,av} = 0.5 * \zeta_{H_2S} + \zeta_{SO_2} \qquad (6)$$

The molar flux of H_2S used in the Figures follows from the average conversion of H_2S as calculated from equation (6) by division by the membrane area.

In Figure 2 the results from the conversion measurements at a temperature of 493 K and a pressure of 220 kPa are presented. In this Figure also the theoretically predicted results are shown. It must be reminded that the calculation of the theoretically predicted molar flux of H_2S involves no fitted parameters but only parameters that have been measured independently.

Figure 2: Results from conversion measurements at a temperature of 493 K

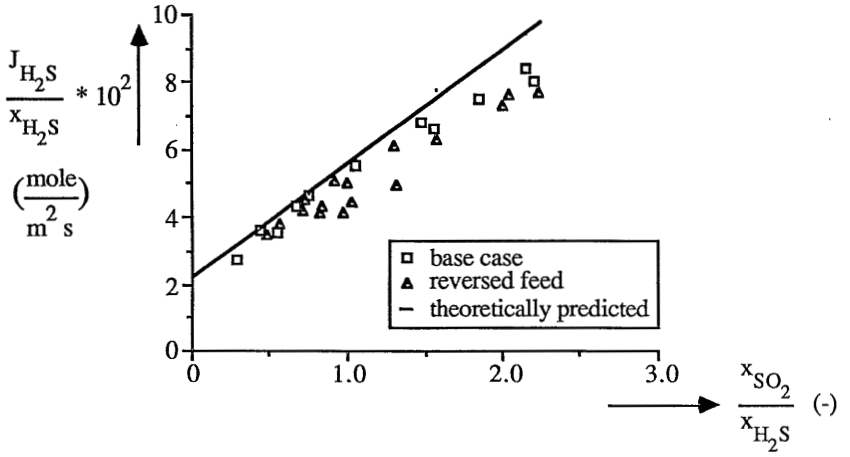

In order to check whether the membrane is homogeneous two series of experiments were performed, the second time using reversed feed, so the H_2S is fed to the SO_2 side of the membrane and vice versa, compared to the first series of experiments. This check is important as the parameters required in the theoretical prediction of molar fluxes were determined using either flow or diffusion measurements without reaction. In these measurements the components are transported through the entire membrane whereas in the conversion measurements H_2S and SO_2 use only part of the membrane before reaction takes place. From Figure 2 it can be concluded that the assumption of a homogeneous membrane is reasonable and that the catalyst is present through the entire membrane. It is also clear from Figure 2 that the experimentally determined molar flux of H_2S divided by the molar fraction of H_2S in the bulk of the gas at the H_2S side of the membrane is somewhat lower compared to the theoretically predicted values, especially at high values of the ratio of the molar fractions of SO_2 and H_2S.

In Figure 3 the data from Figure 2 are plotted in an alternative way, that is by division by the molar fraction of SO_2 instead of the molar fraction of H_2S.

Figure 3: Results from conversion measurements at a temperature of 493 K

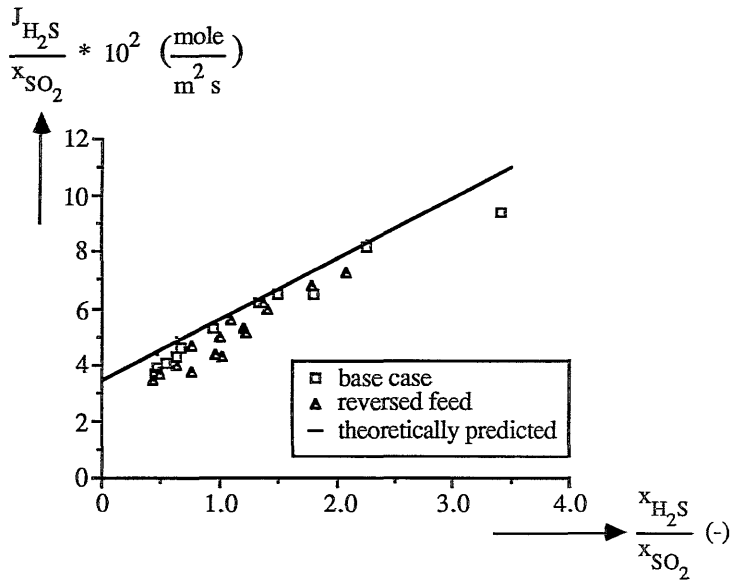

From Figure 3 it can be concluded that the highest deviations of the experimental data from the theoretically predicted values occur at low values of the ratio of the molar fractions of H_2S and SO_2. The fact that the experimental results are systematically lower compared to the results predicted by theory can mainly be attributed to two effects. Firstly, the theoretical model assumes the reaction to be instantaneous whereas in the experiments some influence of kinetics of the Claus reaction might be involved resulting in somewhat lower molar fluxes. Secondly, the parameters, i.e. the surface diffusion parameters of H_2S and SO_2, used by the theoretical model could be overestimated. It is possible that the reaction products, elemental sulfur and water, can adsorb

which results in a decrease of the fraction of the adsorption sites covered by H_2S or SO_2. As a result surface diffusion of H_2S and SO_2 is decreased. Determination of the surface diffusion parameters as presented in Table 1 was carried out in the absence of elemental sulfur and water (Sloot et. al., 1991a).

A further check of the experimental data concerns to what extent the mass balance of H_2S and SO_2 is fulfilled and to check whether the ratio of the conversion of H_2S and SO_2 is independent of the ratio of the molar fractions of H_2S and SO_2. This should be checked as the location of the reaction zone inside the membrane changes with the ratio of the molar fractions of H_2S and SO_2 and as a result part of the membrane that had been in a H_2S containing gas now is in a SO_2 containing gas or vice versa possibly giving a slow reaction between the membrane, or the impregnated catalyst, and H_2S or SO_2. In Figure 4 the ratio of the conversions of H_2S and SO_2 is plotted as a function of the ratio of the molar fractions of H_2S and SO_2.

Figure 4: Check of the mass balance at the conversion measurements at 493 K

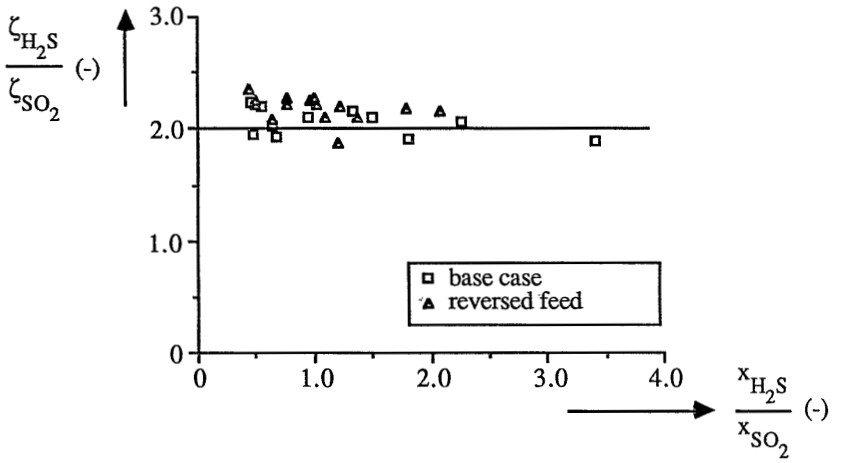

From Figure 4 it is concluded that the agreement of the conversions of H_2S and SO_2 is reasonable although the conversion of H_2S seems to be systematically higher compared to the conversion of SO_2, especially in the situation with the reversed feed.

To determine whether kinetics play a role in the conversion measurements at 493 K, measurements were also performed at a temperature of 542 K. If kinetics of the Claus reaction influenced the values of the molar flux of H_2S divided by the molar fraction of H_2S in Figures 2 and 3 the fit of the experimental data by the results predicted by the theoretical model is expected to be improved at 542 K. In order to study the influence of surface diffusion, conversion measurements were performed at two pressures i.e. at 220 kPa and at 500kPa. In Figure 5 the molar flux of H_2S divided by the molar fraction of H_2S is plotted as a function of the ratio of the molar fractions of SO_2 and H_2S and in Figure 6 the same data are plotted in the alternative way.

Figure 5: Results from conversion measurements at a temperature of 542 K

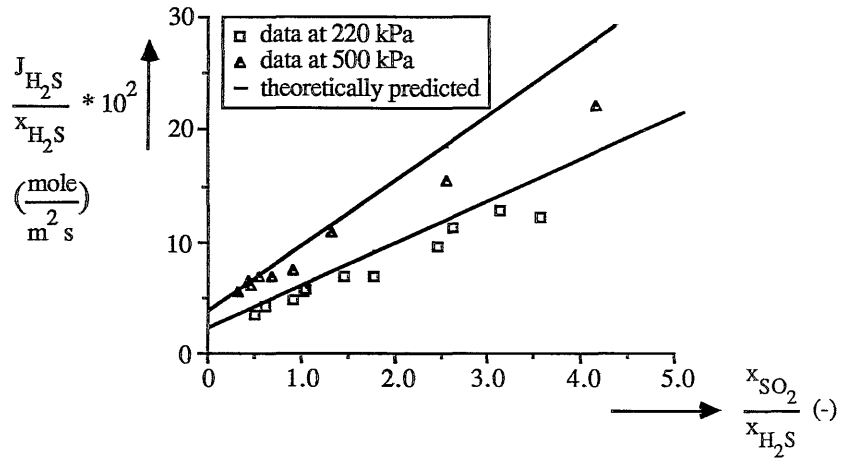

Figure 6: Results from conversion measurements at a temperature of 542 K

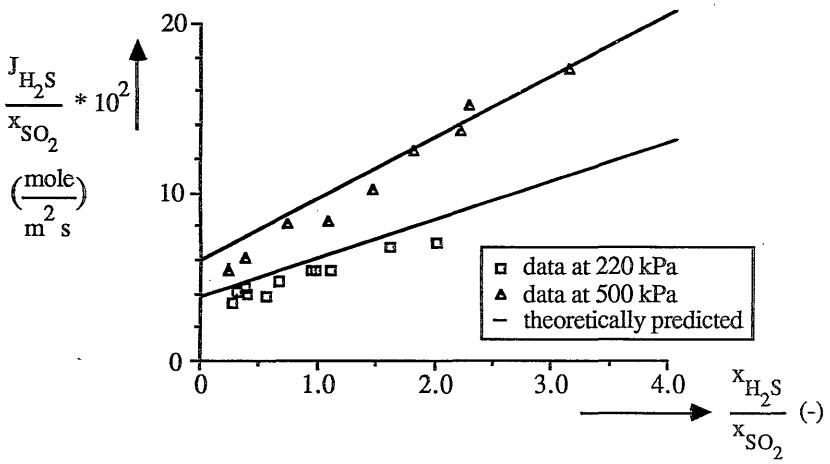

From Figures 5 and 6 it can be concluded that the experimentally determined values are somewhat lower compared to the values calculated by theory. Again it should be noted that the theoretical model uses only parameters that were determined independently (Sloot et. al., 1991b) and contains no fitted parameters. The difference between the results measured at a pressure of 220 kPa and at 500 kPa is remarkable and is caused entirely by the increase of surface diffusion. As the pore diameter of the membrane is 350 nm, transport at a pressure of 220 kPa already takes place completely in the continuum regime. As the continuum diffusion coefficient is inversely proportional to the pressure the molar flux owing to diffusion through the gas phase in the pores of the membrane is independent of the pressure and no difference of the experimental data at 220 kPa and 500 kPa in Figures 5 and 6 is expected. The transport owing to surface diffusion however, is linearly proportional to the pressure provided the fraction of the adsorption sites covered by H_2S or

SO_2 is small. Therefore the total molar flux of H_2S and SO_2 increases with pressure as can be seen in Figures 5 and 6. These experimental data demonstrate that despite the large pore diameter of the membrane surface diffusion causes a considerable part of the total transport.

From the experimental data at a pressure of 500 kPa in Figures 5 and 6 it appears that the agreement with the theoretically calculated data is good in case the molar fraction of H_2S is high compared with the molar fraction of SO_2 and worse at relatively high molar fractions of SO_2. The most likely explanation for this is that the surface diffusion parameters for SO_2, which are important at the pressure of 500 kPa, are not correct although their values have been measured independently (Sloot et. al., 1991a).

To check the agreement of the experimentally determined conversions of H_2S and SO_2 their ratio is plotted as a function of the ratio of the molar fractions of H_2S and SO_2 in Figures 7 and 8 for a pressure of 220 kPa and 500 kPa respectively.

Figure 7: Check of the mass balance for the conversion measurements at 542 K and 220 kPa

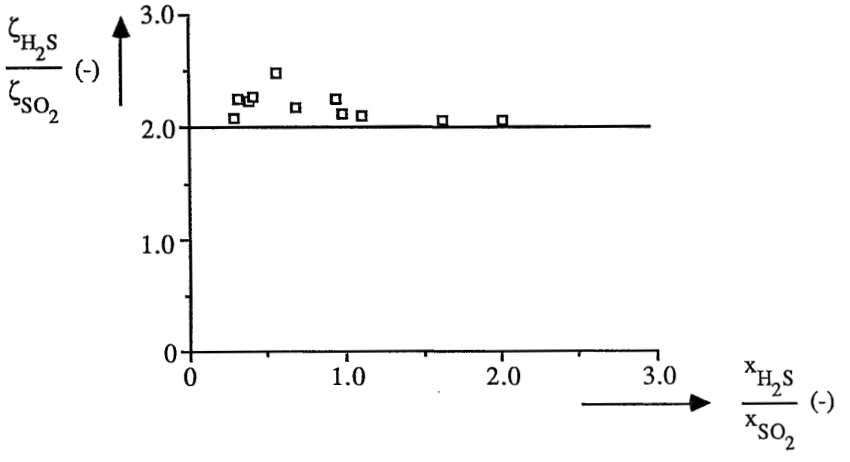

Figure 8: Check of the mass balance for the conversion measurements at 542 K and 500 kPa

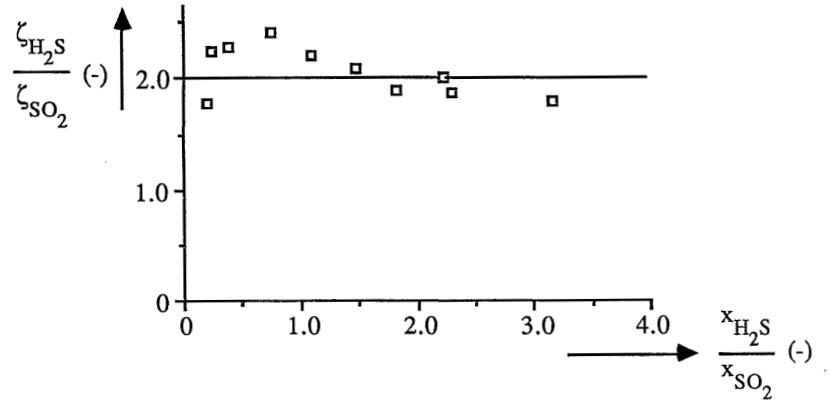

At a pressure of 200 kPa the ratio of the conversion of H_2S and SO_2 is systematically slightly higher compared to the stoichiometric ratio of 2. At a pressure of 500 kPa this ratio is better fulfilled on the average however a slight decrease with the ratio of the molar fractions of H_2S and SO_2 is present. Nevertheless the mass balance is fulfilled reasonably in the experiments.

As in practice a pressure difference over the membrane can occur it is important to check whether such a pressure difference results in slip of the reactant at the high pressure side of the membrane. Some conversion measurements were carried out in which a pressure difference over the membrane is applied with the highest pressure at the H_2S side of the membrane. These measurements were performed at a temperature of 551 K and an average pressure between 365 and 505 kPa. The change of the flows at both sides of the membrane owing to the pressure difference over the membrane was fixed by the mass flow controller in the outlet of the reactor at the SO_2 side of the membrane (see Figure 1). In these measurements no substantial slip of H_2S at the SO_2 side of the membrane was observed. In Figure 9 the ratio of the experimentally observed molar flux of H_2S, using equation 6, and the theoretically calculated molar flux is plotted as a function of the pressure difference over the membrane.

Figure 9: Conversion measurements in the presence of a pressure difference over the membrane.

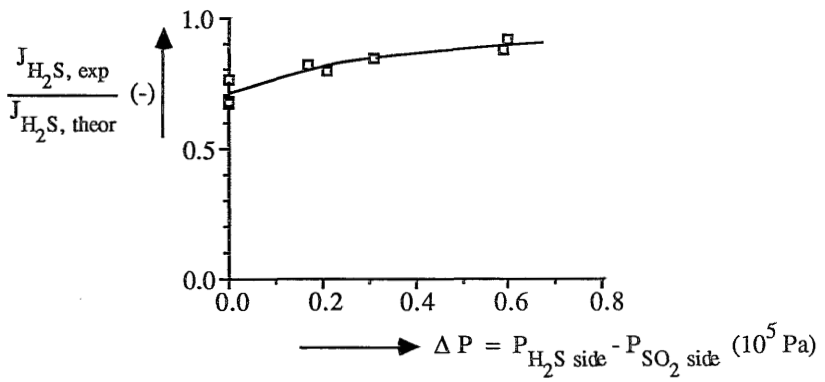

From Figure 9 it can be concluded that the agreement between the experimentally observed molar flux and the theoretically calculated molar flux of H_2S approaches to 1 with higher pressure difference over the membrane. This is probably caused by the fact that at higher pressure differences over the membrane viscous flow becomes important as a transport mechanism thereby shifting the reaction zone towards the low pressure side of the membrane, i.e. the SO_2 side of the membrane. This reduces the relative contribution of surface diffusion of SO_2 as a transport mechanism whose parameters are not accurately known under actual conversion conditions.

5. Conclusions

The mathematical transportmodel describing transport and reaction in the membrane reactor is verified experimentally using the Claus reaction as a model reaction. Results from conversion

measurements at temperatures of 493 K and 541 K are shown to be 10 to 20% lower compared to the molar fluxes predicted by the theoretical model. Conversion measurements performed at pressures of 220 kPa and 500 kPa demonstrate the occurrence of surface diffusion as a transport mechanism despite the large pore diameter of the membrane of 350 nm. Measurement in the presence of a pressure difference over the membrane were performed at a temperature of 551 K. Despite the relatively large pressure difference of up to 0.7 bar no substantial slip of H_2S to the SO_2 side of the membrane was observed. The agreement between the experimentally observed and the theoretically calculated molar flux of H_2S was reasonable.

Notation

b_i	adsorption constant	Pa^{-1}
$c_{i,\,bulk}$	concentration of component i in the bulk of the gas	mole / m^3
c_S	concentration of adsorption sites on the surface	mole / m^2
D^o_i	continuum diffusion coefficient of component i	m^2 / s
$D_{i,\,eff}$	effective difusion coefficient of component i	m^2 / s
$D^o_{i,\,K}$	Knudsen diffusion coefficient	m^2 / s
$D_{i,S\,eff}$	effective surface diffusion coefficient	m^2 / s
d_p	average pore diameter	m
J_i	molar flux of component i	mole / m^2 s
k_g	mass transfer parameter in th gas phase outside the membrane	m / s
N	parameter defined in equation (2)	m
P	pressure	Pa
R	gas constant	J / mole K
T	temperature	K
$x_{i,\,int}$	molar fraction of component i at the membrane interface	-
δ_i	thickness of the stagnant gas film	m
ε	porosity of the membrane	-
τ	tortuosity of the membrane	-
ζ_i	conversion of component i	mole / s

References

Mark H.F., D.F. Othmer, C.G. Overberger and G.T. Seaborg, 1983, Kirk-Othmer, Encyclopedia of chemical technology, vol. 22, pp 276-282, John Wiley & Son, New York

Mason E.A. and A.P. Malinauskas, 1983, Gas transport in porous media: The Dusty-Gas Model, Chemical Engineering Monographs 17, Elsevier, Amsterdam

Sloot H.J., G.F. Versteeg, C.A. Smolders and W.P.M. van Swaaij, 1991a, Surface diffusion of hydrogen sulfide and sulfur dioxide in alumina membranes in the continuum regime, to be published, chapter 3 in this thesis

Sloot H.J., G.F. Versteeg, C.A. Smolders and W.P.M. van Swaaij, 1991b, Mathematical modelling of mass transport combined with an instantaneous, reversible reaction inside a membrane, to be published, chapter 4 in this thesis

Chapter 6

A NON-PERMSELECTIVE MEMBRANE REACTOR FOR THE SELECTIVE CATALYTIC REDUCTION OF NITRIC OXIDE WITH AMMONIA

Abstract

A novel type of reactor is developed for the catalytic reduction of NO_x with NH_3. In this reactor a porous membrane is used to keep the reactants separated from each other and to carry out the reaction in a controlled way inside the membrane. As the rate of reaction is fast compared to the diffusion rate of the reactants, the molar fluxes of both reactants are in stoichiometric ratio and slip of reactants to the opposite side of the membrane is prevented. The advantage of this reactor is the possibility to obtain high conversions of NO_x despite fluctuating concentrations of NO_x without severe slip of NH_3. This membrane reactor has been tested experimentally and it is demonstrated that it is able to cope with a varying ratio of concentrations of NO_x and NH_3 without detectable slip of NH_3 or NO_x at a temperature of 569 K.

1. Introduction

Selective catalytic reduction of NO_x with NH_3, the socalled SCR reaction, using a V_2O_5 catalyst on a TiO_2 support is widely regarded as a promising method to reduce the emission of NO_x. In order to develop processes for this reaction there are two important aspects to be solved; the development of selective, highly active catalysts and the development of a reactor suitable to carry out the catalytic reduction.

In literature most attention is focussed on the development of catalysts for the SCR reaction and an extensive review is given by Bosch (1988). NO_x consists mainly of NO and NO_2, or its dimer N_2O_4 (Gmelin, 1934). The main, desired reactions of NO_x with NH_3 in the presence of oxygen are given in equations (1 - 3).

$$4\,NO + 4\,NH_3 + O_2 \longrightarrow 4\,N_2 + 6\,H_2O \quad (1)$$

$$6\,NO_2 + 8\,NH_3 \longrightarrow 7\,N_2 + 12\,H_2O \quad (2)$$

$$NO + NO_2 + 2\,NH_3 \longrightarrow 2\,N_2 + 3\,H_2O \quad (3)$$

It is known from literature (Kato et. al., 1981a, Tuenter et. al., 1988) that the kinetics of reaction (3) are higher compared to the kinetics of reactions (1) and (2). Besides the reactions (1 - 3) also the formation of N_2O has been reported as a product (Tuenter et. al., 1988), however, occurring mainly at temperatures above 573 K. At these temperatures also the extent of the oxidation of NH_3 increases (Kato et. al., 1981b, Vogt et. al., 1988). In literature it is observed that oxygen plays an important role in the reaction of NO with NH_3 (Kato et. al., 1981a, Inomata et. al., 1982, Tuenter et. al., 1988). The proposed mechanism assumes two oxidation states of the vanadium: V^{5+} and V^{4+}. In the reaction of NO with NH_3 V^{5+} is reduced to V^{4+} which is reoxidized by the oxygen in the gas (Inomata et. al., 1980, 1982, Janssen et. al., 1987a and b).

A number of catalysts have been studied in literature mostly using V_2O_5 on Al_2O_3 (Bauerle et. al., 1978, Inomata et. al., 1982, Nam et. al., 1986, Wong and Nobe, 1986) or on TiO_2 (Inomata et. al, 1982, Wong and Nobe, 1986, Vogt et. al., 1988), the last ones giving the highest kinetics. Also catalysts based on stainless steel have been reported (Sadakata et. al., 1985, Willey et. al., 1985).

Far less attention has been paid in literature to the development of suitable reactors for the SCR reaction although this is a very important issue. As the ammonia content of the flue gas treated must be limited to only 5 ppm (Janssen et. al., 1986) severe restrictions are imposed on the reactor and on the amount of NH_3 that must be fed to the flue gas. In order to obtain high conversions of NO_x the amount of NH_3 added has to be regulated extremely well as insufficient NH_3 supply results in a limited conversion of NO_x whereas an excess of NH_3 gives an undesired slip of NH_3. To complicate this control problem, the concentration of NO_x in the flue gas fluctuates usually. In literature a few suggestions have been presented to solve the problem of NH_3 supply. Vogt et. al. (1988) suggested to use an excess supply of NH_3 and remove the remaining NH_3 after the SCR reaction by selective oxidation to N_2 at a higher temperature. Disadvantages are the increased

amount of NH_3 required for the de-NO_x process and the necessity of heating the flue gas in order to convert the excess of NH_3. The use of a chromatographic reactor with periodically reversing flow was suggested by Agar and Ruppel (1988). By periodically reversing the flow direction NH_3 can be concentrated in the center of the reactor by which the problem of exact stoichiometric addition of NH_3 is solved whereas slip of NH_3 remains negligible. However large reactor volumes will be required or short cycle times will be be necessary.

An alternative solution for the stoichiometric addition of NH_3 could be the membrane reactor which was developed by Sloot et. al. (1990). This membrane reactor was first proposed for the catalytic part of the Claus process in which H_2S reacts with SO_2, a system that suffers from the same problem of stoichiometric supply of reactants. In this reactor a porous, ceramic membrane is used to keep the reactants, NO_x and NH_3 in this case, separated from each other and to obtain a controlled stoichiometric feed of NH_3. Flue gas containing NO_x is fed to one side, a gas with NH_3 added is fed to the other side of the membrane. As no pressure difference over the membrane is applied both reactants diffuse from opposite sides into the membrane, which is impregnated with a catalyst for the SCR reaction, and react inside the membrane. Provided the rate of the reaction is fast compared to the diffusion rates of the reactants, a small reaction zone inside the membrane will occur preventing slip of reactants to the opposite side of the membrane. The location of this reaction zone is such that the molar fluxes of NO_x and NH_3 are in stoichiometric ratio. If the concentration of NO_x increases the molar flux of NO_x into the membrane increases resulting in an excess of NO_x at the reaction zone that diffuses further into the membrane to react with NH_3. As a result the location of the reaction zone shifts towards the NH_3 side of the membrane. As the distance from the membrane interface to the reaction zone is increased for NO_x its molar flux decreases and vice versa for NH_3. Finally the location of the reaction zone inside the membrane will be such that the molar fluxes of NO_x and NH_3 are in stoichiometric ratio again. In Figure 1 the concentration profiles are presented schematically.

Figure 1: Concentration profiles

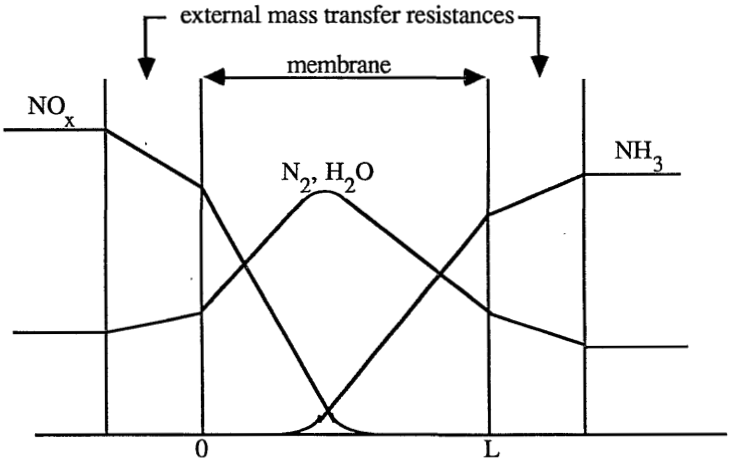

In Figure 1 besides the mass transfer resistance of the membrane also mass transfer resistances in the gas phase outside the membrane are shown. As permselectivity is not of importance in this membrane reactor the pore diameter of the membrane is chosen relatively large in order to operate in the continuum regime. This results in a relatively small mass transfer resistance of the membrane giving high molar fluxes and therefore small membrane area required. Because of the relatively small mass transfer resistance of the membrane, the mass transfer resistances in the gas phase outside the membrane cannot be neglected.

The outlet of the reactor at the NH_3 side of the membrane, containing the excess of NH_3, is recycled after addition of pure ammonia. In this reactor NO_x and NH_3 are always supplied in stoichiometric ratio and slip of NH_3 is prevented by the fast chemical reaction inside the membrane. Instead of instantaneous adjustment of the NH_3 supply as is required when a conventional reactor is used, the NH_3 supply in the membrane reactor has only to be in stoichiometric ratio averaged in time.

Recently at Twente University Zaspalis (1990) studied the applicability of a similar membrane reactor for the de-NO_x process using a Al_2O_3 membrane with a TiO_2 toplayer with 5 nm pores which contained the V_2O_5 catalyst. Slip of NH_3 could, however, only be prevented by using a small pressure difference over the membrane.

2. Theory

If the rate of the irreversible reaction is assumed to be instantaneous compared to the diffusion rate of the reactants, a reaction plane inside the membrane results at location δ_r and the molar flux of NO_x and NH_3 can be expressed by equations (4-5).

$$J_{NO_x} = D^{eff}_{NO_x} \frac{P}{RT} \frac{x^{int}_{NO_x}}{\delta_r} \tag{4}$$

$$J_{NH_3} = D^{eff}_{NH_3} \frac{P}{RT} \frac{x^{int}_{NH_3}}{L - \delta_r} \tag{5}$$

The molar fluxes of NO_x and NH_3 are directed oppositely. The mass transfer resistances in the gas phase outside the membrane are taken into account by equations (6-7).

$$J_{NO_x} = k_{g,NO_x} \frac{P}{RT} \left(x^{bulk}_{NO_x} - x^{int}_{NO_x}\right) \tag{6}$$

$$J_{NH_3} = k_{g,NH_3} \frac{P}{RT} \left(x^{bulk}_{NH_3} - x^{int}_{NH_3}\right) \tag{7}$$

The molar fractions of NO_x and NH_3 at the membrane interface are eliminated by combination of equations (4-7). Finally the location of the reaction plane, δ_r, is eliminated by the condition of stoichiometry of the molar fluxes of NO_x and NH_3 given by equation (8) which results in equation (9).

$$J_{NO_x} = \frac{J_{NH_3}}{\nu_{NH_3}} \tag{8}$$

In equation (8) ν_{NH3} is the stoichiometric coefficient which is equal to the number of NH_3 molecules that react with 1 NO_x molecule. Depending on whether NO_x consists of NO or NO_2 or a combination of both, this coefficient varies between 1 and 1.33 (see equations (1-3)).

$$J_{NO_x} = \frac{\frac{D^{eff}_{NH_3} x^{bulk}_{NH_3}}{\nu_{NH_3}} + D^{eff}_{NO_x} x^{bulk}_{NO_x}}{L + \frac{D^{eff}_{NO_x}}{k_{g,NO_x}} + \frac{D^{eff}_{NH_3}}{k_{g,NH_3}}} * \frac{P}{RT} \tag{9}$$

The denominator in equation (9) consists of three resistances in series, the membrane resistance represented by the membrane thickness L and mass transfer resistances in the gas phase outside the membrane at the NO_x and at the NH_3 side of the membrane. The numerator in equation (9) contains the effective diffusion coefficients of NH_3 and NO_x, the molar fractions of NH_3 and NO_x in the bulk of the gas at the NH_3 and NO_x side of the membrane respectively and the stoichiometric coefficient ν_{NH3}. The mass transfer parameter outside the membrane, k_g, has been measured as a function of pressure in an experimental setup used for the study of the Claus reaction (Sloot et. al., 1991) which was identical to the setup used in the present study. The k_g values measured for SO_2 as a function of pressure at a temperature of 534 K is presented in equation (10).

$$k_g = 7.53 * 10^{-3} * P^{-0.16} \tag{10}$$

with P in 10^5 Pa

The k_g values determined with SO_2 can be used to estimate the k_g values of NO_x and NH_3 in the present experimental setup. With these values of the mass transfer parameter k_g and the effective diffusion coefficients obtained from conversion measurements, the relative contribution of the terms in equation (9) reflecting the mass transfer resistances in the gas phase outside the membrane can be calculated to be about 25% of the membrane thickness L of $4.7 * 10^{-3}$ m. Therefore the denominator in equation (9) is replaced by 1.25 times the membrane thickness L. In order to

reduce the number of variables from three to two, which makes a graphical representation of the experimental data possible, equation (9) is divided by the molar fraction of NH_3 in the bulk of the gas at the NH_3 side of the membrane, resulting in equation (11).

$$\frac{J_{NO_x}}{x_{NH_3}} = \frac{1}{1.25 * L} * \frac{P}{RT} * \frac{D^{eff}_{NH_3}}{\nu_{NH_3}} + \frac{1}{1.25 * L} * \frac{P}{RT} * D^{eff}_{NO_x} * \left(\frac{x_{NO_x}}{x_{NH_3}}\right) \qquad (11)$$

When the molar flux of NO_x divided by the molar fraction of NH_3 in the bulk of the gas at the NH_3 side of the membrane is plotted as a function of the ratio of the molar fractions of NO_x and NH_3 in the bulk of the gas, a straight line must result. From the intercept and the slope of this line the effective diffusion coefficients of NO_x and NH_3 can be calculated respectively. The stoichiometric coefficient, ν_{NH3}, can be determined from the experimentally observed mass balance between NH_3 and NO_x or fixed at some value between 1 and 1.33 (see equations (1-3)).

3. Experimental setup

The experimental setup is given schematically in Figure 2.

Figure 2: Experimental setup

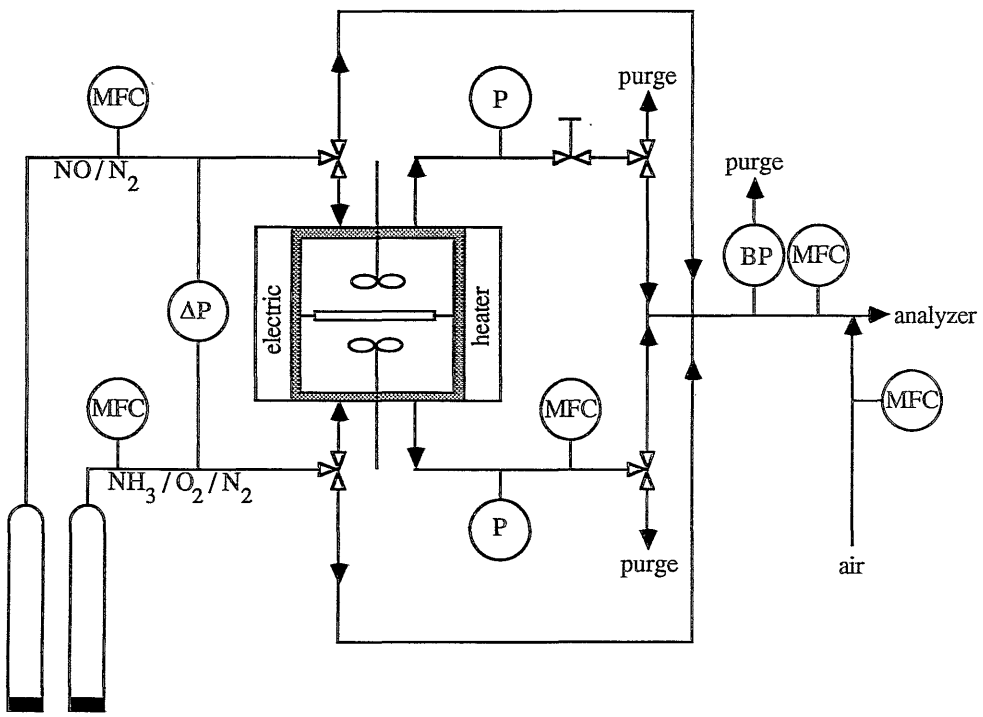

NO in N_2 (1500 ppm) is fed to one side of the membrane and NH_3 in N_2 (1500 ppm) and O_2 (6%) is fed to the other side of the membrane by mass flow controllers. Both reactor chambers are stirred and considered ideally mixed. The reactor is made of stainless steel and consists of three parts, the NO_x chamber, the NH_3 chamber and the membrane holder held together by bolts. The sealing of the membrane has been described in detail in a previous chapter (Sloot et. al., 1991a). The reactor is heated electrically and the temperature is controlled. The outlet of the reactor at the NO_x side of the membrane contains a mass flow controller which is used to control the flow rate out of the reactor and thereby the pressure difference over the membrane. The outlet of the reactor at the NH_3 side of the membrane contains a valve to regulate the pressure in the reactor itself. The pressure difference over the membrane is measured by an U-tube filled with water placed directly at the entrance of the reactor. Both the outlets of the reactor can either be purged or sent to the analyzer. Analysis of NO, NO_2 and NH_3 is performed by a dual channel Monitor Labs chemiluminescent analyzer. As this analyzer requires low concentrations (50 ppm at most) of NO_x and NH_3 and large gas flows only a part of the gas to be analyzed is used for analysis, the remaining gas is purged. The amount of sample gas to be sent to the analyzer is controlled by a mass flow controller as is the flow of air used to dilute the sample gas. A back pressure valve is used to maintain a constant pressure for the mass flow controller in the sample gas.

In Figure 3 the chemiluminescent analyzer is presented schematically.

Figure 3: Chemiluminescent analyzer

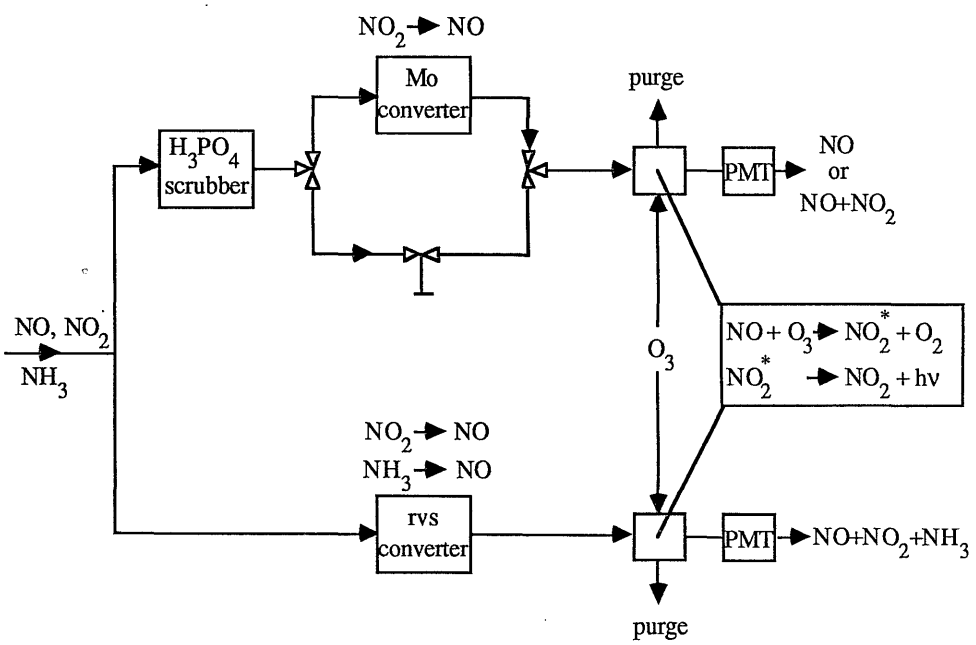

The chemiluminescent analyzer consists of two channels, the NO_x channel and the NH_3/NO_x channel. The NO_x channel contains a molybdenum converter to convert NO_2 to NO and measures NO plus NO_2, bypassing this converter gives the NO content only. The bypass of the molybdenum converter contains an adjusting valve to maintain the pressure drop equal to the pressure drop over the molybdenum converter. It is well known from literature that the molybdenum converter only works properly if NH_3 is removed from the sample which is done by a scrubber containing concentrated phosphoric acid (Wong et. al., 1984, Janssen et. al., 1986). The NH_3/NO_x channel contains a stainless steel converter at a temperature of 750 °C which converts NH_3 and NO_2 to NO.

The membrane used was made of α-Al_2O_3 and was obtained from ECN, Petten, The Netherlands. The membrane was impregnated with a saturated solution of ammoniumvanadate, NH_4VO_3, with oxalic acid, $H_2C_2O_4.2H_2O$ (Bauerle et. al., 1978, Nam et. al., 1986). After drying the membrane was calcined at a temperature of 770 K. The average pore diameter was determined by porosimetry using mercury. The volume averaged pore diameter was determined to be 507 nm.

Although this catalyst cannot be considered as the best suitable for the SCR reaction, its activity is reasonable (Inomata et. al., 1982, Wong et. al., 1986) and the objective of this paper is to demonstrate the possibilities of the membrane reactor for the SCR process and not to optimize the catalyst.

4. Analysis system

Before the performance of the membrane reactor was studied the reactor was first bypassed, and the analyzer was tested. Starting with a mixture of NO in N_2 the analyzer was calibrated by adjusting the signals from the NO_x and NH_3/NO_x channel to the same chosen response. The valve in the bypass of the molybdenum converter was set at a position where bypassing this converter resulted in the same signal.

Next calibration curves of NO and NH_3 were determined by feeding the analyzer with different concentrations of NO in N_2 and NH_3 in N_2 successively. In case of NH_3 in N_2 also 6% of O_2 was present. It was observed that plotting the signal of the analyzer as a function of the NO concentration, a straight line through the origin was obtained, bypassing the Mo-converter resulted in the same signal and therefore no NO_2 formation had occurred. For NH_3 a nearly identical straight line was found. This line did not go precisely through the origin. From these measurements it can be concluded that conversion of NH_3 to NO in the stainless steel converter is complete and selective. Also it can be concluded that a possible reaction of NO produced in this converter with NH_3 does not occur. Therefore quantitative analyses of NO or NH_3 in an air stream is possible.

Next NO was diluted with air and the formation of NO_2 by oxidation of NO was verified, with the reactor still bypassed. In Figure 4 the NO plus NO_2 signal and the NO signal, obtained from bypassing the Mo-converter, are plotted as a function of the concentration of NO fed.

Figure 4: Oxidation of NO to NO_2 in the gasmixing analysis section before dilution

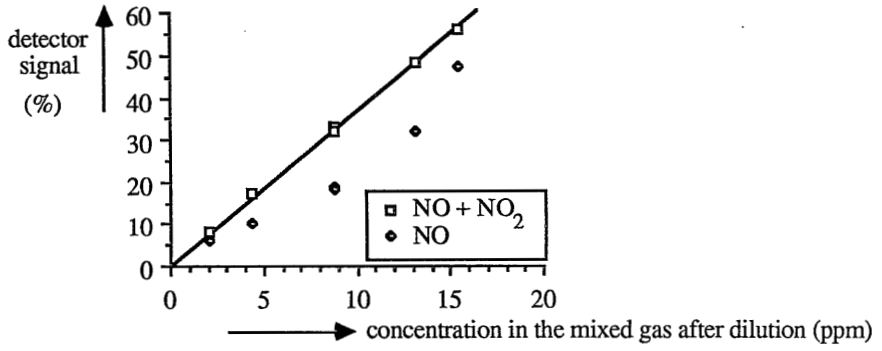

From Figure 4 it is concluded that substantial oxidation of NO to NO_2 occurred. From the straight line obtained for the NO+NO_2 signal it is concluded that the Mo-converter quantitatively and selectively converts NO_2 to NO. So quantitative analyses of NO and NO_2 is possible. As the final dilution of NO in N_2 before the analyzer with air did not result in the formation of NO_2, NO oxidation must have taken place in the setup before dilution with air for the analyzer. To determine the location of this NO oxydation two additional experiments were performed varying the residence time in different parts of the setup. By increasing the flow of NO with air through the setup up to the mass flow controller just before the dilution with air for the analyzer (ϕ_{max} = 0.44 l_n/hr), the residence time in the first part of the setup, up to the back pressure in Figure 2, was decreased. This did not result in any change of the NO conversion measured. Increasing the residence time in the tubing section which contains the mass flow controller before the dilution with air (see Figure 2), however resulted in a considerable increase of the NO conversion to NO_2. Therefore it is concluded that NO oxidation took place in this part of the experimental setup.

Next NO and NH_3 were premixed in different concentration ratios and fed simultaneously to the analyzer, bypassing the reactor. In Figure 5 the observed NO_x and NH_3 signals are presented as a function of the concentration.

Figure 5: NO and NH_3 fed simultaneously to the analyzer

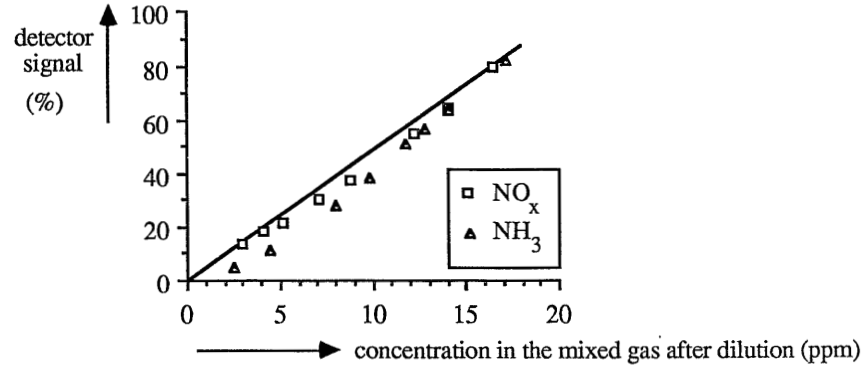

Substantial deviations from the expected straight lines were observed especially for NH_3 at low concentrations. As both the NO_x and the NH_3/NO_x channel show a deviation from the straight line, the cause of these deviations is located somewhere before the sample is split in the analyzer. The most likely explanation is a reaction between NO, or NO_2, with NH_3 in the tubing section which contains the mass flow controller for the dilution with air for the analyzer. Especially the combination of low NH_3 concentrations combined with relatively high NO_x concentrations results in substantial deviations of the NH_3 signal. The simultaneous presence of both NO_x and NH_3 in the gas to be analyzed must therefore be avoided. As in the membrane reactor the gas containing NO_x and the gas containing NH_3 remain separated by the membrane this limitation of the analytical technique is not a problem because both exits of the membrane reactor can be analyzed separately. To determine qualitatively possible slip of NO_x to the NH_3 side of the membrane the analyzer can still be used as the deviations for NO_x at low concentrations are negligible as can be seen in Figure 5. However analyses of NH_3 slip to the NO_x side of the membrane is not possible with this setup, see Figure 5. Therefore analysis tubes (Dräger) containing a solid packed bed reacting selectively with NH_3 giving a change of colour were used to obtain a qualitative impression of the slip of NH_3.

5. Conversions of NO_x and NH_3 in the reactor

Before using the reactor as a membrane reactor oxidation of NO to NO_2 and of NH_3 were determined as a function of temperature. NO in N_2 was mixed with air, fed to the reactor and forced through the membrane. In Figure 6 the conversion of NO to NO_2 is plotted as a function of the temperature in the reactor.

Figure 6: Conversion of NO to NO_2 as a function of temperature

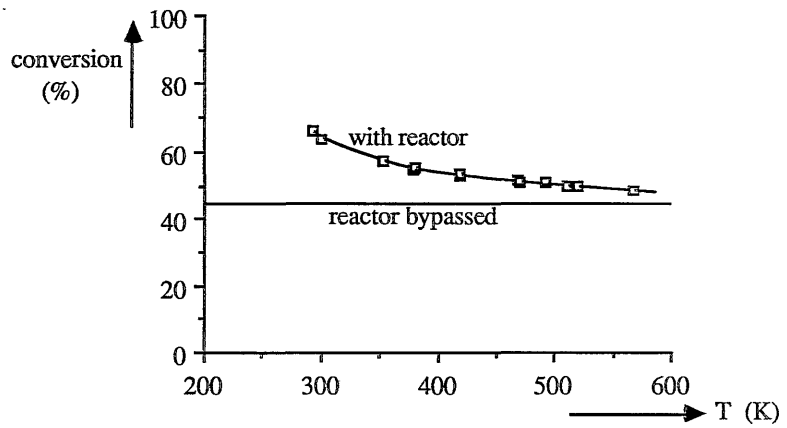

In Figure 6 also the conversion obtained when bypassing the reactor has been plotted. As can be seen from Figure 6 the conversion with the reactor is higher and decreases with temperature. The decrease of the conversion with temperature is caused by decreasing kinetics with temperature as

has been reported in literature (Gmelin, 1934). According to Gmelin (1934) the oxidation of NO to NO_2 takes place in two steps, a fast equilibrium reaction giving an intermediate product followed by a slow consecutive reaction. The equilibrium of the first reaction is shifted to the reactant side by increasing temperature resulting in a decrease of the concentration of the intermediate product and thereby the kinetics of the consecutive reaction which more than compensates the increase of the kinetic constant with temperature. This results in an overall decrease of the kinetics of the oxidation of NO to NO_2 with temperature. The conversion obtained when the reactor is bypassed is caused by the tubing section which contains the mass flow controller for dilution of the gas for the analyzer as was discussed before (see Figure 4). As the reactor is located in front of this tubing section it cannot be concluded from Figure 6 that the conversion obtained in the reactor is equal to the difference between the conversion with and without the reactor. Therefore it can only be concluded that in the reactor both NO and NO_2 are present.

Next the oxidation of NH_3 in the reactor was studied as a function of temperature by forcing a gasmixture of NH_3 in N_2, also containing 6 % of O_2, through the membrane. In Figure 7 the conversion of NH_3 is presented as a function of temperature.

Figure 7: Oxidation of NH_3 as a function of temperature.

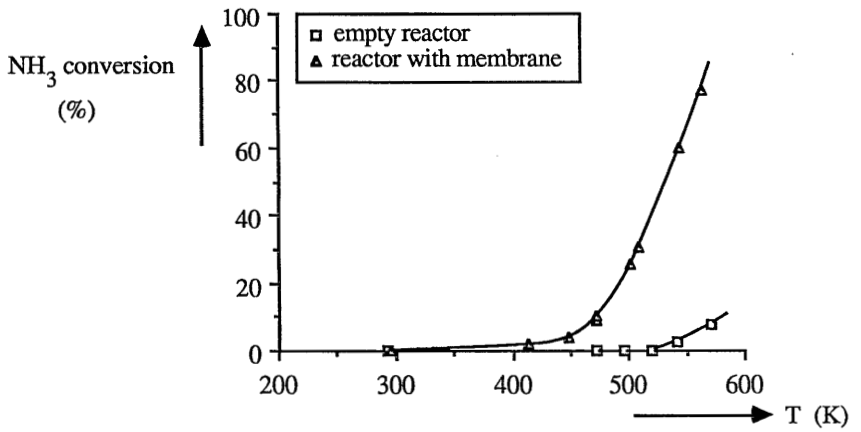

In Figure 7 both the conversion of NH_3 in the empty reactor and the conversion in the presence of the membrane, impregnated with the catalyst, is presented. As can be seen from Figure 7 NH_3 conversion in the empty reactor starts at a temperature of 525 K. However, in the presence of the membrane the oxidation of NH_3 already takes place at a temperature of 425 K. As no NO_x formation has been observed, this in contrast to Odenbrand et. al. (1988), the product of the oxidation of NH_3 is probably N_2 or N_2O, which has not been analyzed. Oxidation of NH_3 either directly results in N_2 formation or the intermediate NO_x reacts fast with the remaining NH_3 giving N_2. The substantial oxidation of NH_3 by the membrane at temperatures above 450 K is a result of the combination of the catalyst and the support used and is contradictory to the results from Kato et. al. (1981b) who observed no oxidation of NH_3 up to 575 K. However, the study of this paper is the development of an alternative reactor for the catalytic reduction of NO_x and not much

attention has been paid to the catalyst and its support.

Finally conversion measurements were carried out to demonstrate the performance and usability of the membrane reactor. NO in N_2 was fed to one side of the membrane and NH_3 in N_2, containing also 6% O_2, was fed to the other side of the membrane. No pressure difference over the membrane was applied. Both exit streams of the reactor were analyzed separately and slip of NH_3 to the NO_x side of the membrane was checked by the test tubes. Conversion measurements were performed at two temperatures, at 467 K and at 569 K. At the temperature of 467 K two series of measurements were carried out at different pressures of 260 kPa and at 600 kPa to check whether the transport mechanism is only diffusion through the gas phase in the pores of the membrane. In case of the Claus reaction, a reaction between H_2S and SO_2 giving S and H_2O, a substantial part of the transport in the membrane appeared to be caused by surface diffusion (Sloot, 1991) despite the large pore diameters of the membrane of 350 nm used. As, owing to the large pore diameter of the membrane, diffusion through the gas phase in the pores of the membrane takes place in the continuum regime the resulting molar flux is independent of pressure. The molar flux owing to surface diffusion, however, is proportional to the pressure provided the fraction of the adsorption sites occupied remains relatively small. This difference in pressure dependence can be used to discriminate between diffusion through the gas phase in the pores of the membrane and surface diffusion.

In Figure 8 the conversion of NO_x, consisting of NO and NO_2, divided by the molar fraction of NH_3 at the NH_3 side of the membrane is plotted as a function of the ratio of the molar fractions of NO_x and NH_3 (see equation 11) both at a pressure of 260 kPa and at 600 kPa.

Figure 8: Conversion measurements at 467 K.

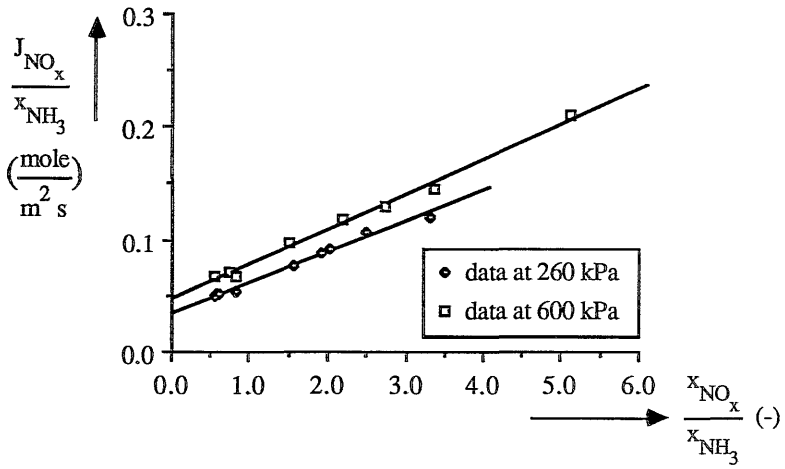

To check the results of the conversion measurements, the slope and the intercept in Figure 8, the same experimental data are plotted in an alternative way i.e. by division by the molar fraction of NO_x instead of NH_3. The result is given by Figure 9.

Figure 9: Conversion measurements at 467 K plotted in an alternative way.

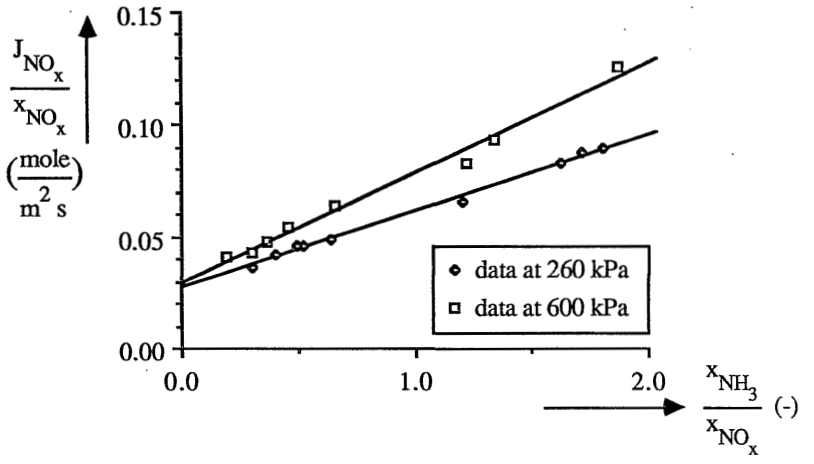

From Figures 8 and 9 it is concluded that in both cases a straight line is obtained that does not go through the origin. The mass balance between NH_3 and NO_x, determined by the ratio of the conversion of NH_3 divided by the conversion of NO_x, varied between 1.00 and 1.16 which is in excellent agreement with the value of ν_{NH3} expected between 1.00 and 1.33 (see equations (1-3)). At a ratio of the molar fractions of NH_3 and NO_x of 1.5 and higher, some slip of NH_3 was detected to the NO_x side of the membrane. Slip of NO_x was not detected at ratio's of the molar fractions of NO_x and NH_3 of 4 and lower. Therefore it can be concluded that at a temperature of 467 K the kinetics of the SCR reaction are not yet high enough to completely prevent slip of reactants.

Conversion measurements were also performed at a temperature of 569 K and a pressure of 260 kPa. The resulting plot of the experimental data is presented in Figure 10.

Figure 10: Conversion measurements at a temperature of 569 K

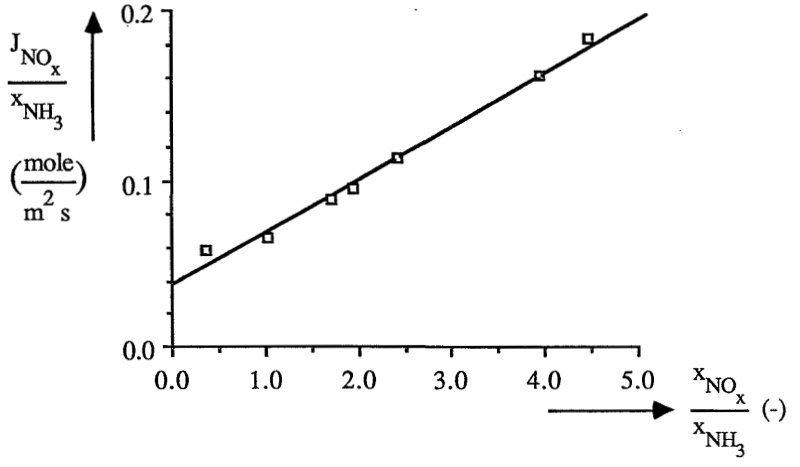

The straight line not going through the origin, expected from equation 11, is observed again. No slip of NH_3 or NO_x was observed. As at the temperature of these experiments substantial oxidation of NH_3 should have occurred, see Figure 7, the ratio of the conversions of NH_3 and NO_x, ν_{NH3}, was studied as a function of the ratio of the molar fractions of NO_x and NH_3 in Figure 11.

Figure 11: Check of the mass balance at the conversion measurements at 569 K

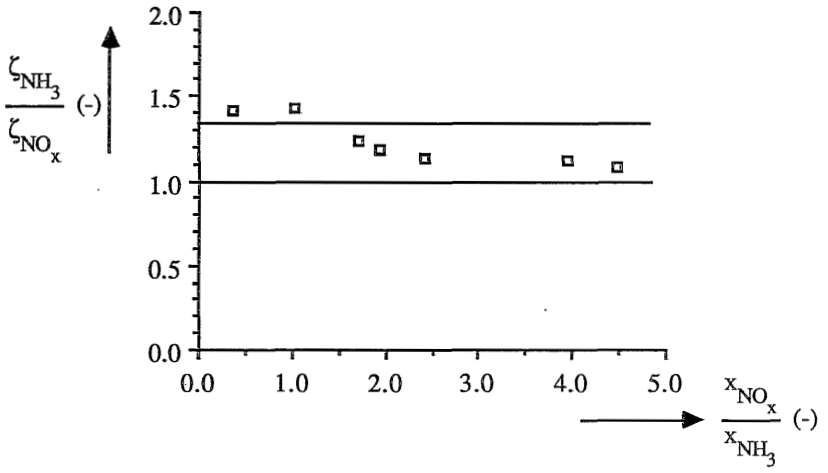

In Figure 11 two straight lines are drawn which present the expected conversion ratio of NH_3 and NO_x, the lower one assuming that NO_x consists entirely of NO and the upper one assuming NO_x present entirely as NO_2. Surprisingly the experimentally observed ratio of the conversions does not deviate substantially from these values. This implies that no substantial oxidation of NH_3 has occurred as this would result in a value of ζ_{NH3}/ζ_{NOx}, which is equal to ν_{NH3}, higher compared to the expected value between 1.00 and 1.33. The decrease of the ratio of the conversion of NH_3 and NO_x with the ratio of the molar fractions of NO_x and NH_3 can be explained by the location of the reaction zone inside the membrane. At high ratio's of the molar fractions of NO_x and NH_3, the reaction zone is shifted towards the NH_3 side of the membrane. As a result the time required for NH_3 to diffuse in the membrane to the reaction zone is relatively small which results in less oxidation of NH_3. To check the results from the oxidation measurements of NH_3 as presented in Figure 7, these experiments were carried out again. The resulting data were however in excellent agreement with those presented in Figure 7.

Next effective diffusion coefficients of NO_x and NH_3 are calculated from the slope and the intercept obtained from Figures 8 to 10. In Table 1 the values of the effective diffusion coefficients of NO_x and NH_3 are presented. In this calculation a membrane thickness of $4.7 * 10^{-3}$ m was used and the stoichiometric coefficient, ν_{NH3}, was set equal to 1.165, the average between 1.0, in case NO_x consists entirely of NO, and 1.33, in case NO_x consists entirely of NO_2.

Table 1: Effective diffusion coefficients at temperatures of 467 and 569 K.

T (K)	P (10^5 Pa)	derived from results of Figure number	$D^{eff}_{NO_x}$ (m^2/s)	$D^{eff}_{NH_3}$ (m^2/s)
467	2.6	8	$2.38 * 10^{-6}$	$3.56 * 10^{-6}$
		9	$2.40 * 10^{-6}$	$3.52 * 10^{-6}$
	6.0	8	$1.18 * 10^{-6}$	$2.08 * 10^{-6}$
		9	$1.13 * 10^{-6}$	$2.17 * 10^{-6}$
569	2.6	10	$3.2 * 10^{-6}$	$4.7 * 10^{-6}$

From Table 1 it can be concluded that the agreement between the effective diffusion coefficients of NO_x and NH_3 at a temperature of 467 K is excellent.

To compare the experimentally determined effective diffusion coefficients with those expected from gas kinetic theory, the diffusion coeficients in the membrane were calculated. As this requires knowledge of the porosity-tortuosity factor of the membrane, this was measured by permeation experiments.

The diffusion coefficient in a straight capillary pore can be calculated theoretically by equation (12).

$$\frac{1}{D^0_i} = \frac{1}{D^0_{i,K}} + \frac{P}{D^0_{i,inert}} \qquad (12)$$

with $D^0_{i,K}$ the Knudsen and $D^0_{i,inert}$ the continuum diffusion coefficient at 10^5 Pa

The continuum diffusion coefficient is calculated from the gas kinetic theory (Reid et. al., 1977) and the Knudsen diffusion coefficient is calculated according to equation (13).

$$D^0_{i,K} = \frac{d_p}{3}\sqrt{\frac{8\,RT}{\pi\,M_i}} \qquad (13)$$

In Table 2 the ratio of the experimentally determined effective diffusion coefficients of NO_x and NH_3 and the diffusion coefficients calculated by equation (12) are presented. This ratio is equal to the porosity-tortuosity factor of the membrane and should be constant, provided that diffusion through the gas phase in the pores of the membrane is the only transport mechanism.

Table 2: Ratio of the effective diffusion coefficient and the diffusion coeffient in a straight capillary pore with a pore diameter of 507 nm.

T (K)	P (10^5 Pa)	$D^{th}_{NO_x}$ (m^2/s)	$D^{th}_{NH_3}$ (m^2/s)	$\frac{D^{exp}_{NO_x}}{D^{th}_{NO_x}}$ (-)	$\frac{D^{exp}_{NH_3}}{D^{th}_{NH_3}}$ (-)
467	2.6	$1.28 * 10^{-5}$	$1.73 * 10^{-5}$	0.19	0.20
	6.0	$5.97 * 10^{-6}$	$7.83 * 10^{-6}$	0.19	0.27
569	2.6	$1.73 * 10^{-5}$	$2.35 * 10^{-5}$	0.19	0.20

From Table 2 it can be concluded that for NO_x the ratio of the experimentally determined effective diffusion coefficient and the theoretically calculated diffusion coefficient in a straight capillary pore is constant. For NH_3 it can be seen that this ratio increases with pressure at a temperature of 467 K. As diffusion through the gas phase in the pores of the membrane almost entirely takes place in the continuum regime, the coefficient for diffusion through the gas phase is inversely proportional to the pressure. For surface diffusion, however, the diffusion coefficient is independent of the pressure provided that the fraction of the adsorption sites occupied is relatively small. The difference in the pressure dependence of both tranport mechanisms is used to determine whether surface diffusion contributes to the total transport. As the ratio of the experimentally determined effective diffusion coefficient of NH_3 and the diffusion coefficient in a straight capillary pore increases with pressure, this seems an indication that surface diffusion of NH_3 plays a role in the transport of NH_3 in the membrane. Although a contribution of surface diffusion in a membrane with a pore diameter of 500 nm is surprising this has also been observed for the transport of H_2S and SO_2 in similar membranes (Sloot et. al., 1991).

The porosity-tortuosity factor of the membrane, ε/τ, was determined by permeation measurements with N_2 at different temperatures. In these permeation measurements pure N_2 is forced through the membrane and the pressure drop over the membrane is measured as a function of the flow through the membrane. The transport through the membrane consists of two contributions; Knudsen diffusion and viscous flow, and can be described by equation (14) (see for instance Mason and Malinauskas, 1983).

$$J_i = -\frac{1}{RT}\left(D^{eff}_{i,K} + \frac{B_o P}{\eta}\right)\frac{dP}{dz} \qquad (14)$$

$$\text{with } B_o = \frac{\varepsilon}{\tau}\frac{d_p^2}{32} \text{ and } D^{eff}_{i,K} = \frac{\varepsilon}{\tau} D^{o}_{i,K} = \frac{\varepsilon}{\tau}\frac{d_p}{3}\sqrt{\frac{8RT}{\pi M_i}}$$

Integration of equation (14) results, after some rearranging, in equation (15).

$$\frac{J_i}{\Delta P} = \frac{1}{RTL}\frac{\varepsilon}{\tau} D^o_{i,K} + \frac{B_o}{RT\eta L}\bar{P} \qquad (15)$$

The average pressure in equation (15) is a direct result from the integration and therefore it is not necessary to have a pressure drop over the membrane that is small compared to the pressure itself. When $J_i / \Delta P$ is plotted as a function of the average pressure a straight line must result. Both from the intercept and from the slope of this line the porosity-tortuosity factor, ε/τ, of the membrane is calculated. In Figure 12 the experimental permeation data are presented, both at a temperature of 293 K and at 562 K.

Figure 12: Permeation measurements carried out with N_2

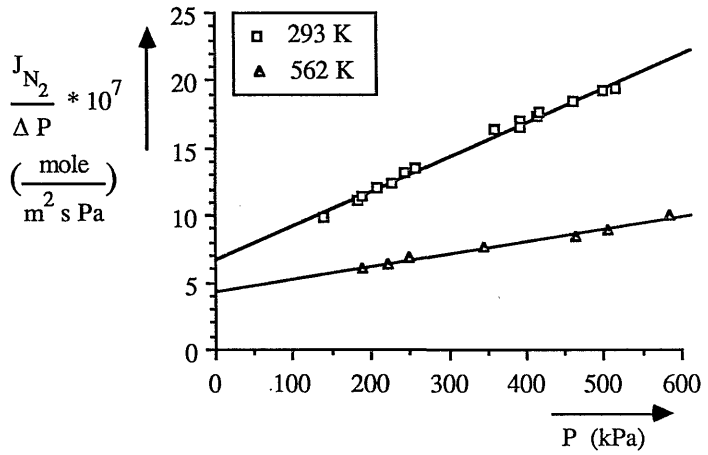

In Table 3 the values of the porosity-tortuosity factor, ε/τ, of the membrane, calculated from the slope and the intercept from Figure 13 are presented.

Table 3: Determination of the porosity-tortuosity factor of the membrane

	293 K	562 K	average
ε/τ from the intercept	0.095	0.105	0.100
ε/τ from the slope	0.069	0.061	0.065

The agreement of the values of the porosity-tortuosity factor, ε/τ, presented in Table 3 is reasonable when the two temperatures are compared. However, the values determined from the intercept and those from the slope deviate about 35%. As the transport during the conversion measurements is diffusion and not viscous flow, the average value of 0.100 as determined from the intercept are used for further interpretation.

When this value is compared to the ratio of the experimentally determined effective diffusion coefficient of NO_x and NH_3 and the diffusion coefficient in a straight capillary pore with a diameter of 500 nm, however, a substantial difference is noticed. The transport rate of NO_x and NH_3 through the membrane is substantially faster compared to the rate estimated from gas kinetic theory using the porosity-tortuosity factor determined from the permeation measurements. This is an indication of surface diffusion although from the conversion measurements at 467 K no contribution of surface diffusion of the magnitude that can explain this difference is observed. More detailed study of the transport in the membrane would be required to explain these observations.

6. Conclusions

A novel type of reactor has been developed for the catalytic reduction of NO_x with NH_3. In this reactor a porous membrane is used to keep the reactants separated from each other. The reaction is carried out inside the membrane and as the rate of reaction is fast compared to the diffusion rate of the reactants the molar fluxes of both reactants are in stoichiometric ratio and slip of reactants to the opposite side of the membrane is prevented. The advantage of this type of reactor is the possibility of treating gas streams with fluctuating concentrations of NO_x. The applicability of this membrane reactor is demonstrated experimentally using an α-Al_2O_3 membrane impregnated with V_2O_5. Temperatures used were between 467 and 569 K. From these conversion measurements it is found that at a temperature of 467 K the reaction rate is not yet high enough to completely prevent slip of reactants, however, at a temperature of 569 K no slip of reactant has been observed. At this temperature the ratio of the NH_3 and the NO_x concentration can vary largely without the occurrence of slip of reactants. No slip of NH_3 to the NO_x side of the membrane has been observed for the experiments performed at a temperature of 569 K. The effective diffusion coefficients of NO_x and NH_3 are higher by about a factor 2 compared to the diffusion coefficients calculated theoretically using the porosity-tortuosity factor of the membrane as determined from permeation measurements with N_2.

This type of reactor offers interesting advantages over a packed bed reactor especially in case of highly fluctuating concentrations of NO_x.

Notation

B_o	membrane specific parameter defined in equation (14)	m^2
D_i^o	diffusion coefficient of component i in a straight capillary pore	m^2 / s
$D_{i,K}^o$	Knudsen diffusion coefficient of component i	m^2 / s
$D_{i,inert}^o$	continuum diffusion coefficient of component i	m^2 / s
D_i^{eff}	effective diffusion coefficient of component i	m^2 / s
d_p	pore diameter of the membrane	m
J_i	molar flux of component i	mole / m^2 s
k_g	mass transfer parameter in the gas phase outside the membrane	m / s

L	membrane thickness	m
M_i	molar mass of component i	kg / mole
P	pressure	Pa
R	gas constant	J / mole K
T	temperature	K
x_i	molar fraction of component i	-
z	location inside the membrane	m
δ_r	location of the reaction zone inside the membrane	m
ε	porosity of the memrbane	-
η	viscosity of the gas	Pa s
ν_{NH3}	stoichiometric coefficient	-
τ	tortuosity of the membrane	-
ζ_i	conversion of component i	mole / s

indices

bulk	in the bulk of the gas
exp	experimental
int	at the membrane interface
th	theoretical

References

Agar D.W. and W. Ruppel, 1988, Extended reactor concept for dynamic de-NO_x design, Chem. Eng. Sci. **43**, 2073-2078

Bauerle G.L., S.C. Wu and K. Nobe, 1978, Parametric and durability studies of NO_x reduction with NH_3 on V_2O_5 catalysts, Ind. Eng. Chem. Prod. Res. Dev. **17**(2), 117-122

Bosch H., 1988, Catal. Today **2**, 369 - 552

Gmelins Handbuch der Anorganischen Chemie, 1934, System-nummer 4: Stickstoff, Lieferung 3, Verbindungen des stickstoffs mit sauerstoff, 8e Auflage, Verlag Chemie GMBH, Berlin

Inomata M., A. Miyamoto and Y. Murakami, 1980, Mechanism of the reaction of NO with NH_3 on vanadium oxide catalyst in the presence of oxygen under the dilute gas condition, J. Catal. **62**, 140-148

Inomata M., A. Miyamoto, T. Ui, K. Kobayashi and Y. Murakami, 1982, Activities of V_2O_5/TiO_2 and V_2O_5/Al_2O_3 catalysts for the Rraction of NO and NH_3 in the presence of O_2, Ind. Eng. Chem. Prod. Res. Dev. **21**, 424-428

Janssen F., F van den Kerkhof, J. Leffers, P. Lodder and L. Luierweert, 1986, The determination of ammonia in flue gas from the selective catalytic reduction of nitric oxide with ammonia, Anal. Chim. Act. **190**, 245-254

Janssen F.J.J.G., F.M.G. van den Kerkhof, H. Bosch and J.R.H. Ross, 1987, Mechanism of

the reaction of nitric oxide, ammonia and oxygen over vanadia catalysts. 1. The role of oxygen studied by way of isotopic transients under dilute conditions, J. Phys. Chem. **91**, 5921-5927

Janssen F.J.J.G., F.M.G. van den Kerkhof, H. Bosch and J.R.H. Ross, 1987, Mechanism of the reaction of nitric oxide, ammonia and oxygen over vanadia catalysts. 2. Isotopic transient studies with oxygen-18 and nitrogen-15, J. Phys. Chem. **91**, 6633-6638

Kato A., S. Matsuda, F. Nakajima, M. Imanari and Y. Watanabe, 1981a, Reduction of nitric oxide with ammonia on iron oxide - titanium oxide catalyst, J. Phys. Chem. **85**, 1710-1713

Kato A., S. Matsuda, T. Kamo, F. Nakajima, H. Kuroda and T. Narita, 1981b, Reaction between NO_x and NH_3 on iron oxide - titanium oxide catalyst, J. Phys. Chem. **85**, 4099-4102

Mason E.A. and A.P. Malinauskas, 1983, Gas transport in porous media: The Dusty-Gas Model, Chemical Engineeriung Monographs 17, Elsevier, Amsterdam

Nam I., J.W. Eldridge and J.R. Kittrell, 1986, Model of temperature dependence of a vanadia-alumina catalyst for NO reduction by NH_3: Fresh catalyst, Ind. Eng. Chem. Prod. Res. Dev. **25**, 186-192

Odenbrand C.U.I., S.T. Lundin and L.A.H. Andersson, 1985, Catalytic reduction of nitrogen oxides 1. The reduction of NO, Appl. Catal. **18**, 335-352

Reid R.C., J.M. Prausnitz and T.K. Sherwood, 1977, The properties of gases and liquids, 3rd edition, McGraw-Hill, New York

Sadakata M., S. Komiyama and T. Sakai, 1985, Rapid reduction of nitric oxide by hydrogen in the presence of stainless and Ni catalyst, Combust. Sci. and Tech. **44**, 195-205

Sloot H.J., G.F. Versteeg and W.P.M. van Swaaij, 1990, A non-permselective membrane reactor for chemical processes normally requiring strict stoichiometric feed rates of reactants, Chem. Eng. Sci. **45**(8), 2415-2421, chapter 2 in this thesis

Sloot H.J., G.F. Versteeg, C.A. Smolders and W.P.M. van Swaaij, 1991, Surface diffusion of hydrogen sulfide and sulfur dioxide in alumina membranes in the continuum regime, to be published, chapter 3 in this thesis

Tuenter G., W.F. van Leeuwen and L.J.M. Snepvangers, 1986, 'Kinetics and Mechanism of the NO_x Reduction with NH_3 on V_2O_5-WO_3-TiO_2 Catalyst', Ind. Eng. Chem. Prod. Res. Dev. **25**, 633-636

Vogt E.T.C., A. Boot, A.J. van Dillen, J.W. Geus, F.J.J.G. Janssen and F.M.G. van den Kerkhof, 1988, Preparation and performance of a silica-supported V_2O_5 on TiO_2 catalyst for the selective reduction of NO with NH_3, J. Catal. **114**, 313-320

Willey R.J., J.W. Eldridge and J.R. Kittrell, 1985, Mechanistic model of the selective catalytic reduction of nitric oxide with ammonia, Ind. Eng. Chem. Prod. Res. Dev. **24**, 226-233

Wong W.C. and K. Nobe, 1984, Kinetics of NO reduction with NH_3 on 'Chemically mixed' and impregnated V_2O_5-TiO_2 catalysts, Ind. Eng. Chem. Prod. Res. Dev. **23**, 564-568

Wong W.C. and K. Nobe, 1986, Reduction of NO with NH_3 on Al_2O_3- and TiO_2-supported metal oxide catalysts, Ind. Eng. Chem. Prod. Res. Dev. **25**, 179-186

Zaspalis V.T., 1990, thesis Twente University

LEVENSLOOP

Henk Sloot werd geboren op 17 april 1964 te Hengelo. Na de lagere school bezocht hij van 1976 tot en met 1982 het Ichthus College te Enschede waar hij in 1982 het Atheneum diploma behaalde.

In september 1982 begon hij aan de studie Chemische Technologie aan de Universiteit Twente te Enschede. In december 1986 studeerde hij af in de vakgroep Proceskunde en Industriële processen en produkten, afstudeerhoogleraar was Prof. dr. ir. W.P.M. van Swaaij.

In februari 1987 begon hij in dezelfde vakgroep aan het promotieonderzoek waarvan het resultaat in dit proefschrift beschreven is.

In maart 1991 is hij in dienst van Shell Research BV te Amsterdam getreden.